Dräger

D-87-2010

Electrical Impedance Tomography: The realisation of regional ventilation monitoring

2nd edition

Eckhard Teschner
Michael Imhoff
Steffen Leonhardt

Dräger. Technology for Life®

Electrical Impedance Tomography: The realisation of regional ventilation monitoring

2nd edition

Eckhard Teschner
Michael Imhoff
Steffen Leonhardt

Important notes

This brochure is for educational purposes only and does not replace the instructions for use. Prior to using the technique of EIT (Electrical Impedance Tomography), the corresponding instructions for use must always be read and complied with.

Medical knowledge is subject to constant change due to research and clinical experience. The authors of this publication have taken utmost care to ensure that all information provided, in particular concerning applications and effects, is current at the time of publication. This does not, however, absolve readers of the obligation to take clinical measures on their own responsibility.

Editor
Drägerwerk AG & Co. KGaA
Moislinger Allee 53–55
D-23542 Lübeck
www.draeger.com

CONTENTS

1. Foreword

This booklet accompanies the introduction of Electrical Impedance Tomography (EIT) as a clinical application for monitoring of regional lung function, especially in intensive care patients. In this context, four questions must be answered:

Why introduce EIT as a supplementary imaging technique in medicine?
What information can be gained from EIT?
Which clinical benefits can be expected?
Why did it take about 30 years to develop appropriate clinical devices?

Today, clinicians are accustomed to rapid improvements of high resolution imaging techniques, such as 128-slice CT scanners, f-MRI methods, SPECT or 3D ultrasound scanning. Do we need EIT with its limited local resolution as an additional tool? The principle answer is that EIT, on the one hand, provides images based on new and different information, such as electrical tissue properties. On the other hand, EIT can be applied at the bedside as a continuous monitoring technique, as it only requires small devices and does not expose patients or users to any ionising radiation. These opportunities justify the search for application fields in which EIT will help to improve the care of patients.

EIT was introduced in the early 1980s by Barber and Brown. Soon thereafter, a wide spectrum of possible applications in medicine was suggested, ranging from gastric emptying to brain function monitoring and from breast imaging to lung function assessment. Our group, which had the opportunity to work with early system versions, predicted that, based on our own experiences, the greatest medical benefit of EIT would lie in monitoring regional lung function in intensive care patients. Before EIT was made available as a bedside monitoring tool, the heterogeneous distribution of lung injury, e.g.

in ARDS (Acute Respiratory Distress Syndrome) patients, was only detectable outside the ICU, either by CT or by non-imaging techniques such as MIGET (Multiple Inert Gas Elimination Technique). EIT is the only method which can directly show whether closed lung regions can be opened by a recruitment manoeuvre and be kept open by optimised ventilator settings, all with the aim of minimising the risk of VALI (Ventilator Associated Lung Injury).

Major drawbacks of early EIT systems included their poor sensitivity and susceptibility to signal interference in clinical settings. Acceptable lung tomograms and ventilation images were only achieved using maximal inspiratory and expiratory hold manoeuvres which are not applicable in intensive care patients. The images did not provide valid information on the patient's pulmonary status. Most of the research interest in EIT development focused on the extension of the technology towards multi-frequency systems which could deliver special information on tissue properties, on the introduction of new image reconstruction algorithms, or 3D imaging. The less spectacular, yet indispensable, goal of improving signal acquisition quality was not in the centre stage of activities.

The deficits of the existing EIT systems have been the motivation for our group to enhance sensitivity and to make improved EIT systems available for scientific studies on clinical issues. A major advantage was our opportunity for technical development, validation experiments in animals, volunteer studies and research with patients by affiliation of our group to the centre of Anesthesiology and Intensive Care of the University Hospital in Göttingen. These special conditions facilitated EIT development and brought it very close to practical clinical use, as it tied together all the essential factors for improving the technology and developing it further for use in the clinical setting.

A further substantial step was the cooperation with those commercial

companies which stood out as leaders in ventilation technology equipment. Even with their commitment to this field and their substantial financial investment, it took many years to improve the system hardware, perform validation studies and develop simple but reliable software tools for bringing EIT into broad and successful clinical use. This booklet will tell the story of the considerable period of time devoted to EIT application and validation in patients in much more detail.

The final assessment of the particularly promising indications of EIT and their establishment in routine clinical work will result from the experience of a critical but constructive community of future EIT users.

by Prof. Gerhard Hellige

D-61-2011

Prof. G. Hellige, born in 1943 in Berlin, Germany, was until his retirement in 2008 Head of the Department of Anaesthesiological Research at the Centre of Anaesthesiology and Vice Dean of the Medical Faculty at the University in Göttingen.

He was the leader of multiple research projects on experimental and clinical validation of EIT and Member Resp. Head of several executive boards, e.g. the Cardiolab module of the International Space Station ISS and the Committee on Measuring Technology in Medicine at the German Ministry of Research and Technology.

2. Introduction

Acute Lung Injury (ALI) is a very common complication in intensive care. It has been shown that mechanical ventilation with ventilator settings which do not suit the individual requirements of the diseased lung can lead to injury of the cellular structures of the lung tissue. As a result, vascular and alveolar permeability increases and interstitial edema formation occurs. Due to the increased weight of the lung, alveolar collapse may predominantly occur in the dependent lung regions, resulting in even more severe arterial hypoxemia [1].

Lung protective ventilation may not only prevent mechanical pulmonary injury but may also reduce the risk of inducing the systemic release of cytokines, which is associated with the development of multi-organ failure [2, 3, 4]. Thus, over the past decades, clinicians have been searching for strategies to optimise alveolar recruitment, maintain an open lung and limit pulmonary overdistension.

However, finding optimal PEEP (Positive End-Expiratory Pressure) and tidal volume settings for the individual patient remains a constant challenge in clinical practice [5, 6].

For more than 30 years, clinicians have been examining various approaches and monitoring devices to guide ventilation management. As the lung of an ALI patient has heterogeneous properties, global parameters reflecting the condition of the lung as a whole have proved to be insufficient to adequately guide lung protective ventilation [7, 8].

CT (Computed Tomography) imaging reveals the underlying problem of treating patients based on global parameters alone. Fig. 1 schematically shows a slice of the lung of an ALI patient with non-aerated, poorly aerated,

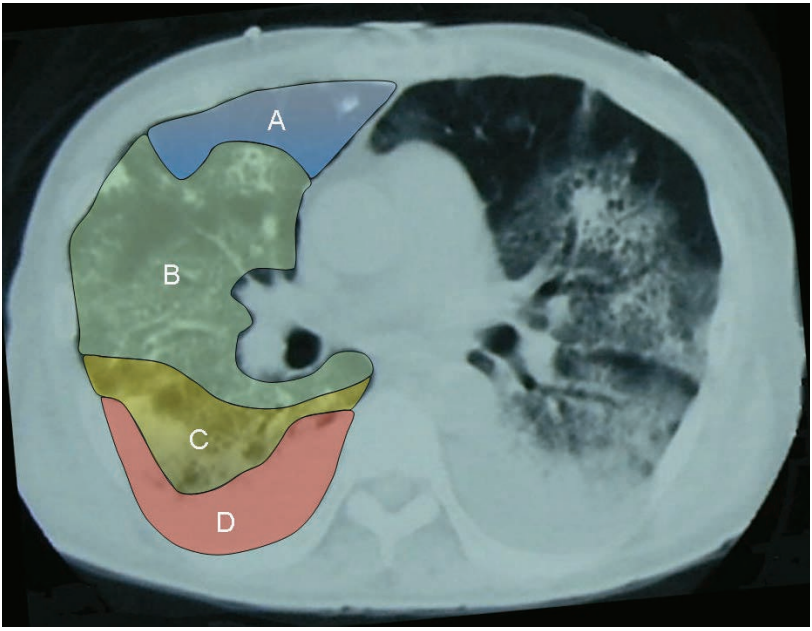

D-3428-2011

Fig. 1: CT image showing hyperinflated (A), normally aerated (B), poorly aerated (C) and non-aerated (D) lung regions

normally aerated and hyperinflated lung regions. In order to achieve a more homogeneous distribution of tidal volume and to keep the lung as open as possible, it has been suggested that therapy settings should be made based on regional information of pulmonary status [9, 10, 11].

Although CT provides detailed regional information about the lung, it is, for obvious reasons, not suited for continuous regional lung monitoring at the bedside and thus cannot be used to guide the routine adjustment of ventilator settings.

Electrical Impedance Tomography (EIT) has emerged as a new modality

for non-invasive, radiation-free monitoring of regional lung function. With the Dräger PulmoVista 500, this unique tool is now available as a mature, clinically usable product for the very first time.

Being complementary to well-established radiological techniques and conventional pulmonary monitoring, EIT can be used to continuously visualise the lung function at the bedside and to instantly assess the effects of therapeutic manoeuvres on regional ventilation distribution.

The purpose of this booklet is to provide an overview of the technological aspects and clinical application of EIT, the appearance of EIT images, the parameters that can be derived and the clinical situations where EIT can be used.

It was written for the clinician who wants to gain a good understanding of EIT, but this booklet may also serve as a valuable source of information for scientists and engineers.

As with every new modality, EIT and its clinical application will evolve over time. If this booklet contributes to our understanding of this new approach to lung function monitoring, thereby accelerating this evolution, then its mission will have been accomplished.

3. The history of EIT

D-60-2011

Fig. 2: GOE MF II system

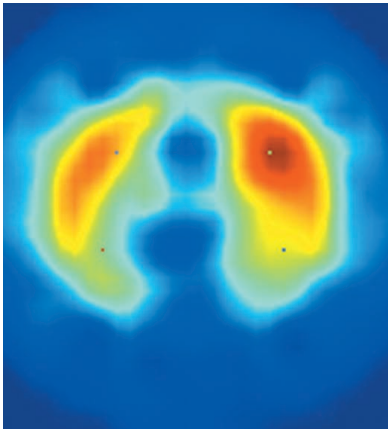

D-62-2011

Fig. 3: First EIT image from 2001 taken at Draeger using the GOE MF II

Ever since the first EIT device (Sheffield Mark I) was developed by Barber and Brown in the early 1980s, EIT has received increasing attention within the scientific community. By the mid-1990s more than 30 research groups were actively engaged in EIT-related research. The first available EIT devices, although technologically limited, have been applied exemplarily in various scientific fields, including the monitoring of gastric emptying, regional lung monitoring, lung perfusion, cardiac function, neurological function, quantification of lung water and breast cancer screening.

By the mid-1990s the EIT Group in Göttingen, represented by G. Hellige and G. Hahn, had developed a predominantly digital EIT prototype (GOE MF II, Fig. 2), which was a further development step beyond the Sheffield Mark I system. It was the world's first EIT system suited for and systematically

BOOKS ABOUT EIT

In 1993, Holder published a book about clinical and physiological applications of EIT which summarised the results of the first conference entirely dedicated to EIT (held in 1992 at the Royal Society in London) [12].

All the studies that Holder presented in his book were performed with the Sheffield Mark I or its derivatives.

In 2004, Holder published a second EIT book in which the state of reconstruction algorithms and hardware developments were described [13].

Additionally, he presented and discussed the experimental use of EIT in specific clinical fields in great detail.

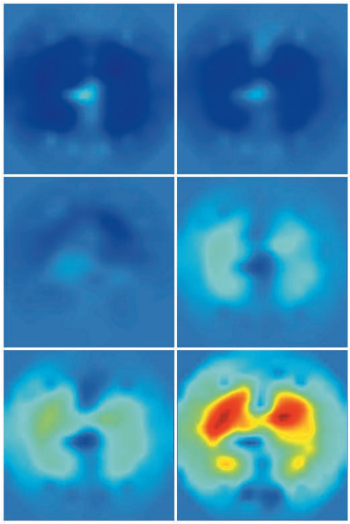

D-64-2011

Fig. 4: Early ventilation images made with the GOE MF II

used in experimental validation studies in animals, physiological studies in volunteers and clinical research. The GOE MF II was specifically designed for the assessment of tidal volume distribution and it was mainly used to evaluate the capability of EIT to monitor regional lung function.

In 2001 the EIT-Group Göttingen and Dräger initiated a scientific exchange of experience in the field of EIT with the mutual objective of improving the technology, design, and software in such a way as to facilitate the use of EIT lung function monitors, not only in experimental research but also in daily clinical practice. Initial measurements on volunteers and subsequent reconstruction of functional EIT images were conducted at Dräger in 2001 (Fig. 3 and 4).

During the initial phase of this cooperative effort, the first major task was to understand why, despite a history of more than 20 years at that time,

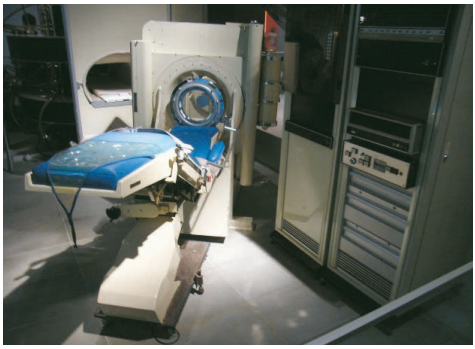

Fig. 5: A historic CT Scanner of EMI

D-59-2011

HISTORY OF CT

By way of comparison, Computed Tomography (CT) was invented by G. N. Hounsfield in 1967, a British engineer who worked for EMI (the record label which marketed the Beatles records). The first prototype (Fig. 5), dedicated to imaging the brain and completed in 1971, had a resolution of 80 × 80 pixels. The first commercial CT system (SIRETOM) developed by Siemens was launched in 1974. In the following years CT rapidly emerged as a well-established diagnostic modality all over the world. So, the history of computed tomography appears to be only about 10 years older than that of EIT.

Up until the introduction of Dräger PulmoVista® 500, the use of EIT for regional lung function monitoring has been limited to a growing, but still small, number of experts and research groups. These groups continue to investigate EIT technology within the context of various scientific studies. However, from today's perspective, it seems that the "path to the Holy Grail" [14] has been much longer than had been initially expected.

EIT had still not found a place in clinical practice, even though the results of all experimental studies had suggested the tremendous potential clinical benefits of EIT when used for regional lung monitoring.

It quickly became obvious that the failure to adopt EIT as a viable clinical tool was closely related to the experience of those who had tried to use it in the clinical setting. EIT devices of that time still were not sufficiently adapted to the "real world" requirements for use in ICUs. This was mainly due to specific limitations in the design of those EIT devices:

D-63-2011

Fig. 6: Application of ECG electrodes in order to perform EIT measurements on an intensive care patient

– Intra-thoracic bioelectric properties are only very slightly changed by ventilation. At the body surface, this may result in voltage changes of less than 100μV. In 2001, the most crucial components of EIT devices had only been developed to a point where they could reliably be used in animal trials and healthy humans but not in all intensive care patients. Yet, patients with e.g. lung edema where EIT measurements can be challenging are precisely those who would be likely to benefit the most from EIT monitoring.

– In previous EIT systems, sixteen single ECG electrodes had to be attached around the patient's thorax and each electrode connected to the corresponding cable (Fig. 6). This resulted in preparation times of at least 20 min. [15] before EIT measurements could be started. It was apparent that the everyday clinical use required an improved method of electrode application.

– Various EIT software tools had been developed to address scientific questions and identify relevant parameters – but all tools were designed for off-line use and thus did not allow clinicians to perform on-line data interpretation, i.e. directly at the bedside.

EIT EVALUATION KIT 2

In 2006 Dräger had finalised the development of a limited series of EIT prototypes (EIT Evaluation Kit 2, Fig. 8). Its design addressed various aspects of the identified obstacles related to data acquisition and clinical usability.

– The electronics for the data acquisition and also the patient cables were completely redesigned to achieve reliable measurements with sufficient signal quality even in those patients with wet lungs and small tidal volumes, where previous EIT systems failed.

– An EIT electrode belt (Fig. 7) was developed which made electrode application and maintenance much easier. Also, the surface of the electrodes became larger and thus stability of the skin-electrode contact improved so EIT measurements were much more reliable and feasible for longer time periods.

– Additionally, the Dräger MonoLead™ cables that had already been successfully introduced by Dräger for ECG measurements were adapted for use with the newly developed electrode belt. This meant that the cables could be attached to the belt before it was applied to the patient. As with the belt the cable also contributed to a significant improvement of signal quality compared to previously used single lead cables.

– The experience Dräger has in software and user interface design was utilised in the development of software for the EIT Evaluation Kit 2. In contrast to previous EIT systems, the EIT Evaluation Kit 2 made the continuous display of EIT images and waveforms possible. The user interface was designed according to principles of the graphical user interfaces of the latest Dräger medical devices at that time.

D-71-2011

Fig. 7: Electrode belt of the EIT Evaluation Kit 2 attached to an intensive care patient after abdominal surgery

D-47-2011

Fig. 8: EIT Evaluation Kit 2

The EIT Evaluation Kit 2 was limited to use within clinical studies in order to answer the most important question: Could EIT emerge as a tool for routine clinical practice or would its previous limitations cause it to remain a research tool?

In an early evaluation, EIT measurements were performed at 11 hospitals around the world. Results from 183 patients mainly suffering from ALI / ARDS were analysed. After each EIT measurement clinicians wrote a report which addressed the general usability of the device.

Also, analysis of the collected EIT data revealed, from a technical point of view, that EIT measurements were successfully performed on all patients.

4. The principles of EIT as applied by Dräger PulmoVista® 500

DYNAMIC DETERMINATION OF REGIONAL BIOELECTRICAL PROPERTIES WITHIN THE THORAX

PulmoVista 500 (Fig. 9) is designed as a lung function monitor for clinical use which continuously generates cross-sectional images of the lung function by applying the technique of electrical impedance tomography (EIT).

To perform bioimpedance measurements, an electrode belt containing 16 electrodes is placed around the chest wall. Additionally, one reference electrode must be attached to a central point on the body (Fig. 10), preferably on the abdomen. The reference electrode ensures that all measurements at different electrode pairs are referenced to the same electric potential.

MEASUREMENT PRINCIPLES

D-101-2010

Fig. 9: Dräger PulmoVista® 500

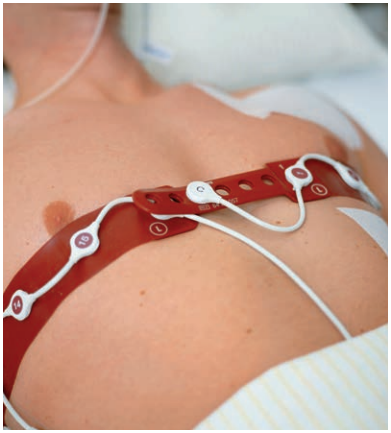

D-28332-2009

Fig. 10: Electrode belt with patient cable connected

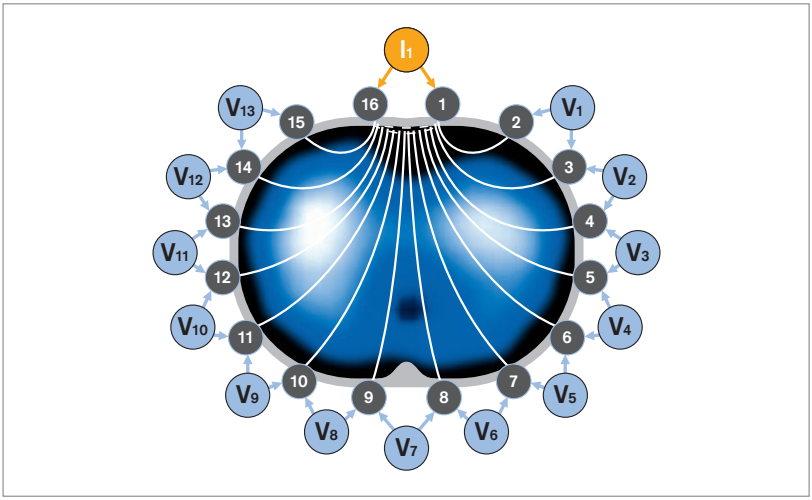

D-3420-2011

Fig. 11: Current application and voltage measurements around the thorax

PulmoVista 500 determines the distribution of intra-thoracic bioimpedance by applying a known alternating current “I1” to a first pair of electrodes and measuring the resulting surface potentials “Vn” at the remaining 13 electrode pairs (Fig. 11). Applying Ohm’s law, the bioelectrical impedance between the injecting and the measuring electrode pairs is determined from the known applied current and the measured voltages. Subsequently, the adjacent electrode pair is used for the next current application and another 13 voltage measurements are performed. The location of the injecting and measuring electrode pairs successively rotates around the entire thorax. One complete rotation creates voltage profiles at 16 electrode positions, each consisting of 13 voltage measurements (Fig. 13). The resulting 208 values, also called a frame, are used to reconstruct one cross-sectional EIT image.

Please see Appendix II for more details about bioimpedance measurements.

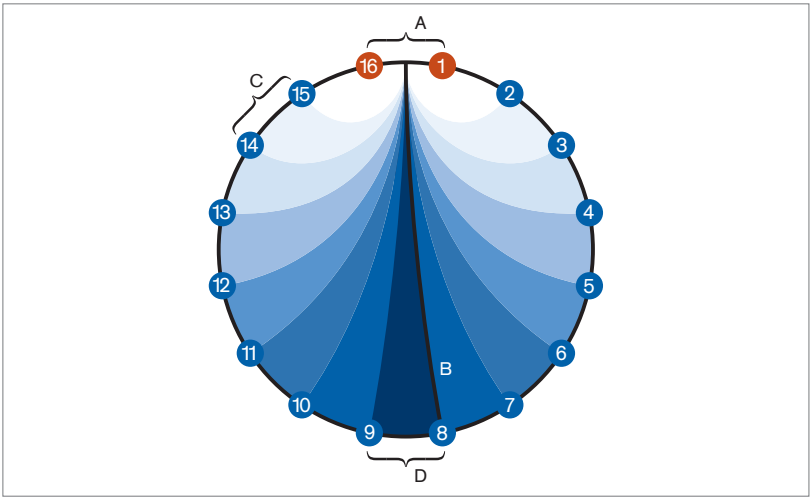

D-82-2011

Fig. 12: Distribution of isopotential lines inside the subject. The voltages (C) next to the current application are the highest, as indicated by the white colour. The voltage (D) on the side opposite the current application is the lowest, indicated by the dark blue colour

IMAGE RECONSTRUCTION

A current application (A) at the surface of a subject with homogenous bioelectric properties causes a reproducible distribution of potentials inside the subject (Fig. 12). The regions in the thorax with the same electrical potential, as a result of current application, are called isopotential lines (B). The distribution of isopotential lines contributes to a predictable voltage profile on the surface of the body.

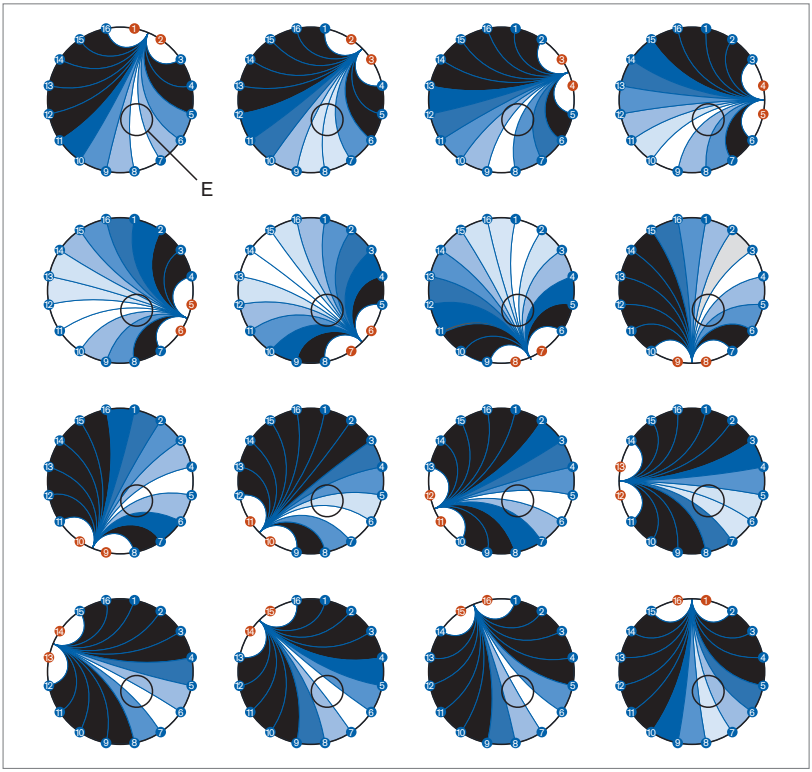

D-83-2011

Fig. 13: Profiles of voltage deviations in the presence of a regional increase of impedance. In this figure, white and light blue colours represent deviations of the voltage distribution in an inhomogeneous medium. Voltages without deviation are indicated by the black colour

A regional increase of impedance (E) of the subject results in a change in each of the 16 voltage profiles which make up one frame. Regardless of where the current is applied, the regional increase of impedance always causes an increase of the voltages “behind” the region of increased impedance.

Originally the Sheffield Back-Projection reconstruction algorithm, described by Barber and Brown [16] and drawing on principles similar to those used for computed tomography, was developed to compile the recorded voltage profiles into cross-sectional images.

The reconstruction algorithm superposes the 16 voltage profiles on each other (Fig. 14). Reconstruction artifacts are eliminated by applying selective boundary filtering. The resulting image (Fig. 15) displays the region of increased impedance (E) at the correct location.

As with CT scans, the projection of the displayed EIT images is from caudal to cranial. This means that the left side of the image displays the right side of the patient. The upper part of the image displays the ventral aspect of the patient.

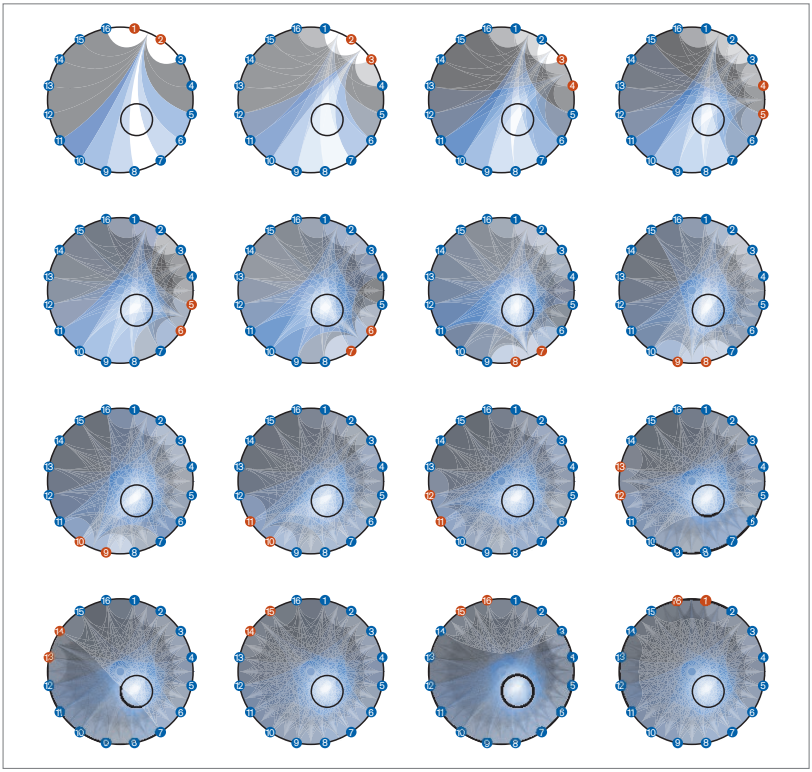

D-3417-2011

Fig. 14: Successive superposition of the 16 voltage profiles

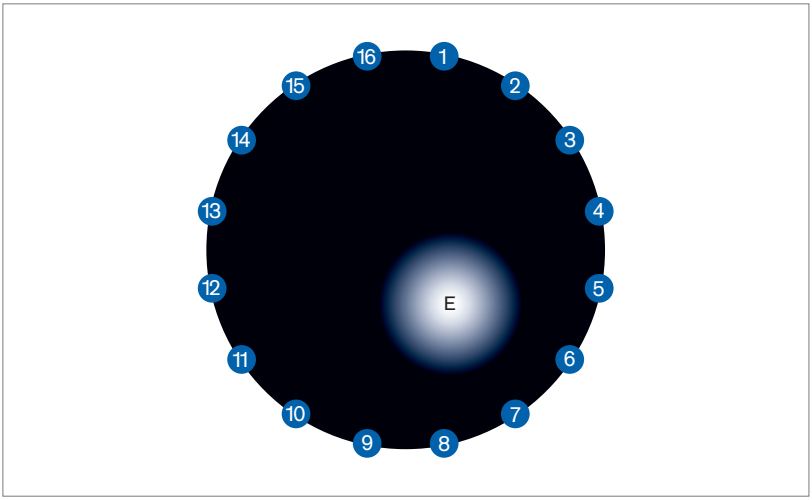

D-3418-2011

Fig. 15: Resulting image after selective boundary filtering

However, as described by Yorkey et al. [17], the Sheffield Back-Projection reconstruction algorithm carries some inherent limitations, such as a geometry fixed to round shaped subjects, no means to suppress corrupt data and no flexibility regarding the sequence of current injections and voltage measurements. It has since been demonstrated that iterative approximation methods, such as the Newton-Raphson algorithms, deliver better results.

For these reasons, PulmoVista 500 uses a Finite Element Method (FEM) based linearised Newton-Raphson reconstruction algorithm to convert the 208 voltages of a frame into an ellipsoid EIT image.

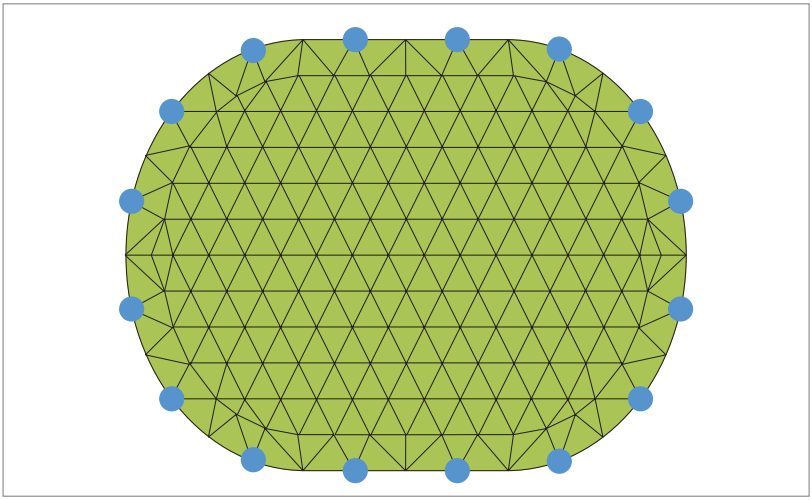

D-3419-2011

Fig. 16: 2D mesh with 340 finite elements for 16 surface electrodes

This method divides the electrode plane into 340 triangular elements, where each element is assigned homogeneous and isotropic bioelectrical properties (Fig. 16).

This method allows the calculation of the resulting surface voltages at the boundary nodes of the model, for any arbitrary distribution of impedance values within this mesh, which is the numerical solution of the so-called „forward problem“.

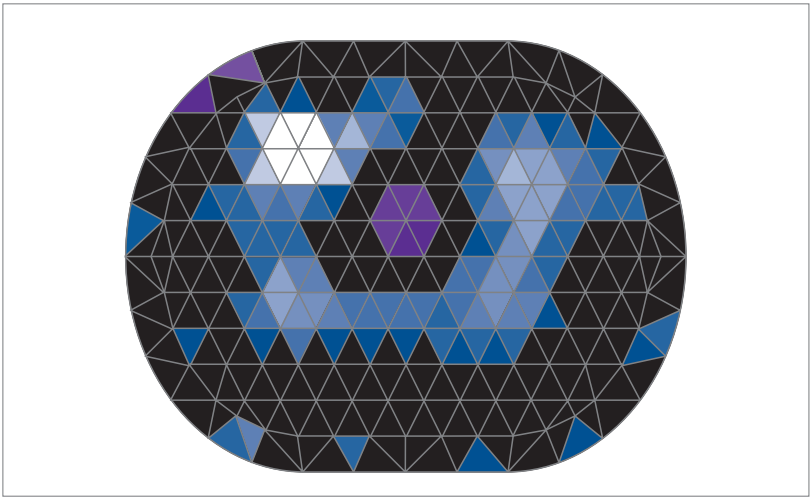

D-3421-2011

Fig. 17: FEM based reconstruction of regional bioimpedance distribution based on 208 measured surface voltages

For reconstruction of EIT images however, the approach is reversed: after the voltages at the body surface have been measured, their relative changes are fed into the Newton-Raphson reconstruction algorithm by multiplying them with a sensitivity matrix. This matrix has been optimized over the last several years by taking into account real EIT data from several hundred patients.

This algorithm assigns a relative impedance change to each individual finite element to achieve a best match for the numerical solution of this so-called „inverse problem“ of the FEM to the actual voltage profile (Fig. 17).

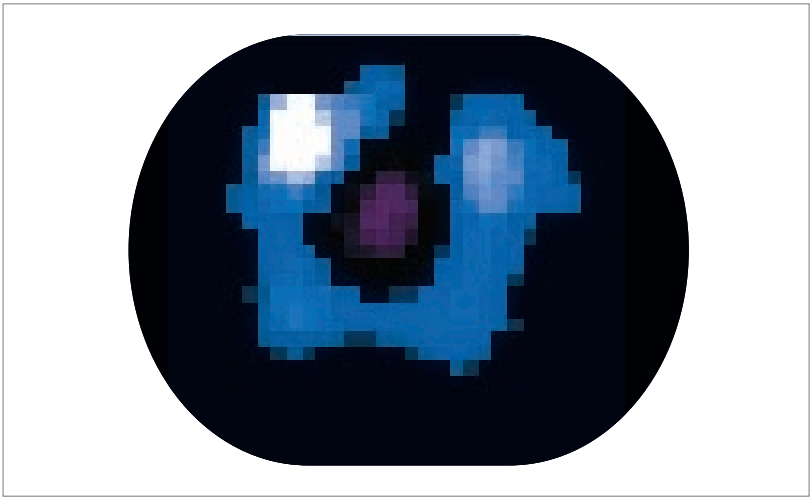

D-3423-2011

Fig. 18: Co-registration and damping of boundary artifacts

Following image reconstruction, the triangular structure is converted into a rectangular pattern (“co-registration”) for further image processing (Fig. 18). Also, damping of boundary artifacts is applied.

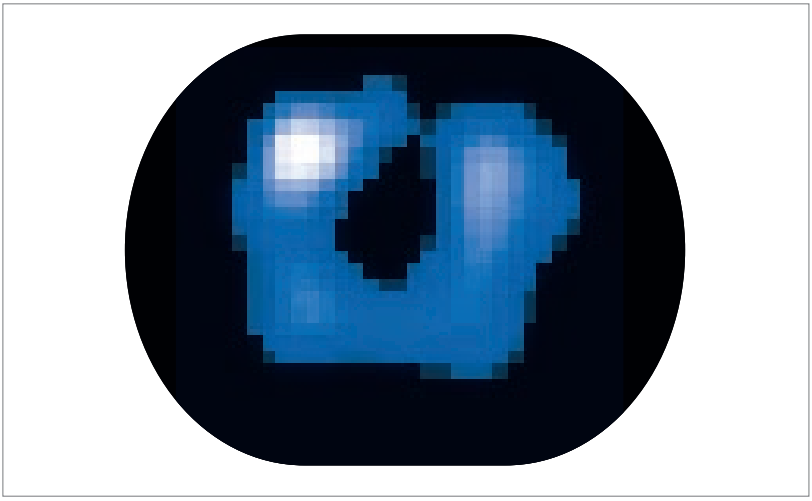

D-3424-2011

Fig. 19: Smoothing by applying Gaussian filtering

In the next step, a Gaussian filter is used to smooth the image (Fig. 19). Gaussian filtering is widely used in graphics software, typically to reduce image noise and details. The visual effect of this technique is that of a smooth blur, which resembles viewing the image through a translucent screen. Gaussian smoothing is also widely used as a pre-processing stage in computer vision algorithms in order to enhance image structures at different scales.

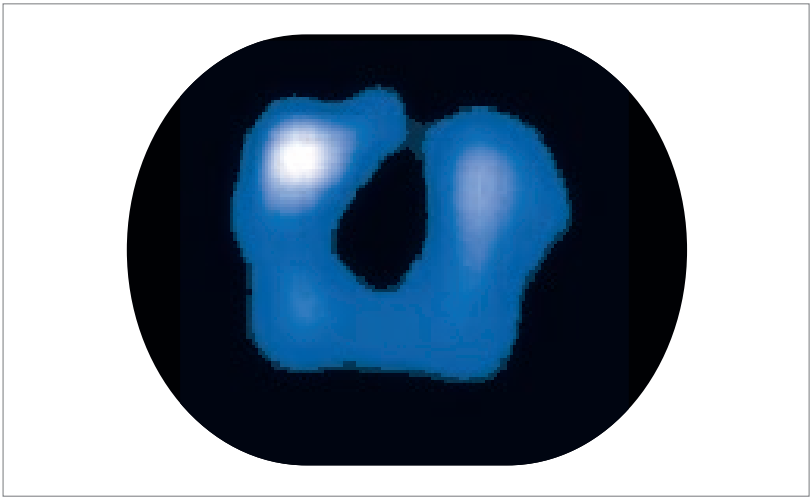

D-3425-2011

Fig. 20: Bilinear filtering

Each EIT image consists of a matrix of 32 × 32 pixels. In order to create larger images for better graphical representation and interpretability, bilinear interpolation allows to increase the virtual resolution of the EIT images to a matrix of any size, as EIT images in a larger format enable better separation of the displayed structures by the viewer (Fig. 20). However, the underlying resolution of the images remains unchanged.

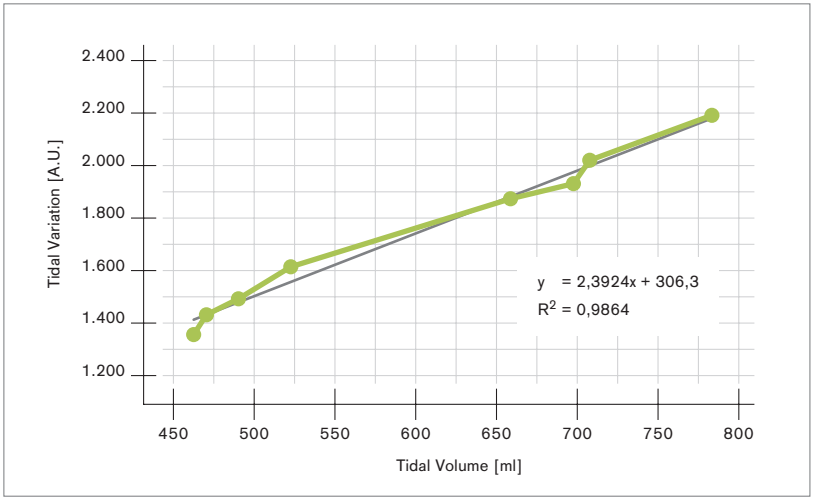

Fig. 21: Correlation of tidal volumes and tidal variations, i.e. ventilation related impedance changes, in a patient with aortic valve replacement after a PEEP reduction from 17 down to 10 cm H_2O

BIOELECTRICAL PROPERTIES OF LUNG TISSUE

As discussed in detail in Appendix II, it is well known that the impedance of lung tissue varies with the air content. Thus ventilation and changes of end-expiratory lung volume that occur within the EIT sensitivity region result in changes of the voltages measured at the body surface. The correlation between Tidal (Impedance) Variations and Tidal Volumes is typically high (Fig. 21) and has been assessed in various validation studies (see chapter 8).

In humans, an inspiration manoeuvre from residual volume to total lung capacity amplifies regional bioimpedance by around 300 % [18, 19]. Cardiac activity and perfusion cause a change in thoracic bioimpedance, from diastole to systole, in the range of 3 % [20].

Extravascular lung water, body movement and the skin-electrode resistance may also have various effects on thoracic bioimpedance.

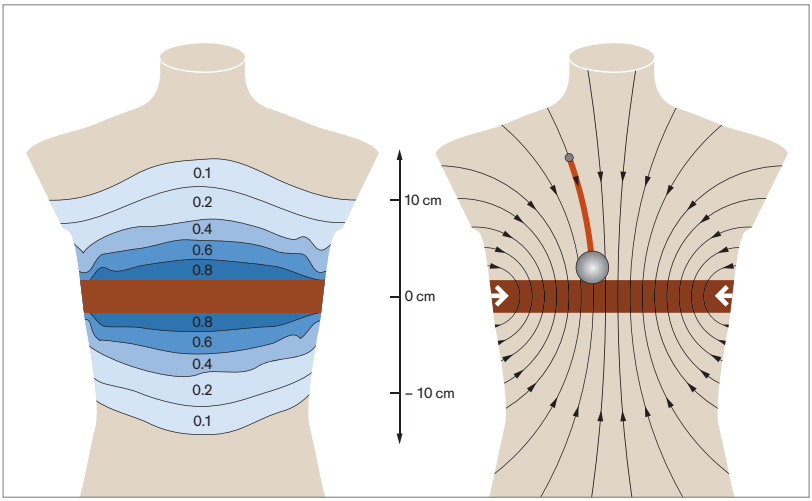

Fig. 22: Left: Contribution of impedance with increasing distance from the cross-section, that is defined by the position of the electrode belt
Fig. 22: Right: Projection lines of impedance changes within the body; impedance changes are moved towards the central region with increasing distance from the transversal plane

THE EIT SENSITIVITY REGION

In the context of EIT, the term “EIT sensitivity region” describes the lens-shaped intra-thoracic volume whose impedance changes contribute to the generation of EIT images.

The actual thickness and the shape of this EIT sensitivity region depend on the dimensions, the bioelectric properties and the shape of the thorax, and particularly on the morphological structures inside of it. Furthermore, the degree of homogeneity of trans-thoracic bioelectric properties also has an effect on the dimension of this EIT sensitivity region.

The electrode belt used with PulmoVista 500 uses electrodes which are 40 mm wide. Hence, close to the body surface the EIT sensitivity region is at least 40 mm thick. The thickness of the sensitivity region increases towards the central region of the body. The contribution of impedance changes is reduced with increasing distance from the cross-sectional plane (Fig. 22 left). Increasing distance from the cross-sectional plane moves the position of impedance changes close to the body surface, towards the central region along the depicted projection lines (Fig. 22 right). However, as the contribution of impedance changes is reduced with increasing distance from the cross-sectional plane, the effect on the image is limited.

FUNCTIONAL EIT

PulmoVista 500 performs functional EIT, meaning that it mainly displays relative impedance changes as a result of lung function, i.e., ventilation and changing end-expiratory lung volume. If the signals are not filtered, cardiac related impedance changes are also displayed. Factors affecting the absolute impedance are eliminated by only displaying relative impedance changes, rather than absolute impedance values.

Thus, the Dynamic Images generated by PulmoVista 500 contain information on the functional condition of different lung regions within the EIT sensitivity region.

5. Clinical information derived from Dräger PulmoVista® 500

D-87-2010

Fig. 23: Dräger PulmoVista® 500 in a clinical setting

PulmoVista 500 (Fig. 23) is the first EIT system of its kind which continuously provides graphical information about the regional distribution of ventilation and changes of end-expiratory lung volume. The temporal resolution of this information is high and can even be presented as trend data. While this opens up a number of new approaches to observing specific conditions of different lung regions, it generally also carries the risk that the information provided by EIT devices may be too complex to be used by clinicians who have limited experience in this field.

With reference to EIT measurements it is important to remember the terms “distribution of ventilation” or “lung volume changes” refer to physiological processes inside the previously described EIT sensitivity region, i.e. the

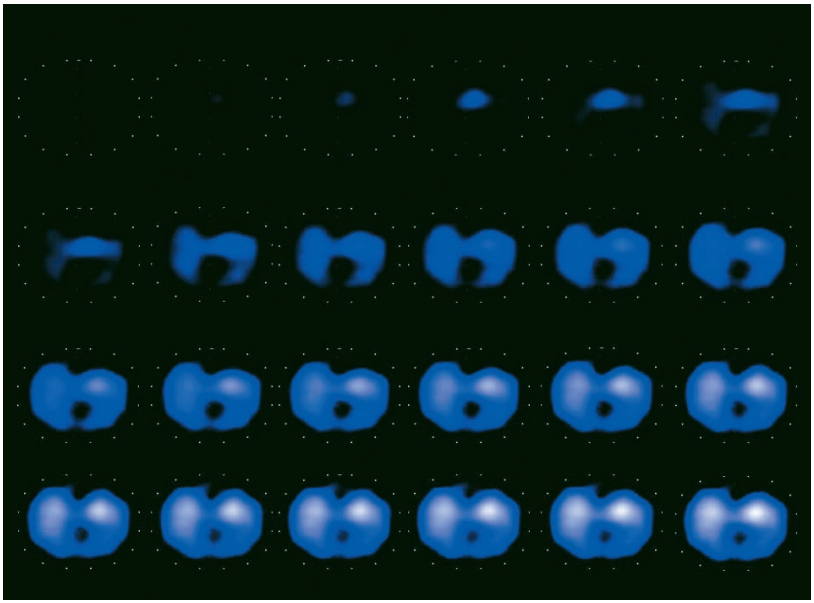

D-46-2011

Fig. 24: Series of dynamic images representing air filling during inspiration

lens-shaped intra-thoracic volume. PulmoVista 500 captures a relatively thick slice of the lung which might represent about 20 % to 30 % of the entire lung.

5.1 SCREEN ELEMENTS DISPLAYED BY PULMOVISTA 500

DYNAMIC IMAGE

The Dynamic Image continuously displays relative impedance changes within the EIT sensitivity region as a movie which represents the dynamics of ventilation (Fig. 24). PulmoVista 500 can generate up to 50 EIT images per second. This high temporal resolution facilitates the visualisation of regional ventilation even at higher respiratory rates. For example, when

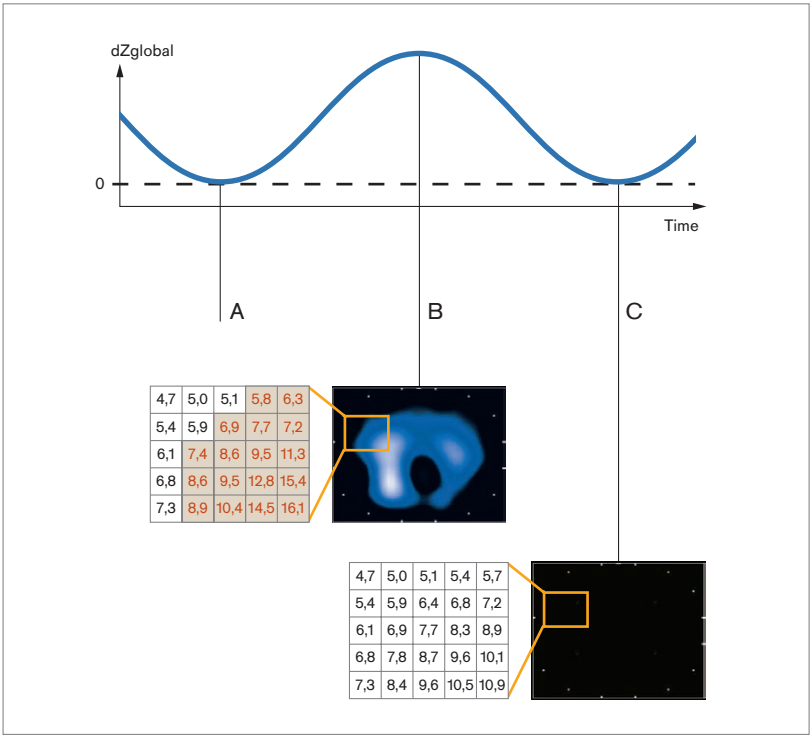

Fig. 25: Generation of EIT images

PulmoVista 500 uses a frame rate of 20 images per second and the respiratory rate is 30 breaths per minute, 40 EIT images per breath will be generated.

Each EIT image is determined by referencing the current frame (B), i.e. the set of 208 voltages, to a baseline frame (A) which represents the end of expiration of the last detected breath (Fig. 25). This results in a frame of relative voltage deviations which then is used for the image reconstruction.

This means that, regardless of the actual values of the baseline frame (which also reflect a certain distribution of absolute impedance), only regional differences between the current frame and the baseline frame are displayed.

If the end-expiratory impedance distribution of the next breath is identical to the former one, the next end-expiratory image (C) is black. As the baseline frame is continuously updated following each detected breath, mainly impedance changes due to tidal ventilation are displayed. Due to this baseline definition, waveform offsets caused by changes in end-expiratory lung impedance are not displayed in the Dynamic Image.

This behaviour is somewhat comparable to the volume waveform of a ventilator, which is calculated from the flow waveform and requires calibration to zero after each detected breath. In the ventilator, the volume waveform is zeroed because the external flow sensor cannot distinguish between differences between inspiratory and expiratory volumes either due to air leaks or those caused by changes in end-expiratory lung volume.

STATUS IMAGES

Further analysis of the lung regions, e.g. comparative evaluation at different times or quantification of regional ventilation distribution, can be achieved using status images. With PulmoVista 500, the status image can be configured as either a Tidal Image, or as a Minute Image.

The Tidal Image is a differential image of the end of inspiration compared to the beginning of inspiration which represents the regional distribution of ventilation of the last detected breath. The Tidal Image is automatically updated after each breath.

The Minute Image represents regional impedance distribution changes as averaged Tidal Images over the last minute. The Minute Images are ideal for the assessment of regional distribution during ventilation with varying tidal volumes.

REGIONS OF INTEREST

A region of interest (ROI) is a user-defined area within a status image. The image can be divided into 4 ROIs and arranged either horizontally, as quadrants or in a customised way (Fig. 26, 27, 28). The area covered by each ROI is represented by the corresponding regional impedance waveform and the regional numeric value.

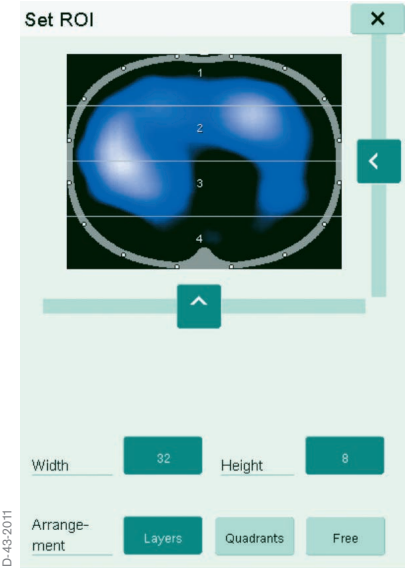

Fig. 26: An arrangement as “Layers” allows assessing the effects of gravity and thus the different properties of dependent and non-dependent lung regions

This arrangement helps to assess the effects of e.g. PEEP changes, recruitment manoeuvres and to monitor any pathology which equally affects both sides of the lungs

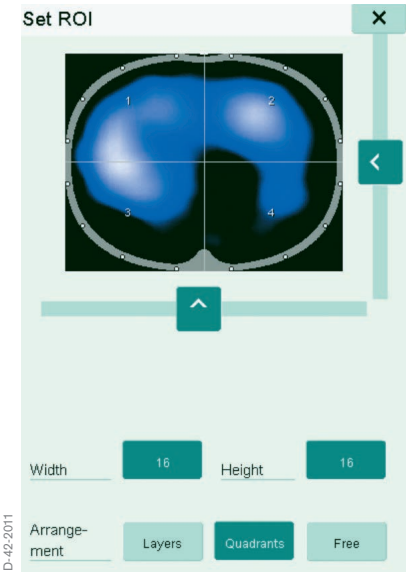

Fig. 27: An arrangement as “Quadrants” allows assessing regional characteristics of the upper and lower left lung vs. the upper and lower right lung

This arrangement helps to assess the effects of e.g. lateral positioning, lung suction, pleural drainages and to monitor any pathology which affects both sides of the lungs differently

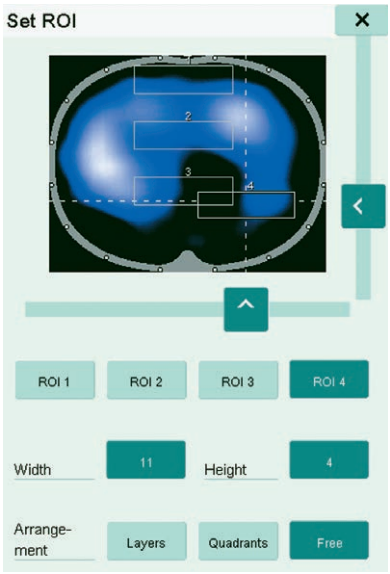

Fig. 28: An arrangement in the “Free” mode allows assessing status images pixel by pixel and comparison of non-adjacent lung regions

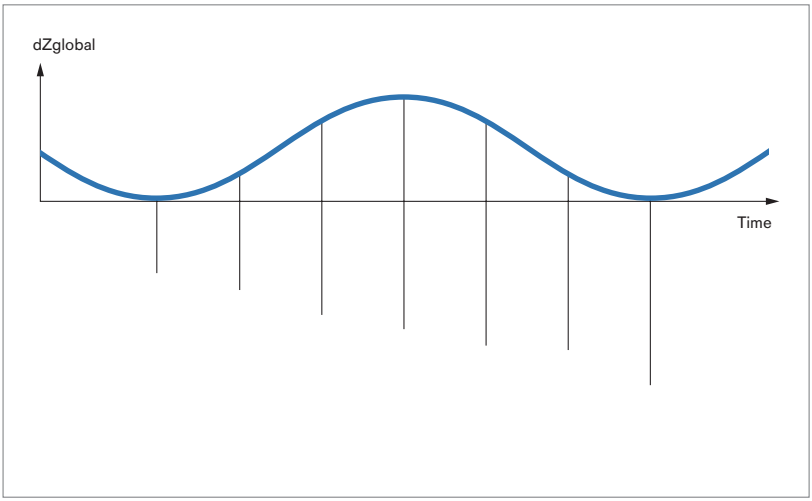

D-76-2011

Fig. 29: Generation of the global impedance waveform

IMPEDANCE WAVEFORMS

The status images present the ventilatory status in a somewhat compressed fashion. The temporal behaviour of the lung regions cannot be assessed just by interpreting those images.

In contrast, the impedance waveforms represent the impedance changes within the EIT sensitivity region over time (Fig. 29). All displayed impedance waveforms, i.e. one global and four regional waveforms, are plotted simultaneously over the same time base. The impedance waveforms can be assessed in a manner similar to the assessment of waveforms on the ventilator.

The global impedance waveform represents the sum of relative impedance changes in all pixels of each Dynamic Image plotted over time.

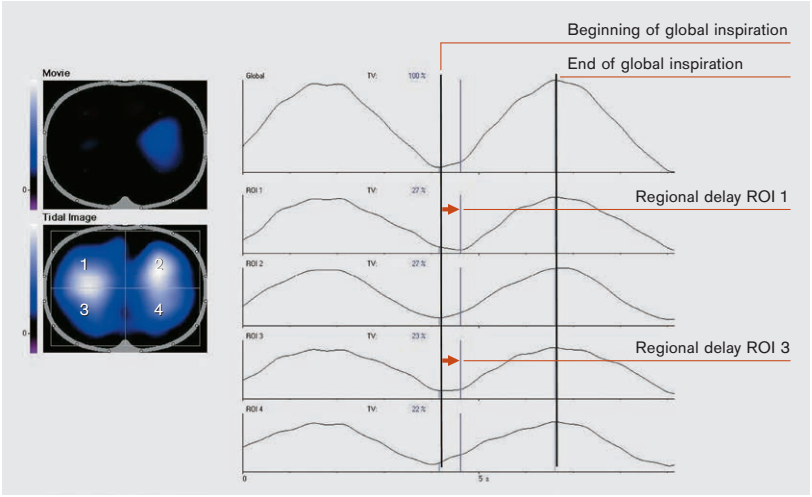

Fig. 30: Impedance waveforms from an individual with delayed air filling in the right lung (ROIs 1 and 3). The dynamics during inspiration in the lung regions can only be seen in the waveforms, and not in the Tidal Image

The global impedance curve primarily displays impedance changes related to ventilation. There is usually a strong correlation between this curve and the volume curve displayed by the ventilator.

In contrast to the global impedance curve, the four regional impedance curves display the sum of impedance changes within the specified ROI over time. The regional impedance curves allow comparison of impedance changes in different lung regions with respect to this temporal behaviour.

In patients with inhomogeneous pulmonary conditions, the shape and potential phase lags of impedance waveforms provide information about regions with delayed air filling (Fig. 30). Also, changes of regional conditions can be analysed in detail over a longer period of time, depending on the selected time scale.

The parameter Tidal Rate, determined from the global impedance curve, typically represents the number of breaths detected per minute.

The parameter TV global (Tidal Variation global) represents the difference between the minimum and maximum value of the global impedance curve for each breath. The TV global is always 100 %, regardless of the tidal volume. It serves solely as a reference for the display of regional tidal variations.

The regional Tidal Variation TV ROIn represents the difference between the minimum and maximum values on the regional impedance curves for each breath, i.e. from end of expiration and the end of inspiration.

End of expiration and inspiration are detected on the global impedance curve and indicated by markers. Regional Tidal Variations show the percentage of impedance change which takes place in the corresponding ROI.

Fig. 31: Numeric values of Dräger PulmoVista® 500

D-3429-2011

NUMERIC VALUES

Numeric values are continuously calculated and displayed so that quantification and comparison of regional impedance changes at different times is possible. PulmoVista 500 uses a very straightforward method to express distribution of ventilation within the EIT sensitivity region – it simply expresses the distribution as regional proportions (Fig. 31).

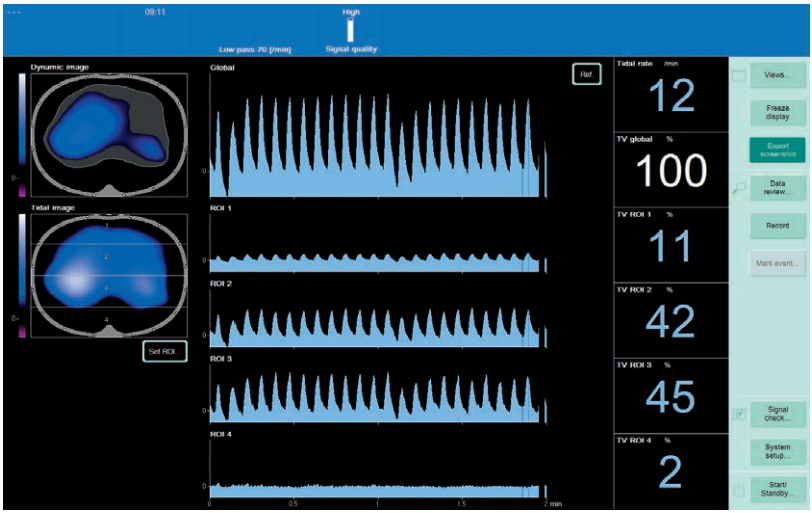

D-7513-2014

Fig. 32: Screenshot of “Main” view

5.2 MAIN VIEW

The “Main” view (Fig. 32) is the usual monitoring screen and displays the following: A “Dynamic Image”, showing impedance changes over time, a “Status Image”, a global impedance waveform at the top, and below this, four regional impedance waveforms, representing relative impedance changes of the Regions Of Interest (ROI) defined in the “Status Image”. On the right side of this screen, parameter fields are arranged which contain the numeric values described.

Based on the feedback provided by more than 30 clinical users of EIT over several years, it had become increasingly obvious that the best way to present EIT data is to combine EIT status images (containing regional information), impedance curves (containing regional and temporal information) and derived numerical parameters (allowing quantitative assessment). Consequently, the “Main” view of the PulmoVista 500 provides EIT data in a graphical layout similar to that which clinicians know from patient monitors.

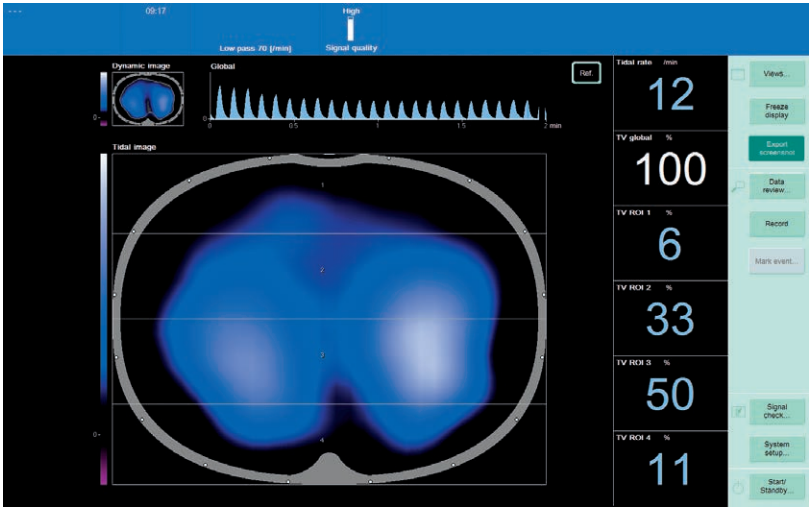

Fig. 33: Full Screen Image view

5.3 FULL SCREEN IMAGE VIEW

The view “Full Screen Image” (Fig. 33) displays contents similar to the “Main” view. However, by providing a large format view of either the Dynamic Image or a status image, it allows users to easily snatch an impression of ventilation distribution from a remote position. Thus this view may be especially helpful during clinical rounds, during training or in other situations when the presentation of EIT images in front of a larger group of people is required.

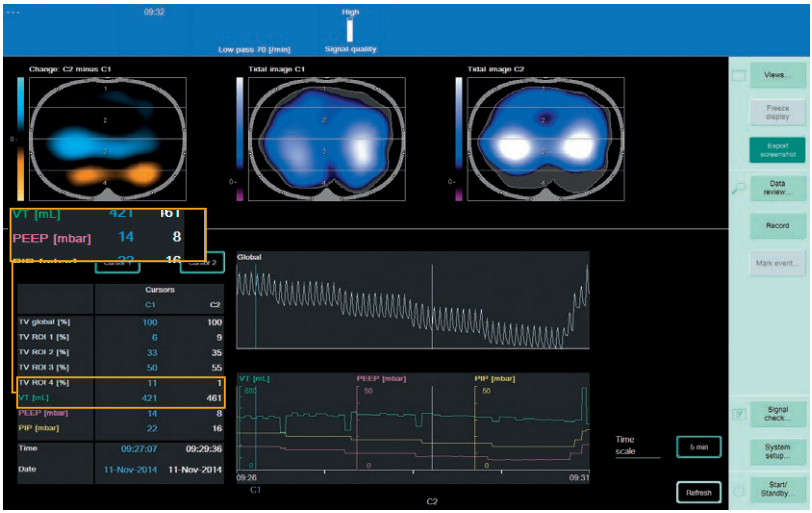

Fig. 34: “End-Inspiratory Trend View”, showing an example of trended distribution of ventilation during a decremental PEEP trial. Comparing PEEP levels of 14 and 8 mbar reveals a massive redistribution of tidal volumes towards ventral regions. This results in a drop of dorsal ventilation from 11% down to 1%, while the global tidal volume even increased from 421 ml to 461 ml

5.4 END-INSPIRATORY TREND VIEW

While a single status image provides an impression of the homogeneity of ventilation and which lung regions may be not ventilated at all, the major clinical use and added value when compared to radiological images comes from the ability of PulmoVista 500 to compare and assess EIT status images before and after therapeutic interventions.

The End-inspiratory trend view (Fig. 34) provided by PulmoVista 500 allows continuous display of two status images generated at different times.

Regional ventilation distribution can thus be reviewed over a time period of up to 120 minutes. Two cursors can be easily navigated through the global impedance curve: an additional image, reflecting the difference between the status images at each cursor position, displays regional changes associated with changed lung conditions or a change of therapy.

If a Dräger Evita family ventilator is connected to PulmoVista 500 via the Medibus interface, ventilation parameters such as e.g. PEEP, which can affect regional distribution, can also be displayed in this view.

5.5 ΔΔEELI TREND VIEW

It is well known that not only ventilation but also changes of the End-Expiratory Lung Volume (EELV) affect the intra-thoracic impedance.

In order to continuously display the impedance changes due to ventilation, all offsets induced by changes of EELV and concurrent changes of End-Expiratory Lung Impedance (ΔEELI) are suppressed in the Main view by referencing all impedance values to a dynamic baseline.

Nevertheless, the ability to continuously display ΔEELI on a regional level provides further information which is potentially as useful as the display of regional ventilation. Continuous information about ΔEELI is especially suited to assess the dynamics of slow recruitment and derecruitment processes within the lungs. Not surprisingly, the early users of EIT devices had consistently asked for a means with which to assess ΔEELI.

Therefore the ΔEELI trend view, dedicated to the display and quantification of global and regional changes in end-expiratory lung impedance over time, has been implemented in PulmoVista 500 (Fig. 35).

The ΔEELI trend displays a differential image “ΔEELI: C2 minus C1”, which represents the difference between end-expiratory images at the two cursor positions C1 and C2.

Up to 120 minutes of global and regional impedance waveforms are displayed, which are referenced to a fixed baseline. Parameter fields display the numerical parameters ΔEELI global and four ΔEELI ROI. The numeric value ΔEELI global displays the deviation of the global end-expiratory status at the cursor positions C1 and C2 in relation to the global tidal variation at C1. The numeric value ΔEELI ROI displays the regional deviations within the respective ROI.

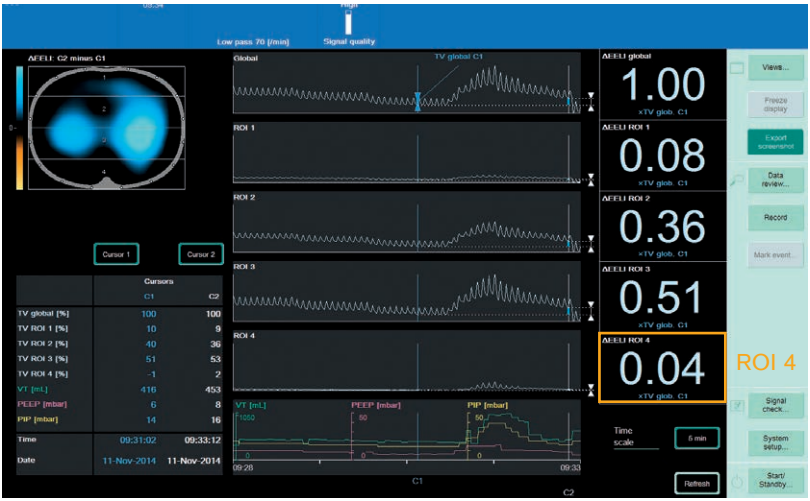

Fig. 35: Trended distribution of ΔEELI, where the status before and after a recruitment manoeuvre is compared. The differential image "ΔEELI: C2 minus C1" reveals an increase of end-expiratory lung volume which was induced by the RM. This increase is equal to the tidal volume, that was present at C1 (416 ml). However, the regional information of ΔEELI ROI 4 also confirms that this RM only led to a minor increase of lung volume (0.04 % of the tidal volume at C1) in the dorsal region

The change in end-expiratory lung impedance ΔEELI at C1 and C2 is expressed as follows:

Zero change (black colour): no difference between values at C1 and C2
Positive changes (turquoise colour): value at C2 is greater than the value at C1
Negative changes (orange colour): value at C2 is less than the value at C1

A positive change in ΔEELI global of 1.00 * TVglobal C1 indicates an increase in end-expiratory lung impedance equal to the global tidal variation (at C1), which in turn is related to the tidal volume, that was present within the EIT sensitivity region at the cursor position C1.

6. Application examples of Dräger PulmoVista® 500

The titration of PEEP after a successful RM is aimed at preventing end-expiratory collapse of depended pulmonary areas. At the same time, the selection of appropriate PEEP levels also plays an important role for achieving homogeneous distribution of tidal volumes and thus lung protective ventilation.

A reasonable approach to determine the “right level of PEEP” requires a comprehensive understanding of the mechanisms establishing alveolar recruitment, the mechanical forces opposing PEEP-induced reopening of atelectatic areas, and the determinants of PEEP-induced lung overinflation and ventilator-induced lung injury (VILI). An important prerequisite for the safe and effective determination of the “right level of PEEP” are clinical tools facilitating the assessment of the effect from therapeutic interventions, for instance, the early detection of overinflation and derecruitment during PEEP trials.

In order to illustrate which role PulmoVista 500 can play in this context, three typical application examples are described below for which data* are used that have been collected from a post-operative patient right after admission to the ICU.

Initially, the patient remained on the ventilator settings according to the hospital’s standard clinical protocol. Then, an RM and a subsequent decremental PEEP trial were performed under pressure controlled ventilation.

After a second RM, PEEP was set according to the highest dynamic compliance (Cdyn) as determined by the ventilator. As Cdyn only started dropping at a PEEP of 6 mbar in this patient, “best” PEEP was set to 8 mbar.

* unpublished data, provided with kind permission by Christiane Grusnick and Hermann Heinze,

Fig. 36: Assessing the patient's response during a RM

UKSH Campus Lübeck, Germany

Ventilator parameters such as Tidal Volume (VT), Compliance (Cdyn), Peak Inspiratory Pressure (PIP) and Positive End-Expiratory Pressure (PEEP) were simultaneously measured by the ventilator and transmitted to and displayed by PulmoVista 500.

6.1 ASSESSING THE PATIENT'S RESPONSE DURING A RECRUITMENT MANOEUVRE

In order to assess the patient's response to the RM, the End-inspiratory trend view of PulmoVista 500 is opened and the first cursor C1 used as a reference. Hence, the Tidal image C1 (mid position) represents the initial ventilation distribution prior to the RM. The second cursor C2 is then set to the position where the RM was performed, represented by the image on the right. (Fig. 36).

This example shows a patient with major increase in dorsal ventilation during the RM, represented by turquoise colour on the differential image Change C2 minus C1 (on the left).

The transient increase of PEEP from 5 to 15 mbar in combination with an increase of peak inspiratory pressure (PIP) from 20 to 39 mbar results in an increase from 2 % to 15 % in Region Of Interest 4 (ROI 4), which represents the ventilation in the dorsal region. Even though this increase in the percentage is partly caused by the decrease of ventral ventilation in the right lung (represented by orange colour), the comparison of the Tidal images C1 and C2 clearly reveals that ROI 4 was not ventilated before but properly ventilated during the RM.

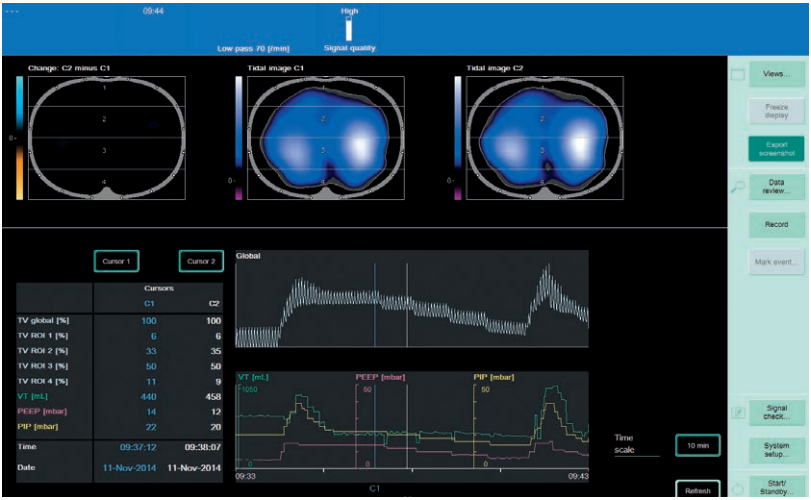

Fig. 37: Identifying the onset of loss of dorsal ventilation (PEEP decrease from 14 to 12 mbar)

6.2 IDENTIFYING THE ONSET OF DERECRUITMENT DURING A DECREMENTAL PEEP TRIAL

In order to monitor potential derecruitment during a decremental PEEP trial, the first cursor C1 again is used as a reference, but now set to the highest PEEP level (14 mbar) after the RM, thus representing the “open lung”. Cursor C2 is set to the next lower PEEP (12 mbar) (Fig. 37).

Even though the decrease of PEEP results in a slight decrease of dorsal ventilation (in ROI 4, from 11 % to 9 %), the Tidal image C2 (on the right) reveals that dorsal ventilation was not significantly reduced by this PEEP reduction.

Consequently, the differential image remains black, indicating that in this patient no significant change of ventilation distribution has occurred when reducing PEEP from 14 to 12 mbar.

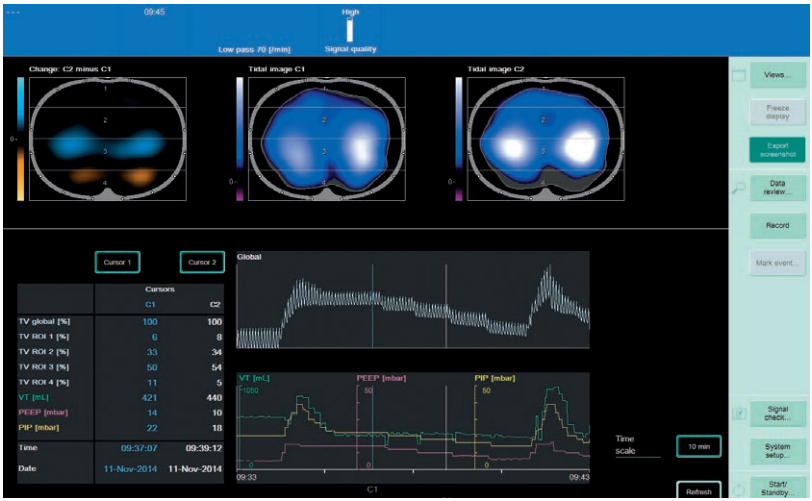

Fig. 38: Identifying the onset of loss of dorsal ventilation (PEEP decrease from 14 to 10 mbar)

However, when comparing PEEP levels of 14 and 10 mbar, a drop in ventilation from 11 % to 5 % can be observed in ROI 4 (Fig. 38). The loss of dorsal ventilation, represented by orange colour, can be interpreted as the onset of derecruitment, which becomes more prominent with further reduction of PEEP.

At a PEEP level of 8 mbar, with 4 % dorsal ventilation in ROI 4, has almost returned to the initial status (2 %).

Interestingly, this derecruitment does not become obvious by monitoring the tidal volume or the dynamic compliance on the ventilator, both of which even slightly increase at a PEEP level of 8 mbar – due to the increase of ventilation in the upper half of the lung, the onset of regional derecruitment is masked in the global information.

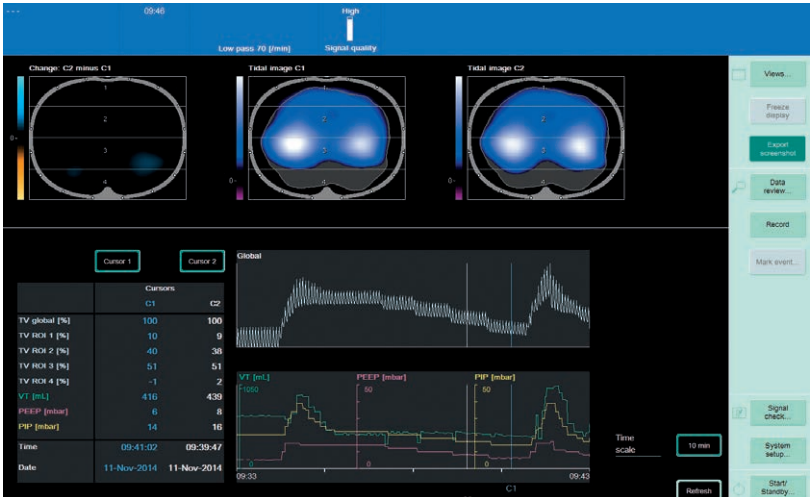

Fig. 39: Estimating the loss of ventral ventilation due to overdistension (PEEP increase from 6 to 8 mbar)

6.3 ESTIMATING THE LOSS OF VENTRAL VENTILATION DUE TO OVERDISTENSION

In order to monitor a potential loss of ventral ventilation induced by overdistension during a decremental PEEP trial, the cursor C1 is again used as a reference, but now set to the lowest PEEP level (6 mbar). It is assumed that no overdistension is present at this relatively low PEEP level. Cursor C2 is now set to the next higher PEEP level (Fig. 39).

Even though the increase of PEEP results in a slight decrease of ventral ventilation in ROI 1 and ROI 2, Tidal image C2 reveals that ventral ventilation is not significantly impaired at a PEEP of 8 mbar.

Consequently, the differential image remains almost black, indicating that there is no significant overdistension at a PEEP of 8 mbar.

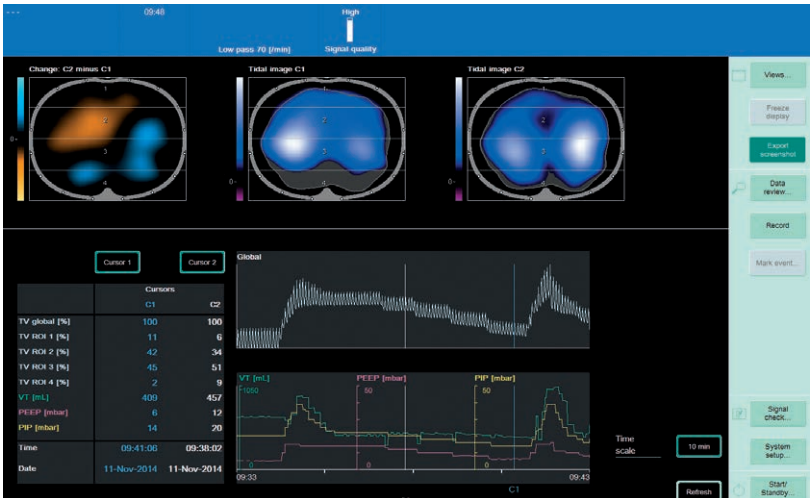

Fig. 40: Estimating the loss of ventral ventilation (PEEP increase from 6 to 12 mbar)

In contrast, comparing the lowest PEEP (6 mbar, C1) with a PEEP of 12 mbar (C2), the upper half of the right lung shows a significant loss in ventilation, as shown in the differential image in orange colour (Fig. 40). This loss of ventral ventilation induced by higher PEEP levels can be interpreted as overdistension.

INTERPRETATION OF THESE APPLICATION EXAMPLES

As discussed previously, the information directly provided by PulmoVista 500 is the distribution of ventilation within the EIT sensitivity region and its changes over time.

Distribution of ventilation typically changes, when therapy, e.g. ventilator settings, is adjusted. During pressure controlled ventilation – where the driving pressure is kept constant – regional volume changes can be interpreted as regional changes in compliance.

Furthermore, it is well known, that regional compliance in ventral parts of the lung tends to be reduced by overdistension at high PEEP levels, and vice versa regional compliance in dorsal parts tends to be reduced by derecruitment at low PEEP levels.

Hence, valuable clinical information can be derived from EIT data collected during decremental PEEP trials, that is not directly available during steady mechanical ventilation.

7. Indications and contraindications

INDICATIONS

PulmoVista 500 is designed to perform thoracic bioimpedance measurements by applying the technique of electrical impedance tomography (EIT). PulmoVista 500 displays regional information on ventilation-related changes of air content within the EIT sensitivity region.

While PulmoVista 500 does not provide absolute values for end-expiratory lung volume, it does display regional information on short-term changes of end-expiratory lung volume within the EIT sensitivity region.

PulmoVista 500 can be used during mechanical ventilation, mask ventilation and spontaneous breathing.

PulmoVista 500 is intended for use on intensive care patients, whose regional (lung) volume distribution is of clinical interest. The electrode belts used with the device have been designed for use on recumbent patients in supine, lateral or prone position.

Generally speaking, in order to perform EIT measurements, the subject can be in an upright, sitting, or supine position, as long as there is no excessive body movement during the measurements. When using an electrode belt for PulmoVista 500, measurements of seated or standing patients may only give satisfactory results when the patient leans against a backrest as some electrodes may, depending on the shape of the posterior muscular structures (latissimus dorsi), not have sufficient skin contact. If required, the belt must be sufficiently secured with adhesive tape during measurements in an upright position.

Due to the fact that EIT monitoring is primarily beneficial in the treatment of patients with severe respiratory complications, PulmoVista 500 is intended for stationary use, at the bedside, in clinical environments and on recumbent intensive care patients.

In principle, EIT measurements can be performed on a wide range of adult patient populations, but also on paediatric and even neonatal patients.

The range of electrode belts which are currently provided with PulmoVista 500 allows EIT measurements on patients with a chest circumference from 70 cm (27.6 in) to 150 cm (59 in).

MEDICAL CONTRAINDICATIONS

GENERAL PRECAUTIONS

PulmoVista 500 should not be used on patients where the application of the electrode belt may pose a risk to the patients, e.g. patients with unstable spinal lesions or fractures.

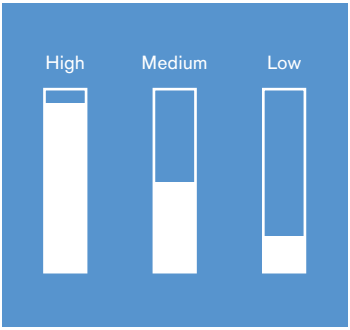

D-3438-2011

LOW SIGNAL QUALITY

Certain, extremely rare patient conditions, such as massive lung and /or tissue edema, can lead to compromised signal quality. When the signal quality indicator reads “Low” and even applying electrode gel or reducing the frame rate do not lead to an improvement, then PulmoVista 500 should not be used on such patients.

Similar precautions apply to obese patients. PulmoVista 500 should not be used on patients with a BMI over 50. The signal quality of obese patients with a BMI less than 50 should be monitored closely. Within the electrode plane, the ratio between lung tissue and fatty tissue surrounding the ribcage is reduced. For this reason, the ventilated lung areas appear smaller in EIT images of massively obese patients (Fig. 50).

EIT measurements are generally relatively sensitive to body movements. For example, lifting the arms will cause the skin over the thorax to shift; a subsequent shift of the belt will also occur, while the position of the lung tissue remains almost unchanged. The resulting change in position of the electrodes relative to the lung tissue will induce impedance changes which are much larger than those related to ventilation.

As sufficient signal quality requires that all electrodes have proper skin contact, the electrode belt must not be placed over wound dressings and the like.

ACTIVE IMPLANTS

So far, little experience exists regarding the interference between active implants and impedance tomography measurements.

For this reason, PulmoVista 500 must not be used on patients with a cardiac pacemaker, an implantable cardioverter-defibrillator (ICD) or any other active implants where the function of PulmoVista 500, especially the alternating current application, may interfere with the function of the active medical device.

In the future, compatibility tests will be performed to identify those devices where interference is likely. In case of any doubt about the compatibility with an implanted active device, the PulmoVista 500 must not be used.

DEFIBRILLATION

PulmoVista 500 must not be used during cardiac defibrillation as the energy needed for defibrillation may disperse into the PulmoVista 500 and decrease the effectiveness of defibrillation.

There is also a risk of damage to the components of the PulmoVista 500 if the patient belt remains connected to the patient during defibrillation, and the electrode belt may mechanically interfere with the correct positioning of the defibrillation electrodes or paddles.

Consequently, before defibrillation is carried out the lateral patient cable connectors should be removed from the patient cable ports and the electrode belt opened.

SKIN CONDITIONS

In contrast to ECG measurements, electrodes must also be placed in the posterior region of the thorax. As the belt is positioned around the thorax, the body weight of the patient always causes parts of the electrode belt to be pressed against the respective skin area, regardless of whether the patient is in a supine, lateral or prone position.

The silicone belt has a cushioning effect and lesions, as a result of the patient lying on the belt, patient cable or its snaps, have been observed only rarely in patients where the belt was attached tightly for many hours or in patients with extremely vulnerable skin, e.g. in septic shock. Shallow indentations and skin redness may occur at the position of the edges of the silicone belt when it has been in place for some time. These marks are similar to those caused by a crease in a bed sheet. The time it takes for these marks to dissipate mainly depends on the skin condition of the individual as well as the tightness of the belt during its application.

In contrast to creases, the EIT belt will remain in exactly the same position for the duration of the measurement period. Thus, prolonged measurement times may increase the risk of skin injury. Therefore the maximum allowable time for the belt to be in place is 24 hours – during this time the skin in the area of the electrode belt must be checked regularly. Special care needs to be taken in patients whose peripheral / skin perfusion is compromised, e.g. septic shock or other severe cardiovascular compromise.

The electrode belt of PulmoVista 500 must not be placed over injured, inflamed or otherwise damaged skin areas.

INTERFERENCE FROM OTHER MEDICAL DEVICES

To date, little experience exists regarding interference of EIT measurements with other electromedical devices and particular other bioimpedance measurements.

This includes non-invasive cardiac output monitors which use bioimpedance measurements, respiration monitors using impedance measurements, instruments for electrocautery and electrosurgery and devices designed for electricity-based therapy.

PulmoVista 500 is not intended for use in the presence of strong magnetic fields, e.g., MRI, as PulmoVista 500 or the respective device may be damaged.

8. Considerations for EIT data interpretation

SPATIAL RESOLUTION

PulmoVista 500 uses 16 electrodes to measure the voltages that are used for image reconstruction. There is a distance of approximately 3 cm between the electrodes of a large size belt (for chest circumferences between 92 cm and 110 cm). Mathematical simulations based on this electrode arrangement demonstrate a spatial resolution of 15% of the thoracic diameter, however the resolution decreases to 20% towards the centre of the body.

While CT scanners typically provide images consisting of 512 × 512 pixels, EIT images from PulmoVista 500 only consist of 32 × 32 pixels, which are 256 times fewer pixels compared to CT images. Even though the first CT scanner, developed in 1970, only provided an array of 80 × 80 pixels, it is not expected that the spatial resolution of EIT images can be improved in the near future to a point comparable with that of CT.

As current pathways do not lead straight through the body (unlike X-rays) and can easily change directions to bypass non-conductive regions, e.g. a pneumothorax, it is assumed that the drawbacks of an increased number of electrodes, such as additional cables and connections, a lower signal strength, and higher crosstalk, will outweigh the potential benefits of a slight increase in spatial resolution.

In contrast to CT and MRI, the intended role of EIT in clinical practice is to guide ventilation therapy rather than the absolute diagnosis; it is unlikely that increased spatial resolution would significantly improve the ability of EIT to guide ventilation therapy.

ONE SINGLE CROSS-SECTIONAL PLANE

PulmoVista 500 displays EIT status images and related information which represent only the distribution of the tidal volume in one single cross-sectional plane.

As previously described, it can be assumed that, due to the three-dimensional current flow, the area at the centre of the thorax which is reflected by EIT data is several centimetres thick; this thickness decreases towards the surface near the electrodes, resulting in a lens-shaped sample volume.

The mapping of complex three-dimensional morphological structures on a two-dimensional template further decreases spatial resolution. Additionally, there is no precise information about the size of the portion of the lungs represented by an EIT image.

When interpreting EIT data, it must be accepted that, as a result of the conditions explained above, the displayed circumference of the electrode plane does not exactly match the geometry of the patient. It also must be taken into account that the displayed position of impedance changes does not always exactly match the position where the impedance changes occur.

Physiological changes, such as increased intra-abdominal pressure, or changes in ventilator settings like the PEEP, may cause caudal-cranial shifts of intra-thoracic structures.

Those shifts have to be considered when relating tidal volumes to tidal variations or changes of EELV to ΔEELI.

Since tidal volume reflects the volume of the entire lung while tidal variations represent only the volume within the EIT sensitivity region, the assumption of a linear relationship between changes in global tidal impedance and tidal volume cannot be used to directly calculate the EELV [21].

As major changes in PEEP can alter the portion of lung tissue which is captured within the EIT sensitivity region, and as recruitment and derecruitment is not necessarily evenly distributed in a caudal/cranial orientation, the strong correlation of volume changes within the EIT sensitivity region and FRC changes reflecting the entire lung, that were previously described by Hinz et al. [22] and Odenstedt et al. [23], is not seen under all clinical circumstances.

Thus, when interpreting the ΔEELI, the fact that this information only reflects changes of end-expiratory lung impedance of one slice of the lung (the EIT sensitivity region), as opposed to the entire lung, must be taken into account.

Nevertheless, assuming that the electrode belt is put at a sufficient distance from the diaphragm, the dynamics of ongoing recruitment or de-recruitment, e.g. after changes in PEEP, can be visualised [24]. Also, with its regional information on end-expiratory lung impedance changes, PulmoVista 500 is the only bedside tool which enables assessment of whether such an increase was caused by hyperinflation (in the ventral regions) or the reopening of atelectatic lung tissue (in the dorsal regions).

When a global FRC parameter is used, regional atelectasis could be masked by increased compliance in other regions during deflation [25]. Hickling [26] has described, in the context of the interpretation of global pressure-volume curves, that recruitment of lung regions and hyperinflation of other lung regions is likely to happen simultaneously in the lungs of ARDS patients.

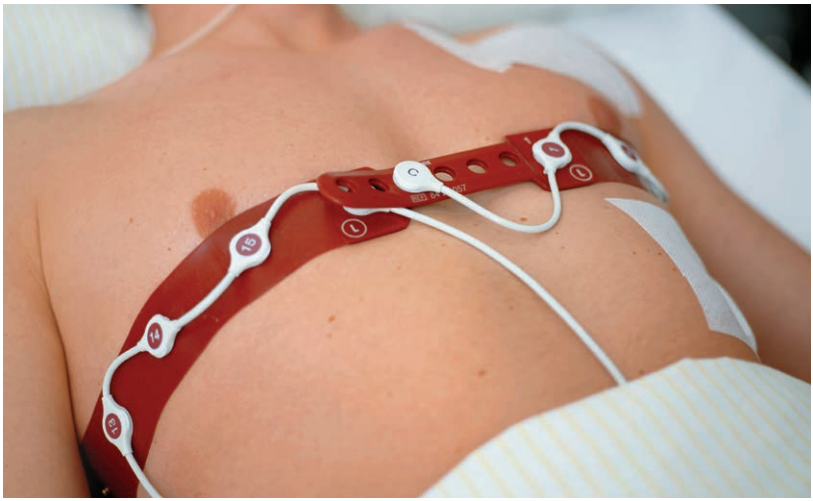

D-28332-2009

Fig. 41: Recommended position of the electrode belt

BELT POSITION

In an experimental study, Reske [27] assessed the correlation between non-aerated lung volume and total lung volume and PaO_2, first using a small number of representative CT slices from different planes rather then 21 CT slices representing the entire lung. It was found that one single juxta-diaphragmatic cross-section reflects the condition of the (atelectatic) lungs better than the conventional combination of apical, hiliar and juxta-diaphragmatic slices. It is known that anaesthesia-induced atelectasis occurs predominantly in dependent juxta-diaphragmatic lung regions, which may account for the superior performance of one single juxta-diaphragmatic slice when assessing atelectasis.

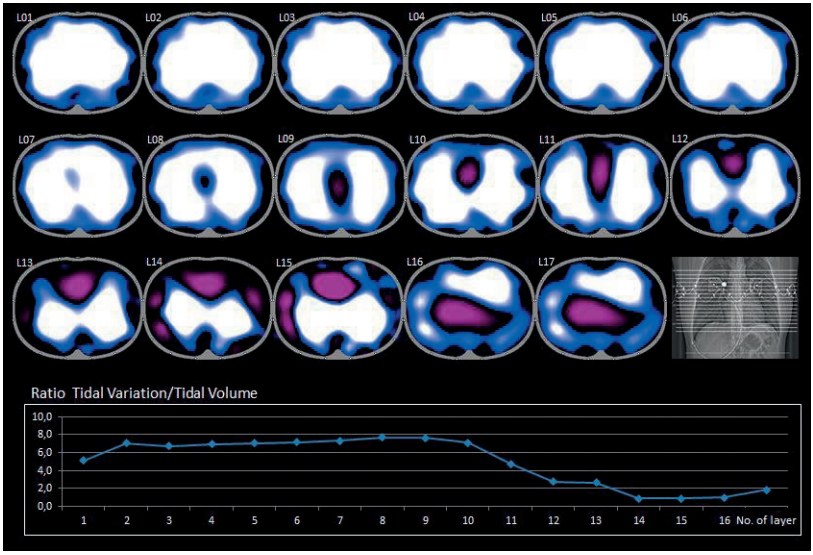

Fig. 42: Impact of belt position on tidal images: L01 was recorded at the highest possible belt position (i.e., below the armpits), for L02 the belt was placed 1 cm further down, and so on. Colours were enhanced to make the effects more obvious. L11 represents ICS 6, where the mediastinum enters into the plane. The diagram reveals that from L02 to L10, the ratio of tidal variation and tidal volume remains almost constant, but begins to rapidly drop from L10. The images L12 to L15 which represent the juxta-diaphragmatic position, can only be interpreted with great caution. At L16 and L17 the ventilation-related signal is inverted and now represented in purple, because the artifacts induced by diaphragmatic movements are larger than the tidal variations

Thus it can be seen that selecting a single plane in the appropriate position – as done with EIT – may provide the best possible representation of those juxta-diaphragmatic lung regions which are most affected by atelectasis, tidal recruitment and overdistension. However, due to the lens-shaped EIT sensitivity region, the belt does not need be placed in the juxta-diaphragmatic position in order to detect recruitment and derecruitment. It is recommended to position the belt at about the 5th intercostal space at the parasternal line (Fig. 41).

In patients where an elevated diaphragmatic position is likely (e.g. obesity, diaphragmatic palsy), the belt should not be positioned below intercostal space 5, in order to avoid artifacts (check spelling with client) caused by diaphragmatic movement. Placement of the belt close to the diaphragmatic position increasingly leads to phase shifts in the mediastinal and lateral regions, which are represented in the tidal images in purple colour (Fig. 42).

A small number of EIT research groups continue to work on prototypes of three-dimensional EIT imaging devices. However, it is not expected that these systems will be developed beyond the research setting within the foreseeable future.

CARDIOPULMONARY INTERACTION

The impedance changes measured by PulmoVista 500 reflect an interaction of different physiological processes rather than the effects of a single, isolated phenomenon. In some publications and review papers, this is perceived as a limitation.

This point of view does not take into account that impedance changes due to ventilation are normally about 10 times greater than impedance changes due to cardiac activity. Also, cardiac-related impedance changes can easily be isolated using low-pass filtering.

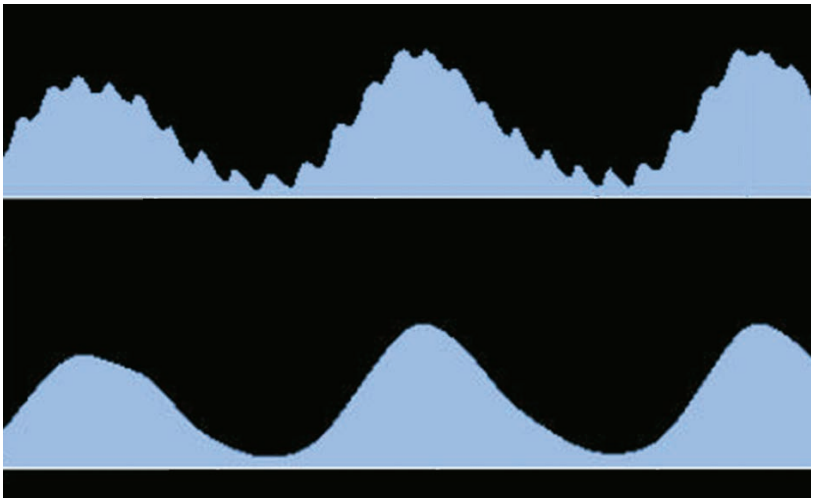

D-65-2011

Fig. 43: Unfiltered impedance waveform (upper curve) and filtered waveform (Cut-off frequency 35 [1/min]) from the same EIT data

As PulmoVista 500 incorporates low-pass filtering, the concurrent presence of impedance signals due to ventilation and cardiac activity does not limit the assessment of regional ventilation distribution and changes of end-expiratory lung impedance (Fig. 43).

ARTIFACTS

PulmoVista 500 was designed to continuously display ventilation related changes of air content within the EIT sensitivity region; however, as with many medical imaging systems, changes in the body position and movement may cause significant artifacts.

Just as moving an ultrasound probe to a different part of the body may change the ultrasound image, so may altering the position of the electrode belt change the distribution of ventilation displayed by EIT; end-expiratory lung impedance values are particularly affected by changes in belt position.

Additionally, changes in position of the electrode belt, or the application of electrode gel, may alter the skin-electrode resistance and thus the EIT data so that the interpretation of the trend data provided by PulmoVista 500 may be compromised. This means that the changes, e.g., from moving the belt, must be taken into consideration when analysing trend data.

End-expiratory lung impedance may also be affected by changes of extravascular lung water content, but in contrast to belt repositioning, changes of extravascular lung water content are relatively slow.

It has occasionally been reported that strong electromagnetic fields in the range of the operating frequency of the EIT device, induced by e.g. CT scanners, have caused major artifacts in EIT data. These electromagnetic fields may exert their effect via the pathway of the patient, the mains power supply, the trunk cable or the patient cable.

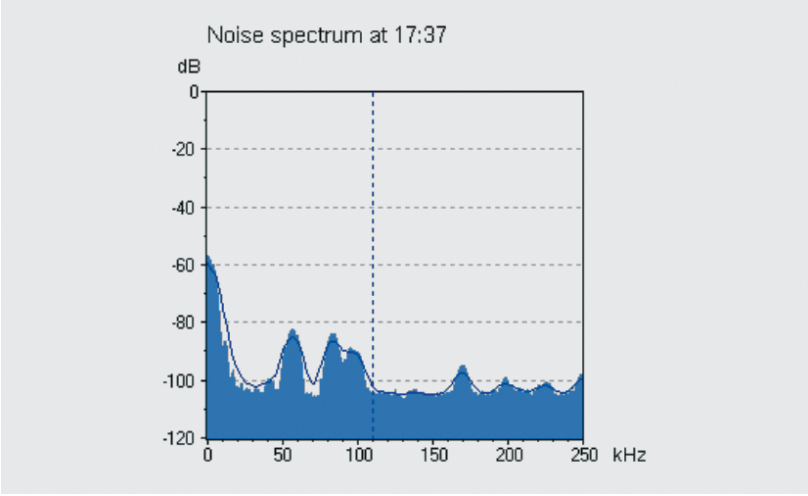

D-72-2011

Fig. 44: Graphical display of the noise spectrum determined by Dräger PulmoVista® 500 during the last calibration

Electromagnetic interference is usually limited to particular frequency bands. PulmoVista 500 prevents superposition of this kind of noise on EIT signals by analysing the relevant spectrum of electromagnetic background noise during the calibration cycle and automatically setting the operating frequency to a range with a low background noise level (Fig. 44). It is this feature of PulmoVista 500 which makes it less sensitive to interference from electromagnetic fields than previous generations of EIT devices.

RELATIVE IMPEDANCE CHANGES

Until now, most studies were performed using functional EIT (f-EIT), which measures impedance changes relative to a baseline. Absolute EIT (a-EIT) may also become clinically useful, as being able to measure absolute regional impedance values would allow one to directly distinguish between lung conditions which result from regions with lower resistivity

(e.g. hemothorax, pleural effusion, atelectasis and lung edema) and those with higher resistivity (e.g. pneumothorax, emphysema).

However, the reconstruction of absolute impedance images requires that the exact dimensions and the shape of the body, as well as the precise location of the electrodes, be taken into account, as simplified assumptions would lead to major reconstruction artifacts.

While initial studies assessing aspects of a-EIT have already been published [28], as of today this area of research has not yet reached the level of maturity which would make it suitable for clinical use. Consequently, PulmoVista 500 does not currently provide a-EIT functionality.

9. Validation studies

Electrical impedance tomography has been extensively validated in animal experiments and clinical (human) studies. In animal experiments, the spatial distribution of pulmonary aeration determined by EIT is well correlated with results from CT, single photon emission CT (SPECT) and electron beam CT (EBCT). These findings were obtained using different EIT devices, and diverse ventilation modes and settings.

Notably a strong correlation between EIT and CT was demonstrated in critically ill patients.

A comprehensive collection of corresponding references can be found in several recent reviews [29, 54, 97].

ANIMAL STUDIES

The correlation of global ventilation with global impedance measurements resulting from EIT image streams has been investigated by several researchers for quite some time. One of the early reports was published in 1997. In 19 dogs, Adler et al. investigated the relation between EIT readings and predefined gas or fluid volume (air, albumin solution) injected with a large syringe into the lungs [30]. Excellent correlations between syringe gas volume and EIT-based estimates for lung volume change were reported.

Similarly, Meier and co-workers [31] reported very good correlations between tidal volume administered by an anaesthesia workstation (Primus, Dräger Medical, Lübeck, Germany) and global impedance changes obtained from EIT readings in 3 pigs.

Of course the validation of regional ventilation is more challenging than global ventilation, as suitable reference techniques are more complex and costly. In 2005, Luepschen et al. compared EIT to CT in 10 domestic

pigs undergoing laparoscopic surgery and pulmonary lavage [32]. The authors found good spatial correlation between EIT images and the CT reference. With the high temporal resolution of EIT, effects of changed ventilator settings can be seen immediately. Functional activity and tidal variation show an excellent linear correlation with tidal volume (i.e. global ventilation). The results of comparing EIT with CT and tidal volume indicate that information on regional ventilation may be gained from EIT images and/or local impedance changes.

Hinz et al. validated EIT for the measurement of regional distribution of ventilation by comparing it to single photon emission CT (SPECT) [33]. In twelve pigs, they investigated whether regional impedance changes obtained by EIT are quantitatively related to regional ventilation as determined by SPECT. Different modes of mechanical and spontaneous ventilation were analysed in this study. A highly significant linear correlation between regional ventilation measured by EIT and SPECT scanning was found ($r^2 = 0.92$; range 0.86 to 0.97). The mode of ventilation, or presence of spontaneous breathing, did not affect the correlation to a relevant extent. Moreover, induced lung injury, induced changes of compliance of the respiratory system or of extravascular lung water content caused no significant effects on the correlation between EIT and SPECT.

Frerichs et al. validated the ability of EIT to detect local changes in air content resulting from modified ventilator settings by comparing data from EIT with data from Electron Beam CT (EBCT), obtained under identical steady state conditions [34]. The experiments were carried out in 6 pigs using 5 different tidal volumes at three PEEP levels. The analysis was performed in 6 regions of interest, located in the ventral, middle and dorsal areas of each lung. Good correlation between the changes in lung air content determined by EIT and EBCT was revealed, with mean correlation coefficients in the ventral, middle and dorsal regions of 0.81, 0.87 and 0.93 respectively.

In another study, Frerichs et al. investigated the reproducibility of EIT images showing lung ventilation distribution at different PEEP levels in 10 pigs [35]. Regional lung ventilation was determined in the right and left hemithorax as well as in 64 regions of interest evenly distributed over each side of the chest in the ventro-dorsal direction. Ventilation distribution in both lungs was visualised as ventro-dorsal ventilation profiles and shifts in ventilation distribution quantified in terms of centres of ventilation in relation to the chest diameter. The proportion of the right lung on total ventilation in the chest cross-section was 0.54 ± 0.04 and remained unaffected by repetitive PEEP changes. In summary, the authors found excellent reproducibility of the results in individual regions of interest with almost identical patterns of ventilation distribution during repeated PEEP changes.

In 2003, van Genderingen et al. investigated the value of EIT for the assessment of regional lung mechanics during high-frequency oscillatory ventilation (HFOV) in eight pigs [36]. Lung volume determined by EIT was estimated by calibrated strain-gauge plethysmography (SGP) during a P-V manoeuvre. Regional lung volume changes were assessed by electrical impedance tomography in various regions of interest. The study showed good agreement between global impedance from EIT and lung volume estimated by SGP, during both the P-V maneuver and subsequent HFOV. However, baseline measurements performed at the end of the experiments suggested that accumulation of intra-thoracic fluid may limit the accuracy for determining small changes in lung volume over a longer period of time.

Meier et al. investigated the capability of EIT to monitor regional lung recruitment and lung collapse using different levels of PEEP in a lavage model of lung injury in six domestic pigs by comparing EIT findings to simultaneously acquired CT images and global ventilation parameters [37]. The authors found a close correlation between end-expiratory gas volumes assessed by EIT and end-expiratory gas volumes calculated from CT

(r = 0.98 – 0.99). Also, correlation of tidal volumes was demonstrated (r = 0.55 – 0.88) for both EIT and CT. The authors concluded that EIT is suitable for monitoring the dynamic effects of PEEP variations on the regional change of tidal volume, and that it is superior to global ventilation parameters in assessing the beginning of alveolar recruitment and lung collapse.

PATIENT STUDIES

In 2003, Hinz et al. compared lung volume changes with end-expiratory lung impedance changes [38]. In their study, 10 intubated patients were enrolled and PEEP was changed from 0 to 15 mbar. During this manoeuvre, ΔEELV was measured by an open-circuit nitrogen washout manoeuvre while EIT was used to assess end-expiratory lung impedance changes ΔEELI. The authors report very high correlation and good accuracy in the Bland-Altman plot.

In 2006, Marquis et al. reported an excellent correlation between global EIT measurement and plethysmography readings used as a reference in 22 healthy volunteers [39].

Victorino et al. performed a validation study comparing EIT with dynamic CT in ten critically ill mechanically ventilated patients [40]. Their data showed that EIT reliably provides a means to assess imbalances in distribution of tidal volume in critically ill patients. When comparing regional ventilation across different thoracic regions, the quantitative information provided by EIT carries good proportionality to changes in air content – as calculated by dynamic CT scanning – but not with CT gas/tissue ratio or CT mean-densities. Further results from this study showed that EIT images from patients undergoing controlled mechanical ventilation were reproducible and presented good agreement to dynamic CT scanning. Moreover, regional impedance changes in the EIT slice were best explained by the corresponding changes in air-content detected in the CT slice (explaining 92 – 93% of its variance). Other CT derived variables, such as

regional X-ray mean-density or regional gas-tissue ratio, did not parallel regional changes in impedance as consistently. It was also noted that good correlation between EIT and CT could only be observed in sufficiently large regions of interest. This finding was to be expected considering the limited spatial resolution of EIT and is in line with results from mathematical calculations.

Riedel et al. evaluated the effect of body position and positive pressure ventilation on intrapulmonary tidal volume distribution in ten healthy adult subjects [41]. EIT measurements and multiple-breath sulphur hexafluoride (SF6) washout were performed. Profiles of average relative impedance change in regional lung areas were calculated. Relative impedance time course analysis and Lissajous figure loop analysis were used to calculate phase angles between dependent or independent lung and total lung (Φ). EIT data were compared to SF6 washout data measuring the lung clearance index (LCI). Proposed EIT profiles allowed inter-individual comparison of EIT data and identified areas with reduced regional tidal volume using pressure support ventilation. The phase angle Φ of dependent lung in various body positions is as follows: supine 11.7 ±1.4, prone 5.3 ±0.5, right lateral 11.0 ±1.3 and left lateral 10.8 ±1.0. LCI increased in the supine position from 5.63 ±0.43 to 7.13 ±0.64 in the prone position. Measured Φ showed an inverse relationship to LCI in the four different body positions. The findings of this study demonstrate that functional EIT measures gravity dependent asynchronous emptying of the lung in different body positions and characterises local tidal volume distribution at different levels of pressure support. Although this study was limited to healthy subjects, and rather large lung areas were analysed, the authors state that the proposed method may be powerful enough to analyse uneven ventilation in diseased lungs and more specific lung regions.

In 2009, Bikker et al. reported on their findings in 25 ventilated ICU patients [42]. They compared EELV measurements performed with a COVX module integrated into an Engström Carestation ventilator (both from GE Healthcare, Helsinki, Finland) with end-expiratory lung impedance readings

obtained by EIT. The authors reported a significant moderate correlation ($r = 0.79$; $r^2 = 0.62$) and a moderate agreement (bias 194 ml, SD 323 ml) between ΔEELV and changes in lung volume calculated from ΔEELI. The results indicate that the relationship between global tidal impedance variation and tidal volume may not be strictly linear. Hence, the authors concluded that such a relationship cannot be used to directly use ΔEELI as a linear surrogate for EELV differences and hence changes in FRC.

Recently, Karsten et al. [43] investigated a similar question in 54 post-operative cardiac patients. The authors used an oxygen wash-in/wash-out technique as a reference and looked at changes during open endotracheal suctioning (OPS) procedures and recruitment manoeuvres (RM) and reported limits of agreement for ΔEELV estimated from ΔEELI between –0.83 and 1.31 l as compared to the reference measurements. These findings led the authors to the conclusion that the correlation between ΔEELI and ΔEELV may not be clinically acceptable.

The different findings in the validation studies can possibly be explained by the impact of belt position: When the belt is placed rather close to the diaphragm and PEEP is changed, the distance between the electrode plane and the diaphragm changes significantly, leading to an alteration of the ratio between impedance changes and lung volume changes. As a result, lung volume changes might get underestimated, when e.g. a PEEP reduction decreases the distance between the diaphragm and the belt significantly and thus the ratio between impedance changes and lung volume changes gets much smaller.

These effects are illustrated and explained in more detail in Fig. 42.

10. Observational Experimental and Clinical Studies

As discussed before, EIT provides a means of visualising the regional distribution of ventilation and changes of lung volume. This ability is particularly useful when therapy changes are intended to achieve a more homogenous gas distribution in mechanically ventilated patients.

Today, the assessment of regional gas distribution can only be based on CT or MRI scans. However, CT involves an exposure to significant doses of ionising radiation [44, 45]. Also, CT and MRI can usually not be performed at the bedside and thus require that the patient is transported to the radiology department. The intra-hospital transport of critically ill ventilated patients represents a significant risk for the patient and increased workload for caregivers.

Moreover, CT and MRI images are static and thus only represent lung volume at one specific point in time. Also, CT and MRI cannot provide real-time quantification of air content in predefined ROIs. Even though CT provides images of the regional gas distribution, experts do not consider CT to be suitable for the individual optimisation of ventilator settings at the bedside [15, 37].

Due to the general properties of EIT and its specific design, PulmoVista 500 can easily be used continuously at the bedside to provide regional information about distribution of ventilation as well as changes of end-expiratory lung volume. No side effects of EIT have ever been reported. Besides the unique information provided by EIT, its convenience and safety contribute to the increasing perception expressed by various authors that EIT has the potential to be used as a valuable tool for optimising PEEP and other ventilator settings [46, 47].

The effects of various therapeutic interventions on ventilation distribution have already been assessed with the help of EIT, and this chapter gives an overview of the literature that has been published in this context.

PEEP TITRATION

Currently, there is no consensus within the medical community on how to optimise ventilator settings such as PEEP. This is, among other issues, related to the fact that before the advent of EIT we did not have a bedside method to assess regional ventilation distribution and dynamic opening and collapse of pulmonary areas. Knowledge about the distribution of ventilation could help the clinicians to set ventilation parameters more appropriately for the individual patient and thus potentially reduce the risk of ventilator associated lung injury (VALI).

EIT-based titration of PEEP to avoid atelectasis on the one hand and regional hyperinflation on the other hand has already been described by Hinz et al. [48]. The authors also interpreted the “filling characteristics”, where local impedance waveforms are plotted over global waveforms and where they found significant differences between dependent and non-dependent lung regions. In the same publication, the ability to find regional upper inflection points in regional pressure-impedance curves was established; this can be used to assess a wide variety of PEEP trials.

Erlandson et al. [47] assessed slopes of the end-expiratory lung impedance (EELI) at different PEEP settings over time; it was hypothesised that a constant level of EELI would correspond to a stable end-expiratory lung volume (within the EIT sensitivity region) and thus would indicate the optimal PEEP setting (Fig. 45).

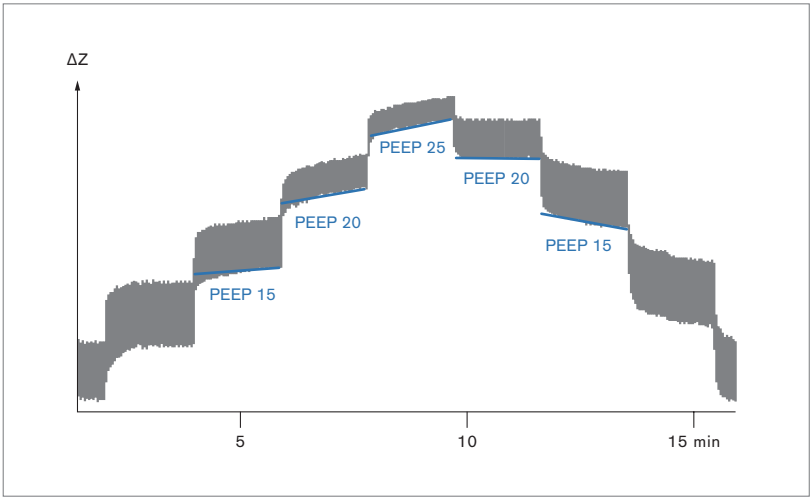

Fig. 45: Defining optimal PEEP settings based on the assessment of ΔEELI. A decrease in slope indicates derecruitment, whereas an increase in slope indicates recruitment. A horizontal tracing during the decremental part corresponds to a stable end-expiratory lung volume, i.e. optimal PEEP [47].

Recently, Mauri et al. investigated the distribution of ventilation in ARDS patients based on the chosen ventilation mode and PEEP levels [49]. In their study, ten intubated patients with ARDS were enrolled, after they were switched from controlled mandatory ventilation to pressure support ventilation. No external reference for regional ventilation was applied. Instead, the redistribution of ventilation was compared within the different lung regions of EIT images. The authors conclude that in ARDS patients, lower pressure support and higher PEEP levels induce a redistribution of tidal ventilation fractions from nondependent to dependent lung regions and increase antero-posterior ventilation homogeneity.

For obese patients scheduled for laparoscopic surgery, PEEP adjustment may be especially important, due to the increased pressure in the abdominal compartment [47, 50]. The results of these studies suggest that in this

patient population, EIT monitoring might be helpful to adjust PEEP levels in order to prevent lung collapse. In morbidly obese patients, the PEEP level required appeared to be higher than previously anticipated.

ASSESSMENT OF RECRUITMENT MANOEUVRES

Recruitment manoeuvres aim at reopening collapsed lung regions, thus improving pulmonary aeration and reducing mechanical stress during subsequent ventilation. The regional effects of recruitment manoeuvres can be visualised and assessed with EIT [10, 37].

Indeed, the question whether patients benefit from a high PEEP or a recruitment manoeuvre has been investigated by many researchers. In 2006, Gattinoni et al. reported a high variability of added lung volume in response to high pressures [51]. However, the Italian authors used CT to determine the responsiveness of patients. To avoid the x-ray load, Lowhagen and co-workers introduced an EIT-based technique of regional P/V-monitoring during recruitment manoeuvres. In their study on 16 ventilated ALI patients [52], the authors presented a new method to quantify potentially recruitable regional lung volume by looking at the difference in regional tidal variations at tidal breathing and at 40 cm H_2O. ΔEELI was calibrated against regional ΔEELV. In accordance with earlier statements about “Recruiters” and “Non-Recruiters” by Gattinoni [51], the authors found that only patients with a higher percentage of potentially recruitable lung benefited from a higher PEEP. The authors concluded that such a technique, after being validated sufficiently, might allow to distinguish recruiters from non-recruiters.

Odenstedt et al. evaluated the effects of different lung recruitment manoeuvres with EIT in fourteen animals with induced lung injury [23]. This study confirmed that EIT is capable of continuously monitoring lung volume changes and that EIT can help to identify responders to recruitment manoeuvres.

Slow de-recruitment after recruitment manoeuvres, caused by insufficient

post-manoeuvre PEEP levels, can also be identified.

SPONTANEOUS BREATHING

Frerichs et al. [53] performed EIT studies in infants and concluded that EIT is capable of displaying the effect of spontaneous breathing on the distribution of ventilation.

In [54], Putensen presented a case of an intubated patient with acute respiratory failure breathing spontaneously with APRV. When spontaneous breathing in this patient was discontinued, ventilation in the right dorsal region almost disappeared, indicating that during mechanical ventilation regional ventilation was predominantly redistributed to the ventral lung areas. Even though these effects are well known and the positive effects of spontaneous breathing on gas exchange, particularly in the dorsal regions, are widely accepted, witnessing the disappearance of dorsal ventilation in association with sedation should provide valuable information for making clinical decisions.

MONITORING OF DE-RECRUITMENT FOLLOWING SUCTIONING PROCEDURES

Endotracheal suctioning is a very common procedure to remove secretions from the airways of intubated and mechanically ventilated patients. While this procedure is often inevitable, it carries the risk, especially in ALI or ARDS patients, of lung de-recruitment, further compromising gas exchange. Using EIT, it has been shown that in some patients, a relatively long period of time passes before end-expiratory lung impedance is restored to levels observed prior to airway suctioning.

In an experimental animal setup, Lindgren et al. [55] used EIT to assess lung volume and compliance changes during open and closed suctioning and were able to confirm that EIT is capable of monitoring rapid lung volume changes such as those induced by endotracheal suctioning.

These results were replicated in a subsequent clinical study by the same

group in 2008 where the effect of endotracheal suctioning on pulmonary aeration was investigated in 13 ventilated ICU patients [56]. Using EIT the authors were able to monitor the derecruitment, as a direct result of suctioning, as well as the slow recruitment that occurred afterwards in some patients.

In 2009, van Veenendaal et al. described the results of their prospective observational clinical study involving 11 preterm infants with RDS treated with open lung high frequency ventilation (HFV) [57]. The authors measured changes in global and regional lung volume with EIT during routine closed suctioning procedures. Tracking the global impedance values, the authors concluded that closed ETT suction may cause an acute, transient and heterogeneous loss of lung volume followed by a gradual recovery within the first minute after suctioning.

Tingay et al. investigated the differences between closed and open suctioning in an animal trial [58]. In this paper published in 2010, three suction methods (open, closed inline and closed using a side-port adapter) and two catheter sizes were applied to six two-week old piglets in random order. The authors concluded that ETT suction causes transient loss of EELI throughout the lung. The catheter size was of greater influence than the suction method, with closed suction only protecting against derecruitment when a small catheter was used, indicating that the resistance to airflow is an important factor.

In 2012, Corley et al. reported on the differences between closed and open suctioning in humans [59]. In a randomised crossover study examining 20 patients post cardiac surgery, the authors examined the effects of open and closed suction on lung volume loss using EIT. Interestingly, the authors found that closed suctioning minimised lung volume loss during suctioning but, counterintuitively, resulted in a slower recovery of EELI compared with open suctioning.

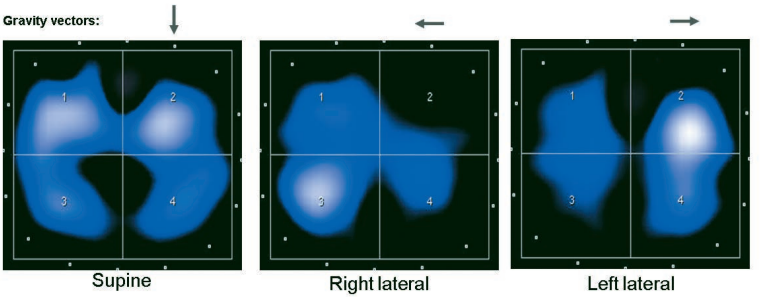

D-48-2011

Fig. 46: Redistribution of ventilation in a healthy volunteer; while a typical left / right distribution of 52 % / 48 % is seen in supine position (left), in a right lateral position this ratio changed to 72 % / 28 % (centre), in a left lateral position to 35 % / 65 % (right)

MONITORING THE EFFECTS OF PATIENT POSITIONING

During lateral positioning, typically much more ventilation occurs in the dependent lung (in left lateral position, the left lung) than in the non-dependent lung. This is because at the end of expiration, gravity causes the dependent lung to be more compressed than the upper lung; however, in a healthy individual the dependent lung is fully inflated at the end of inspiration. This means that larger changes of air content occur in dependent regions (Fig. 46).

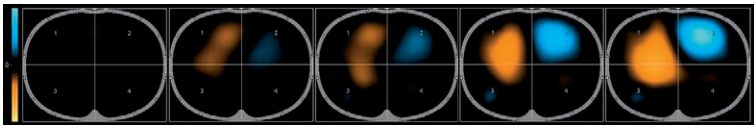

D-7534-2014

Fig. 47: Changes of ventilation distribution – assessed with the End-inspiratory trend view of Dräger PulmoVista® 500 – in a chest trauma patient in a rotation bed, while being turned from supine to a 60° left lateral position. The first image represents supine position (reference), the following images represent a rotation of 15°, 30°, 45° and 60°. The images depict how ventilation increases in the upper right lung due to the gravity vector which changes over time during the rotation

While these phenomena are well known and quite intuitive in clinical practice, EIT allows visualisation and assessment of these dynamic changes at the bedside: see Fig. 47

In the last 20 years, prone positioning has been used increasingly in the treatment of ARDS patients [60, 61]. EIT may help to monitor ventilation redistribution due to such changes of position. Moreover, it may help to identify responders to this kind of treatment. It may also help identify the best body position in case of a highly uneven distribution of ventilation [62, 63].

POSITIONING OF DOUBLE LUMEN ENDOTRACHEAL TUBES

Steinmann et al. [64] used EIT to assess the correct placement of double lumen endotracheal tubes (DLT) and compared the findings with those obtained using fibreoptic bronchoscopy (FOB). While EIT enables immediate recognition of misplaced left-sided DLTs, EIT did not provide

a method to detect incorrectly positioned endobronchial cuffs (as diagnosed by FOB). Thus, EIT cannot replace FOB as a means of determining correct placement of DLTs. Nonetheless, the authors stated that EIT could be used as an additional tool, complementing auscultation as a non-invasive method of assessing DLT placement.

In 2013, Steinmann and co-workers reported on the use of EIT to position endotracheal tubes (ETT) in paediatric anaesthesia applications [65]. The authors concluded that a correct ETT placement correlated very well with a homogeneous distribution of ventilation between left and right lung.

DETECTION OF PNEUMOTHORAX

For intensive care patients, the incidence of acquiring an iatrogenic pneumothorax, which is a life-threatening complication, was reported to be 3% [66].

As the pneumothorax represents a lung region with an extremely high impedance, it has been assessed by different groups whether EIT may be useful not only to detect to detect a pneumothorax, but also to track the potential success of therapeutic interventions. In 2006, Hahn et al. reported that they were able to monitor pathological fluid and air accumulation in 5 pigs and 4 patients [67].

In a controlled experimental setting including 39 pigs, Costa et al. [68] demonstrated that EIT is able to quickly detect the development of an artificial pneumothorax. In the same year, Preis et al. reported on the time course of an accidental pneumothorax which unexpectedly occurred during an open lung animal experiment. The incident could be nicely monitored using EIT [69].

The first human neonatal case of a pneumothorax monitored by EIT was reported by Miedema et al. in 2011 [70]. In this case report, Chest X-ray and functional EIT images from a male preterm infant both clearly showed a right-sided pneumothorax.

In 2012, Bhatia et al. [71] reported on the results obtained from 6 anaesthetised and muscle-relaxed piglets having surfactant-depleted lungs. The authors repetitively injected air volumes of 10–20 ml into the pleural space to a maximum volume of 200 ml. A good correlation of global and regional end-expiratory intra-thoracic volumes (EEV) measured by EIT was found and the authors concluded that EIT may accurately detect even very small pneumothoraces before physiological parameters change.

However, while the capability of EIT to detect an iatrogenic pneumothorax certainly represents a clinical benefit, continuous pneumothorax monitoring using EIT would require a long-term application of EIT, which currently seems impractical in clinical routine due to the need to attach the electrode belt to the patient permanently.

QUANTIFICATION OF PULMONARY EDEMA AND PLEURAL FLUID

So far, only a few studies have investigated whether EIT can be used to quantify the amount of fluid volume in the lung. So far, only preliminary data is available in this specific application field.

In 1999, Kunst et al [72]. investigated whether EIT and the so-called impedance ratio (IR index) correlates to the amount of extravascular lung water (EVLW) determined by the thermal dye double indicator dilution technique (TDD). They enrolled 14 ALI/ARDS patients into the study and a significant correlation between changes in EVLW as measured by TDD and EIT ($r = 0.85$; $p < 0.005$) was found.

In 2009, Arad et al. demonstrated that the decrease in mean tissue resistivity in the thorax correlated well with the fluid removal from the thorax [73]. This study is different from other EIT-related work in that absolute tissue properties, namely tissue resistivity in Ωcm, was studied. The authors used an eight electrode EIT device and included 11 patients with pleural effusion into their study.

11. EIT-derived numerical indices

While the interpretation of EIT images provides a rough visual impression of ventilation distribution, these images alone may not be sufficient for quantification of the impact of therapeutic procedures in clinical routine. EIT-derived numerical indices may be particularly useful for comparing the ventilation distribution at different points in time and for assessing the trend of ventilation distribution. Hence, the clinical community expressed its need for simple yet discriminative numerical indices which are also an important prerequisite for establishing thresholds, limits and proper target ranges for therapy. In the last decade, the race for the best approach to interpret EIT-based information was opened.

In 2000, Kunst et al. [9] introduced an index called the "impedance ratio" (IR) which divided the ventilation activity in the upper (ventral) region $VA_{ventral}$ of EIT images by the dorsal ventilation activity VA_{dorsal}. The IR index turned out to be a sensitive parameter for monitoring vertical ventilation changes induced by e.g. recruitment, derecruitment or overdistension.

The idea of using the "centre of gravity" (COG) as an index to characterise the shape of functional EIT images was first introduced by Frerichs et al. [74]. Originally named the "geometrical centre" of ventilation, this index was later renamed either "centre of ventilation" (COV) or "centre of gravity" (COG). In fact, Luepschen et al. demonstrated in 2007 that COG may serve as a sensitive index to describe vertical shifts in ventilation due to lung opening and closing during incremental and decremental PEEP trials [25].

Radke et al. [75] recently investigated the impact of spontaneous breathing on the COV during general anaesthesia. As is generally known, controlled ventilation tends to ventilate ventral lung regions more than dorsal regions during anaesthesia. Hence, the authors assumed that spontaneous breathing and pressure support ventilation would reduce the extent of the

redistribution of ventilation as detected by electrical impedance tomography. 30 non-obese patients without severe cardiac or pulmonary comorbidities scheduled for elective orthopaedic surgery were enrolled in their study. To quantify the distribution of ventilation, the authors used the COV from EIT recordings, as the COV is a single number, has a good reproducibility, and simplifies the comparison of EIT recordings. The authors conclude that according to the changes in COV, both PCV and PSV induce a redistribution of ventilation towards the ventral region. Spontaneous breathing prevented this redistribution.

In 2011, Luepschen et al. [76] demonstrated that EIT-based numerical indices like COV can be used as a guide for open-lung manoeuvres. In particular, the authors demonstrated that automatic open-lung manoeuvres based on EIT-COV can be part of closed-loop ventilation strategies. While earlier attempts for automatic ventilation of the same group used PaO_2 as a controlled output variable and EIT images as well as CT scans as independent references [25], this was the first time that EIT has actually been made part of the ventilation control loop.

In 2009 and 2010, Zhao et al. proposed another simple index called the "global inhomogeneity" index (GI). To calculate this index, the median value of regional impedance changes from ventilated regions within the tidal image has to be computed, then the sum of differences between the median and every pixel value needs to be calculated, and the result must be normalised by the sum of impedance values within the lung area. As reported, this index was applied to quantify ventilation inhomogeneity during one-lung ventilation in a study enrolling 50 patients, out of which 40 patients were intubated with double-lumen endotracheal tubes (test group) and another 10 patients were serving as a control group [77]. The authors concluded that using the GI index, one-lung ventilation was clearly distinguishable from double-lung ventilation in all patients. The same authors also found the GI index useful for PEEP titration in a pig trial where it correlated well with maximum compliance [78].

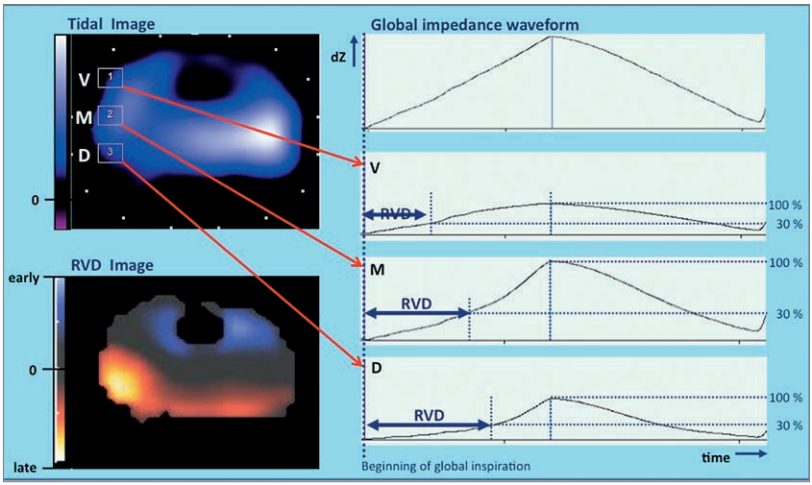

Fig. 48: Distribution of regional ventilation delay during a slow inflation manoeuvre: While the Tidal Image represents the distribution of ventilation, the RVD approach determines the delay of the beginning of regional inspiration relative to the beginning of global inspiration. In the RVD image, the regional ventilation delay is calculated for each pixel and plotted in a colour-coded map. A completely black RVD Image indicates a homogeneous beginning of inspiration, orange regions indicate a delayed and blue regions an early beginning of inspiration (preliminary colour scale).

In 2009, Muders et al. [79] described a new index of homogeneity of regional lung mechanics, the so-called "regional ventilation delay" (RVD) index (Fig. 48). Based on this RVD index, RVD maps may be generated from which the RVD standard deviation called SDRVD may be computed. This SDRVD index describes the variation of regional delays of the beginning of inspiration compared to the global beginning of inspiration during a slow inflation manoeuvre. Preliminary data showed an excellent correlation of SDRVD with cyclic opening and closing, suggesting that this index could also be a promising approach to titrate PEEP settings to prevent tidal recruitment.

Two more indices which allow quantifying regional overdistension and atelectasis were introduced in [80]. Based on the assumption of a uniform

pressure distribution within the lung, Costa et al. introduced the concept of the so-called “pixel compliance”, i.e., ΔZ/(Pplateau - PEEP). By comparing the pixel compliance at each PEEP level to the maximum pixel compliance during a decremental PEEP trial, the so-called “Cumulated Hyperdistension” index quantifies the drop of compliance at higher PEEP levels due to overdistension. Vice versa, the so-called “Cumulated Collapse” index (both in %) quantifies the drop of compliance at lower PEEP levels as a result of atelectasis. These indices were applied to two cases of hypoxemic respiratory failure due to pneumonia.

In 2010, a concept for analysis of intratidal gas distribution (ITV) was presented by Lowhagen et al. [81]. In fact, using the intratidal global impedance change as a reference, the authors discretised the impedance change spatially into four horizontal layers and temporally into eight isovolume parts and were thus able to quantify the local fraction of air flowing into the different regions of interest (ROIs) during the eight inspiratory phases as a function of global tidal volume fraction. The authors also presented regional intratidal pressure-volume loops and introduced the concept of regional intratidal compliance computation. They reported on how regional intratidal compliance changes during a breath and as a function of PEEP during a moderate recruitment manoeuvre followed by a decremental PEEP trial. Finally, the authors presented results from a study involving 10 ARDS patients and demonstrated nicely in 3 selected cases how differently patients may respond to recruitment manoeuvres. In fact, regional intratidal compliance changes may serve as an indicator for responsiveness to recruitment, a subject which certainly deserves additional future investigations.

The concept of regional compliance was recently extended in an investigation involving 4 Yorkshire swine during a stepwise recruitment manoeuvre [82]. Gomez-Laberge et al. nicely demonstrated the reduction in compliance in the non-dependent layers and the corresponding increase in compliance in the

dependent layer of the lung when PEEP was increased stepwise.
By using two EIT silicone belts at the same time in different layers, Bikker et al. investigated the effect of varying the belt location in the cranio-caudal axis [83]. In a decremental PEEP trial following a recruitment manoeuvre (40 cmH_2O × 40 s), 12 mechanically ventilated post cardiac surgery patients were studied. The authors found that tidal impedance variation divided by tidal volume decreased in caudal EIT images, whereas it increased on the cranial EIT images. They also measured COV and found that this index decreased when PEEP decreased on both belt levels. The authors concluded that during a decremental PEEP trial, at least in this patient population, ventilation distribution may not only shift from the dorsal to ventral direction, but also from the caudal to cranial direction.

Besides assessing lung function in ventilated intensive care patients, EIT may also be used for extending diagnostic lung function procedures to include regional information in pneumological patients. Recently, new indices have been introduced for this specific application. In 2012, Zhao et al. studied the GI index in 14 patients with cystic fibrosis and in 14 healthy volunteers [84] and introduced the concept of regional MEF25/MEF75 maps to quantify regional obstruction during forced expiration manoeuvres.

In the same year, Pikkemaat et al. reported on preliminary results of the regional effects of using Salbutamol for broncho-spasmolysis in 8 paediatric patients with bronchial asthma [85]. For this, the authors introduced the new concept of the so-called “regional time constant maps” and were able to demonstrate diverse regional changes in the mechanical time constants, indicating inhomogeneous administration or effectiveness of the drug.

In 2012, Adler et al. published a comprehensive review and consensus paper [86] indicating different levels of maturity for EIT-based ventilation monitoring (quite mature) as compared to monitoring of perfusion, ventilation-to-perfusion mismatch and edema which still are at an early stage of investigation. The authors mentioned that various EIT measures have already been published which may capture different phenomena, but not the complete

12. EIT for guidance of respiratory therapy

More recently EIT has also been used to guide therapy directly, indicating its clinical relevance.

Based on regional compliance, Wolf et al. recently presented a three-step algorithm to adjust ventilation based on EIT. Mainly, the authors proposed to reverse atelectasis in the dorsal regions by raising PEEP in gradations of 5 cm H_2O ("recruitment") and then reduce overdistension in the ventral regions by decrementing PEEP in gradations of 2 cm H_2O while observing a potential decrease of compliance in the dorsal regions (PEEP titration). Their concept was evaluated in twelve Yorkshire swine, out of which 6 animals were ventilated based on the EIT algorithm and 6 were ventilated based on the ARDSnet protocol serving as a control group [87]. Ventilation time was 6 h. The authors concluded that EIT-guided ventilation resulted in improved respiratory mechanics, improved gas exchange, and reduced histologic evidence of ventilator-induced lung injury.

Bikker et al. investigated an oleic acid ARDS model in eight pigs and calculated regional ventilation loops from EIT [88]. Comparing ventilation distribution in EIT during an incremental and decremental PEEP trial, the authors could determine the optimal PEEP level.

In 16 piglets with a lavage model of ARDS, representing a neonatal model, Dargaville et al. used EIT to determine the best PEEP level [89]. In this experiment, the best PEEP level was defined by the most even ventilation distribution and regional ventilation loops displayed by EIT. While this approach may be arbitrary, this endpoint represents a clinical rationale and pathophysiological understanding.

The use of EIT to guide ventilation was also studied in four prospective

interventional trials.
In a study by Zhao et al. [78] EIT was used to find the “optimal” PEEP setting, i.e., the PEEP level that resulted in the most even distribution of ventilation across all lung regions. The authors analysed the EIT image for homogenous distribution of ventilation in 10 healthy patients during anaesthesia. They increased PEEP from 0 to 28 mbar in 2 mbar increments and analysed homogeneity at each PEEP level. In their patients, they found the best homogeneity of ventilation at a PEEP level of 14 mbar.

Lowhagen et al. used EIT in 16 patients with early acute lung injury to determine the potentially recruitable lung volume [52]. Based on this and the regional ventilation distribution shown in EIT, the authors could determine the best PEEP level.

A similar approach was chosen by Camporota et al. in two patients with severe ARDS [90]. Assessing the dynamic changes of ventilation distribution in EIT, the investigators could determine the potentially recruitable lung volume in both patients, and identify the one patient where a recruitment manoeuvre was possibly successful, while in the other patient no recruitable lung volume was identified.

Another study was conducted by Mauri et al. [49] in which EIT was used to identify the best combination of pressure support level and PEEP level. 10 patients with ARDS being ventilated with pressure support ventilation (PSV), the best combination of high-low PEEP with high-low pressure support was determined with EIT. The authors wanted to find the pressure combination that resulted in the best ventilation distribution. The combination of low pressure support with high PEEP appeared to be the best combination for this patient population.

The results of these studies clearly indicate that EIT provides useful information for optimising lung-protective ventilation. It is expected that more studies will investigate the value of EIT for guidance of respiratory therapy in the near future.

13. A Call for Consensus

As has been proposed in several publications already, EIT is considered to be about to become one of the central means to guide mechanical ventilation. In fact, In 2012, Adler et al. answered the hypothetical question “How could EIT improve outcomes?” by claiming that “EIT can guide lung protective ventilator settings” and “EIT can set lung protective ventilator settings faster” [86].

In this paper, the authors nicely sketch the past and future EIT research roadmap agenda by a subsequent series of steps which they called the “4 R series”: Firstly, EIT had to become “Reliable” (i.e. it had to correspond to gold standards like CT, SPECT, etc.) and “Reproducible” (which both have finally been achieved with the market introduction of Pulmovista 500).

It now has to become “Relevant” (i.e. EIT calculates parameters relevant to clinical practice) and it will finally become “Rewarding” (i.e. EIT will be capable of guiding therapy that results in better outcomes).

14. Examples of EIT status images

While radiological and EIT images both provide information about the regional distribution of air in the lungs, the image characteristics provided by these modalities are quite different.

The difference in spatial and temporal resolution has previously been discussed.

Radiological images of the lung provide information on the air content and reflect, depending on the moment the images were taken, the end-inspiratory or end-expiratory status, or a lung condition somewhere in between.

EIT images reflect the lung function, not the lung itself, which means EIT displays ventilated lung regions rather than morphological or anatomical structures of the lung.

Nonetheless, the regional information contained in EIT and CT images is closely related to each other when pathological conditions such as pleural effusion or atelectasis lead to non-aerated and non-ventilated lung regions. While CT images display lung regions with trapped air (e.g. pneumothorax) in black because of the large air content, EIT also displays those regions in black because they are not ventilated. Conversely a CT image may indicate a region of consolidated lung tissue in a white colour because of the high fluid content, while this region might be displayed in the EIT image in a black or dark blue colour, if this region is not or only partially ventilated.

In this chapter, various examples of EIT status images are provided as an introduction to the world of EIT images. Where available, radiographic chest images from the same patient are shown as well.

Please note that the comparability of the displayed EIT images and the related radiographic chest images or CT images may be limited due to the

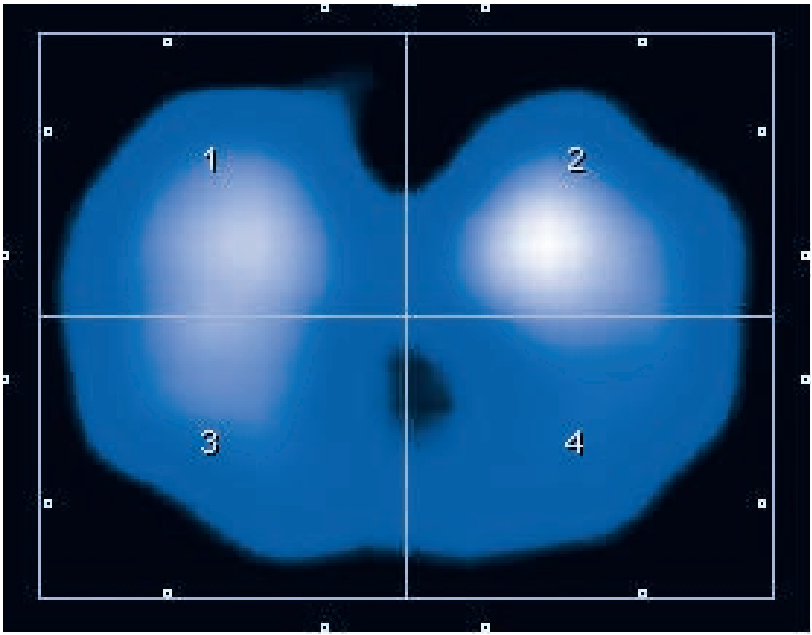

D-50-2011

Fig. 49: Tidal image of a healthy individual

fact that the images were taken at different times, and there may also be some variation in the caudo-cranial aspect of the images.

EXAMPLE 1: HEALTHY LUNG

Ventilation is quite evenly distributed over the quadrants of the image (ROI 1 = 28 %, ROI 2 = 26 %, ROI 3 = 25 %, ROI 4 = 21 %). Typically, the right lung (ROI 1 and ROI 3 in this ROI arrangement) receives 50 – 55 % of global ventilation (100 %) in a sitting or supine individual, which corresponds to findings in the literature [91]. This distribution changes significantly, even in healthy volunteers, during lateral positioning.

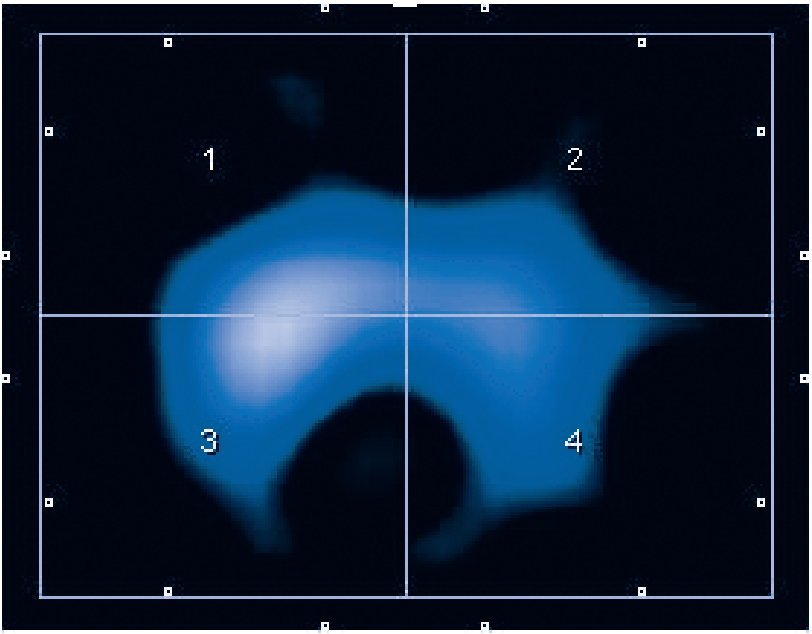

D-55-2011

Fig. 50: Tidal image of a healthy obese individual

EXAMPLE 2: HEALTHY LUNG OF AN OBESE VOLUNTEER

In obese individuals with healthy lungs, the distribution within the quadrants does not differ significantly (ROI 1 = 24 %, ROI 2 = 20 %, ROI 3 = 29 %, ROI 4 = 26 %) from individuals with normal body weight. However, the ventilated regions appear to be much smaller, as the lungs are surrounded by a large area of fatty tissue.

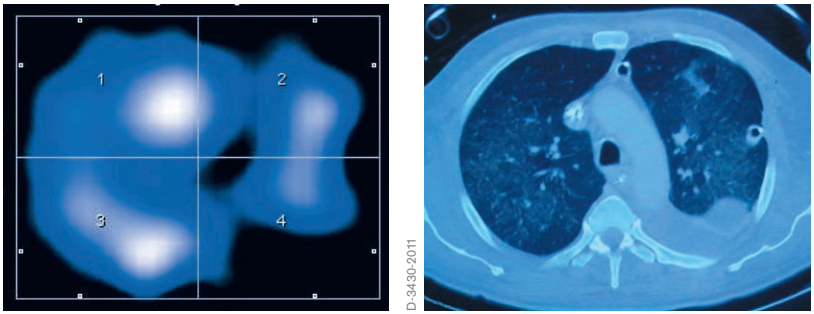

Fig. 51: Tidal image and corresponding CT image of a patient with pleural effusion in the left lung

EXAMPLE 3: PLEURAL EFFUSION

Fluid accumulation, such as a pleural effusion, represents a non-ventilated area; in the EIT image, this is displayed as a black area. On the CT image this region, due to its density, is shown as an area of higher contrast than the surrounding lung tissue.

The EIT image suggests a mediastinal displacement towards the left lung which was not visible in the CT image (taken about 5 hours earlier).

The non-ventilated area is reflected by significant reduction of regional ventilation in the lower right quadrant. The distribution of ventilation was ROI 1 = 35 %, ROI 2 = 20 %, ROI 3 = 31 %, ROI 4 = 14 %.

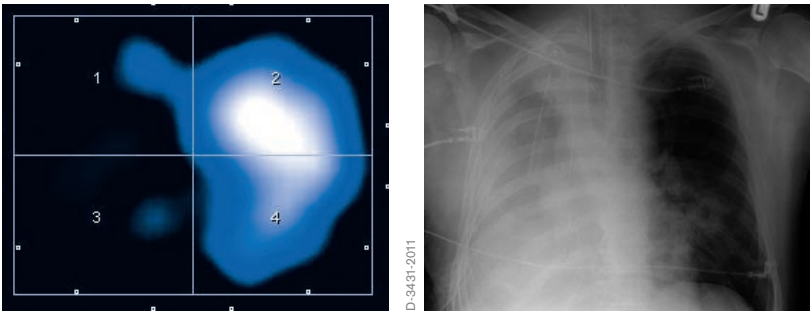

Fig. 52: Tidal image and corresponding chest X-ray of a patient with pneumonectomy

EXAMPLE 4: RIGHT SIDED PNEUMONECTOMY

As there is no ventilation in the right hemithorax after a pneumonectomy, the corresponding area on an EIT image (transverse plane) is black. In contrast on a chest X-ray (frontal plane) this area is white, as the right hemithorax is filled with fluid and connective tissue. The distribution of ventilation was ROI 1 = 2 %, ROI 2 = 55 %, ROI 3, = 1 %, ROI 4 = 42 %.

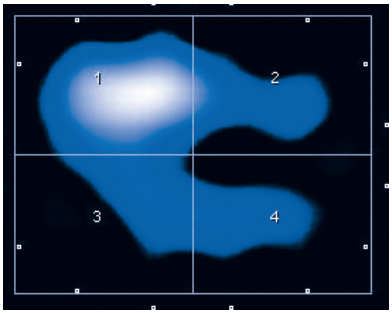

D-52-2011

D-3432-2011

Fig. 53: Tidal image and corresponding CT image of a patient with a pneumothorax in the left lung

EXAMPLE 5: PNEUMOTHORAX

This EIT image reveals that most of the ventilation is occurring in ROI 1; the cause of the poor distribution is revealed by the more anatomically specific CT image: a pneumothorax (marked by the blue line) in the ventral region of the left lung and bilateral dorsal atelectasis and effusion.

ROI 1 is receiving 56 % of the “Tidal Variation” while, due to the pneumothorax, ROI 2 is receiving just 16 % of the global “Tidal Variation” and due to the dorsal pathology ROI’s 3 and 4 are receiving just 15 and 13 % respectively.

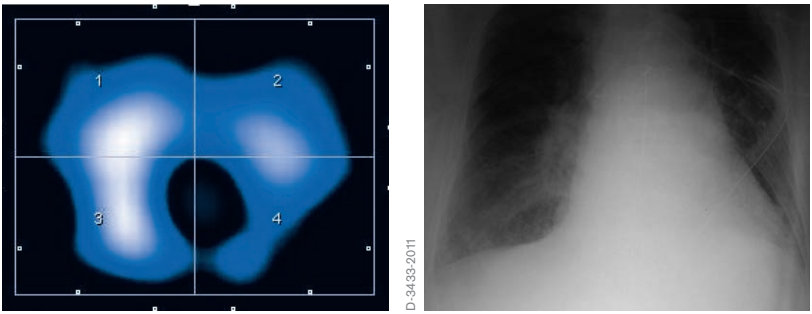

Fig. 54: Tidal image and corresponding chest X-ray of a patient with dorsal atelectasis

EXAMPLE 6: ATELECTASIS

The EIT image shows that the functional impairment of the two basal lung regions was not symmetrical even though the chest X-ray indicates bilateral atelectasis. The basal portions of the right lung, (ROI 3) still received 31 % of the global “Tidal Variation” while the corresponding area of the left lung, (ROI 4) only received 15 %.

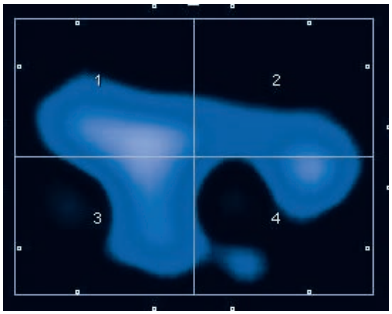

D-57-2011

D-3434-2011

Fig. 55 Tidal image and corresponding CT image of a patient with dystelectasis

EXAMPLE 7: DYSTELECTASIS

The CT Scan shows marked dystelectasis in the dependent (dorsal) region of the left lung with fluid accumulation, and smaller dystelectic areas in the dependent areas of the right dorsal lung. The shape of the ventilated regions as displayed in the EIT image does not match the lung regions filled with air in the CT image. However, the impaired ventilation in the left lower lobe is clearly reflected in ROI 4 of the EIT image.

"Tidal Variations" were highly unevenly distributed within ROI 1 (35 %) and ROI 2 (19 %). The lack of ventilation in the upper part of those regions suggests overdistension of the upper lung regions.

ROI 3 received 27 % of the global "Tidal Variation", while the regional "Tidal Variation" (20 %) in ROI 4 was only accessing the upper third of ROI 4, due to the dystelectasis.

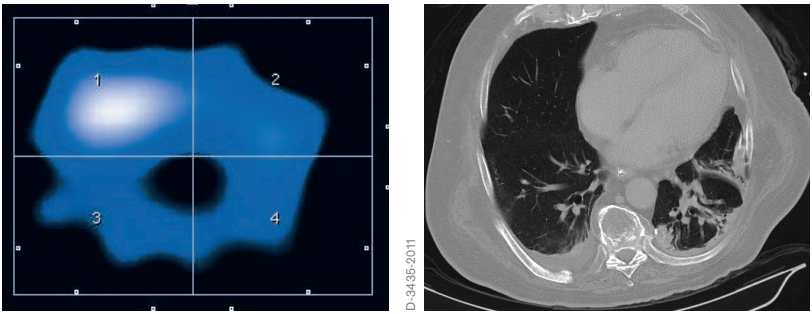

Fig. 56: Tidal image and corresponding CT image of an ARDS patient

EXAMPLE 8: ARDS

The CT scan shows a typical inhomogeneous air distribution of an ARDS patient. The dorsal parts of both lungs (left more than right) were especially impaired. In the EIT image, this inhomogeneity is reflected by reduced ventilation in both dorsal quadrants: 16 % (ROI 3) and 14 % (ROI 4), while the ventral regions received 46 % (ROI 1) and 23 % (ROI 2).

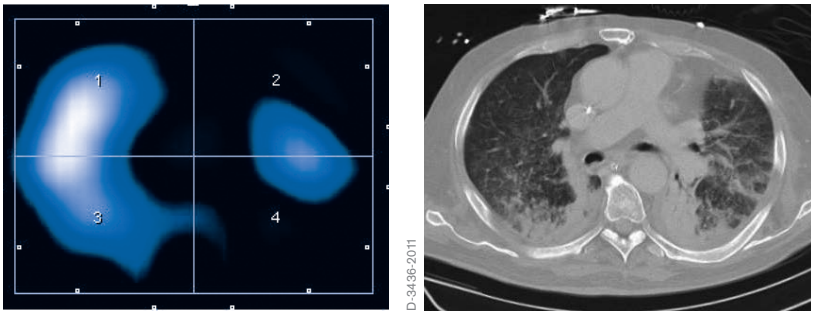

Fig. 57: Tidal image and corresponding CT image of an ARDS patient

EXAMPLE 9: ARDS

The CT scan shows the typical picture of late ARDS with diffuse infiltrates throughout nearly all lung regions. While the CT scan seems to show no major difference in the severity of alteration between both lungs, the EIT image shows a very uneven distribution of Tidal Variations. The upper right lung (ROI 1) received 46 %, the lower right lung (ROI 3) 39 %. The impedance waveforms revealed a significantly delayed filling in ROI 2 and ROI 4, leaving just 15 % of the tidal volume (ROI 2 = 5 %; ROI4 = 10 %) for the left lung. This example shows how EIT can provide additional information compared with other non-dynamic imaging modalities.

15. Outlook

Prior to the introduction of PulmoVista 500, all EIT devices were solely used in clinical and pre-clinical research, which means that at present there is still limited experience in using information from EIT in daily clinical practice.

It is anticipated that, initially, experts in mechanical ventilation and respiratory monitoring will rapidly gain further experience in using EIT in daily clinical practice now that PulmoVista 500 has been made available by Dräger.

At the same time however, the availability of PulmoVista 500 will probably also boost further research activities, as from now on EIT data can conveniently and reliably be collected over hours with an approved medical device.

For example, various approaches to the extraction of diagnostic information from EIT data have already been described by researchers: in the future these methods might be established as being suitable to notify the clinician about lung conditions that need to be avoided, such as overdistension or cyclic opening and closing of lung regions.

Costa et al. [80] have described an algorithm that estimates recruitable alveolar collapse and hyperdistension utilising EIT data collected during a decremental PEEP trial. Recently Löwhagen et al. [92] developed an algorithm to assess the regional redistribution of gas throughout the inspiratory phase during a decremental PEEP trial, subsequent to a recruitment manoeuvre.

It becomes more and more obvious that the greatest value in the diagnostic interpretation of EIT data can be obtained when algorithms are applied

during therapeutic manoeuvres that induce regional redistribution of tidal volumes and changes of end-expiratory lung volumes. It is this specific information that reveals how the lungs of the individual patient respond to different ventilation strategies.

Not surprisingly, initial approaches have already been described [25] about using EIT-based diagnostic information as an input source for future expert systems which automatically adjust ventilator settings according to the requirements of the individual patient, thus continuously maintaining lung protective ventilation strategies.

Another application field receiving increasing interest within the research community is the EIT-based estimation of regional distribution of pulmonary perfusion. While the approaches described so far [93, 94, 95] certainly need further validation, such supplementary information would be of even greater clinical value to the physician, as for the first time, not only the distribution of ventilation but also the regional ventilation/perfusion ratio could be determined non-invasively and continuously at the bedside.

In the research setup, early EIT devices have also been used with promising results to assess the amount of extravascular lung water [72], thus providing means to monitor lung edema. The latest experiments in this field [96, 97] utilised impedance spectroscopy where – in contrast to EIT – the frequency of the applied alternating current varies over a broad band. The generation of spectral information allows a classification or separation of different tissue types, a method which is also utilised by conventional body composition monitors.

In conclusion, even after 30 years of research and development, the field of EIT remains dynamic and vibrant, stimulating clinicians, researchers and developers in their quest for further enhancement and new applications. The market introduction of PulmoVista 500 is clearly a significant milestone

Appendix I: Literature references

1 Gattinoni L, Pesenti A, Bombino M, Baglioni S, Rivolta M, Rossi F, Rossi G, Fumagalli R, Marcolin M, Mascheroni D, Torresin A. Relationships between lung computed tomographic density, gas exchange, and PEEP in Acute Respiratory Failure. Anesthesiology 1988; 69: 824-832

2 Slutsky AS, Tremblay LN. Multiple system organ failure. Is mechanical ventilation a contributing factor? Am J Respir Crit Care Med 1998; 157: 1721-1725

3 Simon BA, Easley RB, Grigoryev DN et al. Microarray analysis of regional cellular responses to local mechanical stress in acute lung injury. Am J Physiol Lung Cell Mol Physiol 2006; 291: L851-L86

4 Ranieri VM, Suter PM, Tortorella C, et al. Effect of mechanical ventilation on inflammatory mediators in patients with acute respiratory distress syndrome – A randomized controlled trial. JAMA 1999; 282: 54-61

5 Gentile MA, Cheifetz IM. Optimal positive end-expiratory pressure: The search for the Holy Grail continues. Crit Care Med 2004; 32: 2553-2554

6 Markhorst D, Kneyber M, van Heerde M. The quest for optimal positive endexpiratory pressure continues. Crit Care 2008; 12: 408

7 Crotti S, Mascheroni D, Caironi P et al. Recruitment and derecruitment during acute respiratory failure: a clinical study. Am J Respir Crit Care Med 2001; 164: 131-140

8 Pelosi P, Goldner M, McKibben A et al. Recruitment and derecruitment during acute respiratory failure: an experimental study. Am J Respir Crit Care Med 2001; 164: 122-130

9 Kunst PW, Vazquez de Anda G, Bohm SH, Faes TJ, Lachmann B, Postmus PE, de Vries PM. Monitoring of recruitment and derecruitment by electrical impedance tomography in a model of acute lung injury. Crit Care Med 2000; 28: 3891-3895.

10 Kunst PW, Bohm SH, Vazquez de Anda G, Amato MB, Lachmann B, Postmus PE, de Vries PM. Regional pressure volume curves by electrical impedance tomography in a model of acute lung injury. Crit Care Med 2000; 28: 178-183

11 Genderingen HR, Vught AJ, Jamsen JRC. Estimation of regional volume changes by electrical impedance tomography during a pressure-volume maneuver. Intensive Care Med 2003; 29: 233-240

12 Holder DS. Clinical and physiological applications of Electrical Impedance Tomography. UCL Press 1993; ISBN 1-85728-164-0 HB

13 Holder DS. Electrical Impedance Tomography Methods, History and Applications. IOP 2005; ISBN 0 7503 0952 0

14 Arnold JH. Electrical impedance tomography: On the path to the Holy Grail. Crit Care Med 2004; 32: 894-895

15 Hinz J, Hahn G, Quintel M. Elektrische Impedanztomographie – Reif für die klinische Routine bei beatmeten Patienten? Anaesthesist 2008; 57: 61-69

16 Barber DC, Brown BH. Recent developments in applied potential tomography-APT. In: Proceedings of 9th Conference on Information Processing in Medical Imaging. Ed. S.L. Bacharach, Martinus Nijhoff, Dordrecht 1986; pp. 106-121

17 Yorkey TJ, Webster JG, Tompkins WJ. Comparing Reconstruction Algorithms for Electrical Impedance Tomography. IEEE Trans. On Biomedical Engineering 1987; vol 34, no. 11, pp. 843-852

18 Faes TJ, Meij HA van der, Munck JC de, Heethaar RM. The electric resistivity of human tissues (100 Hz–10 MHz): a meta-analysis of review studies. Physiol Meas 1999; 20: R1-10

19 Barber DC. A review of image reconstruction techniques for electrical impedance tomography. Med Phys 1989; 16 (2): 162-169

20 Eyuboglu BM, Brown BH. Methods of cardiac gating applied potential tomography. Clin Phys Physiol Meas 1988; 9 (Suppl A): 43–48

21 Bikker IG et al. Lung volume calculated from electrical impedance tomography in ICU patients at different PEEP levels. Intensive Care Med. 2009 Aug; 35(8): 1362-7. Epub 2009 Jun 10

22 Hinz et al. End-expiratory lung impedance change enables bedside monitoring of end-expiratory lung volume change. Intensive Care Med 2003; 29:37–43

23 Odenstedt H, Lindgren S, Olegard C, Erlandsson K, Lethvall S, Aneman A, Stenqvist O, Lundin S. Slow moderate pressure recruitment maneuver minimizes negative circulatory and lung mechanic side effects: evaluation of recruitment maneuvers using electric impedance tomography. Intensive Care Med 2005; 31: 1706-1714.

24 Bikker IG, Leonhardt S, Miranda DR, Bakker J, Gommers D. Bedside measurement of changes in lung impedance to monitor alveolar ventilation in dependent and non-dependent parts by electrical impedance tomography during a positive end-expiratory pressure trial in mechanically ventilated intensive care unit patients. Critical Care 2010; 14: R100 1-9

25 Luepschen H, Meier T, Grossherr M, Leibecke T, Karsten J, Leonhardt S. Protective ventilation using electrical impedance tomography. Physiol Meas 2007; 28: S247-S260.

26 Hickling KG. Reinterpreting the pressure-volume curve in patients with acute respiratory distress syndrome. Current Opinion in Critical Care 2002; Vol 8-1, 32-38

27 Reske AW. Analysis of the nonaerated lung volume in combinations of single computed tomography slices – is extrapolation to the entire lung feasible? Critical Care Volume 11 Suppl 2, 27th International Symposium on Intensive Care and Emergency Medicine 2007; P206, p.85

28 Hahn G. et al. Imaging pathologic pulmonary air and fluid accumulation by functional and absolute EIT. Physiol. Meas. 2006; 27 1-12

29 Leonhardt S, Lachmann B. Electrical impedance tomography: the holy grail of ventilation and perfusion monitoring? Intensive Care Med. 2012 Dec; 38(12):1917-29. doi: 10.1007/s00134-012-2684-z.

30 Adler A, Amyot R, Guardo R, Bates JH, Berthiaume Y. Monitoring changes in lung air and liquid volumes with electrical impedance tomography. J Appl Physiol 1997; 83:1762–1767.

31 Meier T, Leibecke T, Eckmann C, Gosch UW, Grossherr M, Bruch HP, Gehring H, Leonhardt S. Electrical impedance tomography: changes in distribution of pulmonary ventilation during laparoscopic surgery in a porcine model. Langenbecks Arch Surg 2006; 391:383–389.

32 Luepschen H et al. Clinical applications of thoracic electrical impedance tomography. 6th Conference on Biomedical Applications of Electrical Impedance Tomography. London, June 22-24, 2005.

33 Hinz J, Neumann P, Dudykevych T, Andersson LG, Wrigge H, Burchardi H, Hedenstierna G. Regional Ventilation by Electrical Impedance Tomography: A Comparison With Ventilation Scintigraphy in Pigs. Chest 2003; 124:314-32.

34 Frerichs I, Hinz J, Herrmann P, Weisser G, Hahn G, Dudykevych T, Quintel M, Hellige G. Detection of local lung air content by electrical impedance tomography compared with electron beam CT. J Appl Physiol 2002; 93:660-666.

35 Frerichs I, Schmitz G, Pulletz S, Schadler D, Zick G, Scholz J, Weiler N. Reproducibility of regional lung ventilation distribution determined by electrical impedance tomography during mechanical ventilation. Physiol Meas 2007; 28:S261-267.

36 Van Genderingen HR, Vught AJ, Jamsen JRC. Estimation of regional volume changes by electrical impedance tomography during a pressure-volume maneuver. Intensive Care Med 2003; 29:233-240.

37 Meier T, Luepschen H, Karsten J, Leibecke T, Grossherr M, Gehring H, Leonhardt S. Assessment of regional lung recruitment and derecruitment during a PEEP trial based on electrical impedance tomography. Intensive Care Med 2008; 34: 543-550.

38 Hinz J, Hahn G, Neumann P, Sydow M, Mohrenweiser P, Hellige G, Burchardi H. End-expiratory lung impedance change enables bedside monitoring of end-expiratory lung volume change. Intensive Care Med 2003; 29:37–43

39 Marquis F, Coulombe N, Costa R, Gagnon H, Guardo R, Skrobik Y. Electrical impedance tomography's correlation to lung volume is not influenced by anthropometric parameters. J Clin Monit Comput 2006; 20:201–207.

40 Victorino JA, Borges JB, Okamoto VN, Matos GF, Tucci MR, Caramez MP, Tanaka H, Sipmann FS, Santos DC, Barbas CS, Carvalho CR, Amato MB. Imbalances in regional lung ventilation: a validation study on electrical impedance tomography. Am J Respir Crit Care Med 2004; 169: 791-800

41 Riedel T, Richards T, Schibler A. The value of electrical impedance tomography in assessing the effect of body position and positive airway pressures on regional lung ventilation in spontaneous breathing subjects. Intensive Care Med 2005; 31: 1522-1528

42 Bikker IG, Leonhardt S, Bakker J, Gommers D. Lung volume calculated from electrical impedance tomography in ICU patients at different PEEP levels. Intensive Care Med 2009; 35:1362–1367. DOI 10.1007/ s00134-009-1512-6.

43 Karsten J, Meier T, Iblher P, Schindler A, Paarmann H, Heinze H. The suitability of EIT to estimate EELV in a clinical trial compared to oxygen wash-in/wash-out technique. Biomed Tech (Berl). 2014; 59(1): 59-64. doi: 10.1515/bmt-2012-0076

44 Brenner D, Elliston C, Hall E, Berdon W. Estimated risks of radiation-induced fatal cancer from pediatric CT. AJR Am J Roentgenol 2001; 176: 289-296.

45 Brenner DJ, Hall EJ. Computed tomography – an increasing source of radiation exposure. N Engl J Med 2007; 357: 2277-2284.

46 Wrigge H. et al. Electrical impedance tomography compared with thoracic computed tomography during a slow inflation maneuver in experimental models of lung injury. Crit Care Med 2008; 36(3): 1-7.

47 Erlandson K et al. Positive end-expiratory pressure optimization using electric impedance tomography in morbidly obese patients during laparoscopic gastric bypass surgery. Acta Anaesthesiol Scand 2006; 50: 833-839.

48 Hinz J, Gehoff A, Moerer O, Frerichs I, Hahn G, Hellige G, Quintel M. Regional filling characteristics of the lungs in mechanically ventilated patients with acute lung injury. Eur J Anaesthesiol 2007; 24: 414-424.

49 Mauri T, Bellani G, Confalonieri A, Tagliabue T, Turella M, Coppadoro A, Citerio G, Patroniti N, Pesenti A. Topographic Distribution of Tidal Ventilation in Acute Respiratory Distress Syndrome: Effects of Positive End-Expiratory Pressure and Pressure Support. Critical Care Med 2013; 41(7). DOI: 10.1097/CCM.0b013e318287f6e7.

50 Karsten J, Luepschen H, Grossherr M, Bruch HP, Leonhardt S, Gehring H, Meier T. Effect of PEEP on regional ventilation during laparoscopic surgery monitored by electrical impedance tomography. Acta Anaesthesiol Scand 2011; 55:878 – 86.

51 Gattinoni L, Caironi P, Cressoni M, Chiumello D, Ranieri VM, Quintel M, Russo S, Patroniti N, Cornejo R, Bugedo G. Lung recruitment in patients with the acute respiratory distress syndrome. N Engl J Med 2006; 354: 1775–86.

52 Lowhagen K, Lindgren S, Odenstedt H, Stenqvist O, Lundin S. A new non-radiological method to assess potential lung recruitability: a pilot study in ALI patients. Acta Anaesthesiol Scand 2011; 55: 165–174.

53 Frerichs I. et al. Topographic distribution of lung ventilation in artificially ventilated babies. In: Heart and Lung Assistance (Lecture Notes of the ICB Seminars), Eds. Z. Religa, Z. Rondio, G. Ferrari, M. Darowski; International Centre of Biocybernetics, Warsaw, 2000; 115-121.

54 Putensen C. Electrical impedance tomography guided ventilation therapy. Current Opinion in Critical Care 2007; 13: 344-350.

55 Lindgren S, Odenstedt H, Olegård C, Söndergaard S, Lundin S, Stenqvist O. Regional lung derecruitment after endotracheal suction during volume- or pressure-controlled ventilation: a study using electric impedance tomography. Intensive Care Med 2007; 33: 172-180.

56 Lindgren S, Odenstedt H, Erlandsson K, Grivans C, Lundin S, Stenqvist O. Bronchoscopic suctioning may cause lung collapse: a lung model and clinical evaluation. Acta Anaesthesiol Scand. 2008; 52: 209-218.

57 van Veenendaal MB, Miedema M, de Jongh FHC, van der Lee JH, Frerichs I, van Kaam AH. Effect of closed endotracheal suction in high-frequency ventilated premature infants measured with electrical impedance tomography. Intensive Care Med 2009; 35:2130–2134.

58 Tingay DG, Copnell B, Grant CA, Dargaville PA, Dunster KR, Schibler A. The effect of endotracheal suction on regional tidal ventilation and end-expiratory lung volume. Intensive Care Med 2010; 36:888–896.

59 Corley A, Spooner AJ, Barnett AG, Caruana LR, Hammond NE, Fraser JF. End-expiratory lung volume recovers more slowly after closed endotracheal suctioning than after open suctioning: a randomized crossover study. J Crit Care 2012 Dec; 27(6): 742.e1-7.

60 Alsaghir AH, Martin CM. Effect of prone positioning in patients with acute respiratory distress syndrome: a meta-analysis. Crit Care Med 2008; 36: 603-609.

61 Sud S, Sud M, Friedrich JO, Adhikari NK. Effect of mechanical ventilation in the prone position on clinical outcomes in patients with acute hypoxemic respiratory failure: a systematic review and meta-analysis. CMAJ 2008; 178: 1153-1161.

62 Heinrich S, Schiffmann H, Frerichs A, Klockgether-Radke A, Frerichs I. Body and head position effects on regional lung ventilation in infants: An electrical impedance tomography study. Intensive Care Med 2006; 32: 1392-1398.

63 Bein T, Ploner F, Ritzka M, Pfeifer M, Schlitt HJ, Graf BM. No change in the regional distribution of tidal volume during lateral posture in mechanically ventilated patients assessed by electrical impedance tomography. Clin Physiol Funct Imaging 2010; 30(4): 234-240.

64 Steinmann D. Electrical impedance tomography to confirm correct placement of double-lumen tube: a feasibility study. British Journal of Anaesthesia 2008; 101(3): 411-418.

65 Steinmann D, Engehausen M, Stiller B, Guttmann J. Electrical impedance tomography for verification of correct endotracheal tube placement in paediatric patients: a feasibility study. Acta Anaesthesiol Scand. 2013 Aug; 57(7):881-7.

66 de Lassence A, Timsit JF, Tafflet M, Azoulay E, Jamali S, Vincent F, Cohen Y, Garrouste-Orgeas, M, Alberti C, Dreyfuss D. Pneumothorax in the Intensive Care Unit. Anesthesiology 2006; 104:5–13.

67 Hahn G, Just A, Dudykevych T, Frerichs I, Hinz J, Quintel M, Hellige G. Imaging pathologic pulmonary air and fluid accumulation by functional and absolute EIT. Physiol. Meas 2006; 27:S187–S198. doi:10.1088/0967-3334/27/5/S16

68 Costa EL, Chaves CN, Gomes S, Beraldo MA, Volpe MS, Tucci MR, Schettino IA, Bohm SH, Carvalho CR, Tanaka H, Lima RG, Amato MB. Real-time detection of pneumothorax using electrical impedance tomography. Crit Care Med 2008; 36:1230–1238.

69 Preis C, Luepschen H, Leonhardt S, Gommers D. Experimental case report: development of a pneumothorax monitored by electrical impedance tomography. Clin Physiol Funct Imaging 2009 29:159–162.

70 Miedema M, Frerichs I, de Jongh FHC, van Veenendaal MB, van Kaam AH. Pneumothorax in a Preterm Infant Monitored by Electrical Impedance Tomography: A Case Report. Neonatology 2011; 99:10–13.

71 Bhatia R, Schmoelzer GM, Davis PG, Tingay DG. Electrical impedance tomography can rapidly detect small pneumothoraces in surfactant-depleted piglets. Intensive Care Med 2012; 38:308–315.

72 Kunst PW, Vonk Noordegraaf A, Raaijmakers E, Bakker J, Groeneveld AB, Postmus PE, de Vries PM. Electrical impedance tomography in the assessment of extravascular lung water in noncardiogenic acute respiratory failure. CHEST 1999; 116:1695–1702.

73 Arad M, Zlochiver S, Davidson T, Shoenfeld Y, Adunsky A, Abboud S. The detection of pleural effusion using a parametric EIT technique. Physiol Meas 2009; 30:421–428.

74 Frerichs I, Hahn G, Golisch W, Kurpitz M, Burchardi H, Hellige G. Monitoring perioperative changes in distribution of pulmonary ventilation by functional electrical impedance tomography. Acta Anaesthesiol Scand 1998; 42:721–726.

75 Radke OC, Schneider T, Heller AR, Koch T. Spontaneous Breathing During General Anesthesia Prevents the Ventral Redistribution of Ventilation as Detected by Electrical Impedance Tomography – A Randomized Trial. Anesthesiology. 2012 Jun; 116(6):1227-34. doi: 10.1097/ALN.0b013e318256ee08.

76 Luepschen H, Meier T, Muders T, Konowalczyk S, Leonhardt S, Putensen C. Individualized, Automated Lung Recruitment Using Electrical Impedance Tomography In A Porcine ARDS Mode. 2011 American Thoracic Society (ATS) International Conference, May 13-18, 2011 / Denver, Colorado. Abstract 19952

77 Zhao Z, Moller K, Steinmann D, Frerichs I, Guttmann J. Evaluation of an electrical impedance tomography-based global inhomogeneity index for pulmonary ventilation distribution. Intensive Care Med 2009; 35:1900–1906.

78 Zhao Z, Steinmann D, Frerichs I, Guttmann J, Moller K. PEEP titration guided by ventilation homogeneity: a feasibility study using electrical impedance tomography. Crit Care 2010; 14:R8.

79 Muders T, Luepschen H, Putensen C. Regional Ventilation Delay Index: Detection of Tidal Recruitment using Electrical Impedance Tomography. Yearbook of Intensive Care and Emergency Care 2009; 405-412.

80 Costa EL, Borges JB, Melo A, Suarez-Sipmann F, Toufen C Jr, Bohm SH, Amato MB. Bedside estimation of recruitable alveolar collapse and hyperdistension by electrical impedance tomography. Intensive Care Med 2009; 35:1132–1137

81 Lowhagen K, Lundin S, Stenqvist O. Regional intratidal gas distribution in acute lung injury and acute respiratory distress syndrome – assessed by electric impedance tomography. Minerva Anestesiol. 2010 Dec; 76(12):1024-35.

82 Gomez-Laberge C, Arnold JH, Wolf GK. A unified approach for EIT imaging of regional overdistension and atelectasis in acute lung injury. IEEE Trans Med Imaging 2012; 31:834–842

83 Bikker IG, Preis C, Egal M, Bakker J, Gommers D. Electrical impedance tomography measured at two thoracic levels can visualize the ventilation distribution changes at the bedside during a decremental positive end-expiratory lung pressure trial. Critical Care 2011, 15:R193.

84 Zhao Z, Fischer R, Frerichs I, Müller-Lissed U, Möller K. Regional ventilation in cystic fibrosis measured by electrical impedance tomography. Journal of Cystic Fibrosis, September 2012; 11(5): 412–418.

85 Pikkemaat R, Tenbrock K, Lehmann S, Leonhardt S. Electrical impedance tomography: New diagnostic possibilities using regional time constant maps. Applied Cardiopulmonary Pathophysiology 2012; 16:212-225.

86 Adler A, Amato MB, Arnold JH, Bayford R, Bodenstein M, Böhm SH, Brown BH, Frerichs I, Stenqvist O, Weiler N, Wolf GK. Whither lung EIT: Where are we, where do we want to go and what do we need to get there? Physiol. Meas. 2012; 33:679–694.

87 Wolf GK, Gómez-Laberge C, Rettig JS, Vargas SO, Smallwood CD, Prabhu SP, Vitali SH, Zurakowski D, Arnold JH. Mechanical ventilation guided by electrical impedance tomography in experimental acute lung injury. Crit Care Med. 2013; May; 41(5):1296-304.

88 Bikker IG, Blankman P, Specht P, Bakker J, Gommers D. Global and regional parameters to visualize the ‚best' PEEP during a PEEP trial in a porcine model with and without acute lung injury. Minerva Anestesiol. 2013 Sep; 79(9):983-92.

89 Dargaville PA, Rimensberger PC, Frerichs I. Regional tidal ventilation and compliance during a stepwise vital capacity manoeuvre. Intensive Care Med. 2010 Nov; 36(11):1953-61.

90 Camporota L, Smith J, Barrett N, Beale R. Assessment of regional lung mechanics with electrical impedance tomography can determine the requirement for ECMO in patients with severe ARDS. Intensive Care Med. 2012 Dec; 38(12):2086-7.

91 Pierre AF. Pneumonectomy: historical perspective and prospective insight. Eur J Cardiothorac Surg 2003; 23:439-445

92 Löwhagen K, Lundin S, Stenqvist O. Regional intratidal gas distribution in acute lung injury and acute respiratory distress syndrome. Minerva Anestesiol 2010; 76 (12): 1024-1035

93 Fagerberg A, Stenqvist O, Åneman A. Monitoring pulmonary perfusion by electrical impedance tomography: an evaluation in a pig model. Acta Anaesthesiol Scand 2009; 53: 152-158

94 Smit HJ et al. Electrical impedance tomography to measure pulmonary perfusion: is the reproducibility high enough for clinical practice? Physiol. Meas. 2003; 24: 491-499

95 Deibele JM, Lüpschen H, Leonhardt S. Dynamic separation of pulmonary and cardiac changes in electrical impedance tomography. Physiol. Meas. 2008; 29: S1–S14

96 Mayer M, Brunner P, Merwa R, et al. Direct reconstruction of tissue parameters from differential multi-frequency EIT in vivo. Physiol Meas 2006; 27: S93–S101

97 Beckmann L, Cordes A, Saygili E, Schmeink A, Schauerte P, Walter M, Leonhardt S. Monitoring of body fluid in patients with chronic heart failure using Bioimpedance-Spectroscopy. World Congress on Medical Physics and Biomedical Engineering 2009; Munich; Sep. 7-12

98 Bodenstein M, David M, Markstaller K. Principles of electrical impedance tomography and its clinical application. Crit Care Med 2009; Vol. 37, No. 2, p. 1-12

99 Geddes LA, Baker LE. The specific resistance of biological material – a compendium of data for the biomedical engineer and physiologist. Med Biol Eng 1967; 5: 271–293

100 Heyward VH. Practical body composition assessment for children, adults, and older adults. Int J Sport Nutr 1998; 8: 285–307

101 Nopp P, Rapp E, Pfützner H, Nakesch H, Ruhsam Ch. Dielectric properties of lung tissue as a function of air content. Phys. Med. Biol. 38 1993; p. 699-716

102 Nopp P, Harris ND, Zhao TX, Brown BH. Model for the dielectric properties of human lung tissue against frequency and air content. Med. & Biol. Engin. & Computing 1997; p 695-702

103 Bernard GR, Artigas A, Brigham KL, Carlet J, Falke K, Hudson L, Lamy M, Legall JR, Morris A, Spragg R. The American-European Consensus Conference on ARDS. Definitions, mechanisms, relevant outcomes, and clinical trial coordination. Am J Respir Crit Care Med. 1994 Mar; 149(3 Pt 1):818-24.

104 Ferguson ND, Fan E, Camporota L, Antonelli M, Anzueto A, Beale R, Brochard L, Brower R, Esteban A, Gattinoni L, Rhodes A, Slutsky AS, Vincent J-L, Rubenfeld GD, Thompson BJ. The Berlin definition of ARDS: an expanded rationale, justification, and supplementary material. Intensive Care Med (2012) 38:1573–1582

Appendix II: Determining the biological impedance of the lung

Before the term bioimpedance can be fully understood, a basic understanding of electrical impedance is necessary.

DEFINITION OF ELECTRICAL IMPEDANCE

Electrical impedance, or simply impedance, describes a measure of opposition of a material to a sinusoidal alternating current (AC).

Electrical impedance extends the concept of resistance R described by Ohm's law (V=I*R) to AC circuits. Impedance describes not only the relative amplitudes of the voltage V and current I, but also their relative phases.

As both capacitors and inductors cause either negative or positive phase shifts between voltage and current, the term impedance is generally applied when electrical AC circuits contain capacitive and/or inductive elements.

HOW TO EXPRESS IMPEDANCE

Mathematically, electrical impedance $\tilde{Z}$ describes a complex number: it consists of a real and an imaginary component. Dimensionally, impedance is the same as resistance; the SI unit is the Ohm (Ω) for both entities.

There are two ways to express impedance mathematically:

Polar Form: $\tilde{Z} = Ze^{j\theta}$

The polar form conveniently captures both magnitude and phase characteristics, where the magnitude Z represents the ratio of the amplitude of the voltage difference to the current amplitude, while the argument θ gives the phase difference between voltage and current and j is the imaginary unit.

Cartesian Form: $\tilde{Z} = R + jX$

In the Cartesian representation, the real part of impedance is the resistance R and the imaginary component is the reactance X.
In the literature, the graph displayed in fig. 58 is often used to illustrate the relationship between resistance R, reactance X and impedance $\tilde{Z}$.

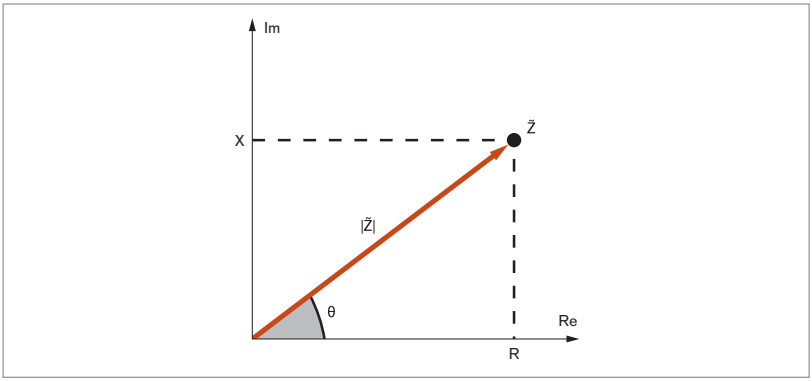

Fig. 58: Relationship between R, reactance X and impedance $\tilde{Z}$

The impedance of an ideal resistor is purely real and is referred to as a resistive impedance $\tilde{Z}_R = R$

Ideal inductors L and capacitors C have a purely imaginary reactive impedance. $\tilde{Z}_L = j\omega L$ $\tilde{Z}_C = \frac{1}{j\omega C}$

The term ω equals 2πf. This means that the impedance of an inductor and a capacitor, and thus the electrical behaviour of inductive or capacitive AC circuits, is a function of the frequency of the applied alternating current. Thus, the impedance expresses the effects of those AC circuits or materials on phase shifts between voltage and current.

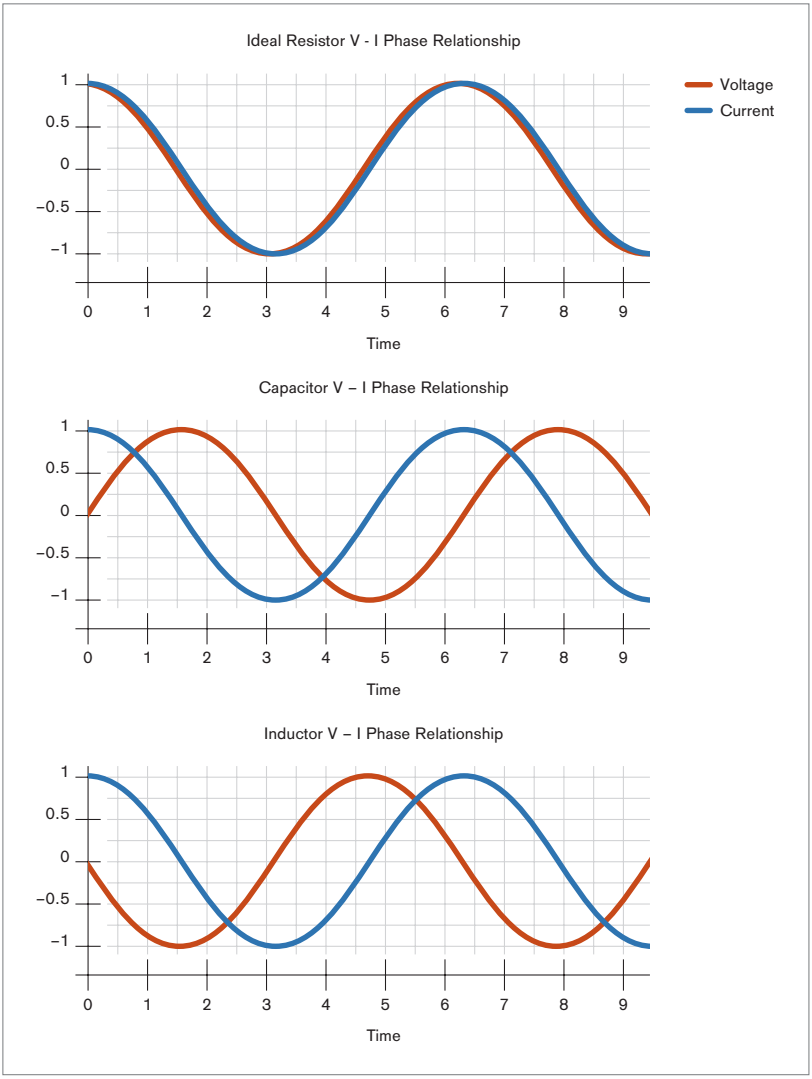

Fig. 59: V-I phase relationships of resistors, inductors and capacitors

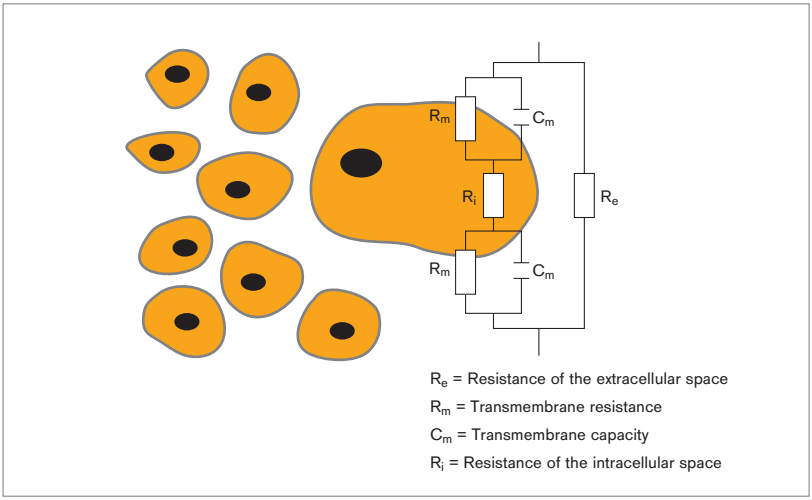

D-78-2011

Fig. 60: Equivalent circuit diagram of biological tissue

BIOIMPEDANCE

Bioimpedance is a term used to describe the response of a living organism to an externally applied alternating electric current. It is a measure of the opposition of biological tissue to the flow of that electric alternating current.

The living organism mainly consists of cells of various different structures and the extracellular fluid which is located in the interstitial space.

With regard to bioelectric properties, biological tissue can be thought of as a complex microscopic network of electrical circuits. As the structures of adjacent cells act as trans-membrane capacitors, biological tissue has, in addition to its resistive properties, a capacitance as well, which is illustrated in Fig. 60.

As in the electric circuits described above, the bioelectrical properties of a specific tissue depend on the frequency of the applied alternating current.

The transition from a microscopic to a macroscopic view leads to a simplified electrical circuit (Fig. 61), where the specific tissue impedance is simulated by a parallel connection of a capacitor C and a resistor $R_0 - R_{00}$.

It can be mathematically expressed with the following formula:

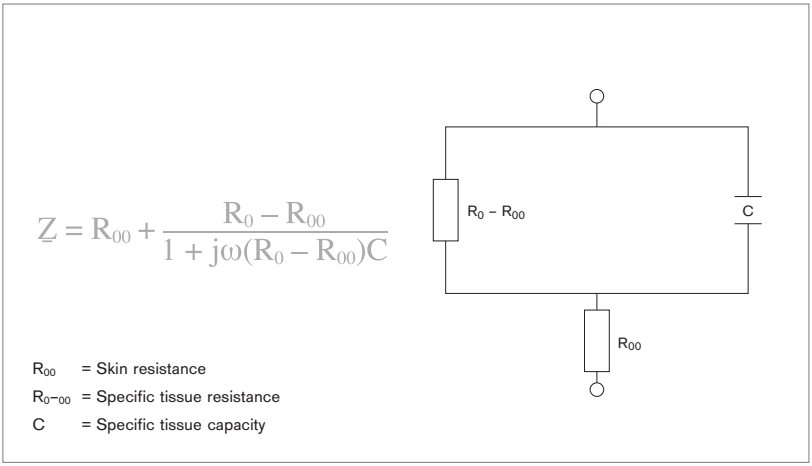

Fig. 61: Simplified equivalent circuit diagram of biological tissue

While the capacity depends on characteristics of the biomembranes of a specific tissue (ion channels, fatty acids, gap junctions, etc.), its resistance mainly depends on characteristics of the extracellular fluid (e.g., composition and amount).

Consequently, it is the specific composition (e.g., lipids, water, electrolytes in the extracellular fluid) of biological tissue which leads to distinct impedance characteristics.

Increased extra-cellular water content, high concentration of electrolytes, large cells, and a high number of cell connections via gap junctions reduce impedance (e.g., in blood and muscle). In contrast, fat accumulation, bone, and air act as electrical resistors and thus increase regional impedance. Regional impedance can be predicted by tissue resistivity (Table 1) [98].

Although in vivo measurements of electrical properties of specific biological tissues are not easily obtained and depend heavily on the experimental setup, impedance values for specific types of biological tissue can be found in the literature [15, 99, 100].

Tissue	Impedance / Resistivity	
Blood		150 Ω * cm
Lung	expiration	700 Ω * cm
	inspiration	2400 Ω * cm
Fat		2000–2700 Ω * cm
Bones		16600 Ω * cm
Muscle	longitudinal	125 Ω * cm
	transversal	1800 Ω * cm
Heart Muscle	longitudinal	160–575 Ω * cm
	transversal	420–5200 Ω * cm

When bioimpedance measurements are performed to assess the lung function, the deviations between end-inspiratory and end-expiratory electrical properties are of particular interest. It is misleading to explain the increased end-inspiratory impedance by the fact that air as such is a poor electric conductor. In contrast to X-rays, the pathways of electrical current never pass through the air inside the bronchi, alveoli or pathological structures such as emphysema bulla or a pneumothorax.

The explanation for the concomitant increase of bioimpedance with increasing pulmonary air content was delivered by Nopp et al. [101, 102]:

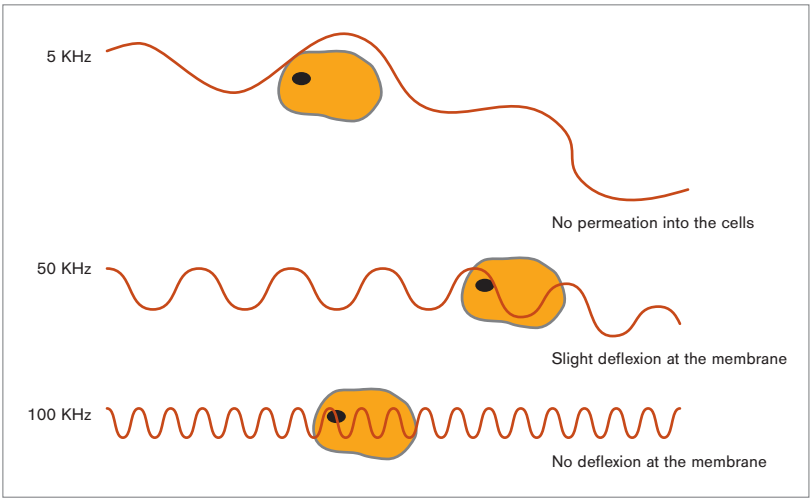

Fig. 62: Pathways of electrical current at different frequencies

With increasing air content, the cellular structures of the lung parenchyma are stretched, increasing the length of the pathways while the diameter of the conducting cellular structure decreases.

According to the formula Z = L/S, where L is the length and S the section of a conductor, the impedance increases during inflation as the conductive cellular structures are stretched.

The electric current only passes through either intracellular or extracellular structures, depending on the frequency applied (Fig. 62).

At frequencies below 5 kHz, electrical current does not permeate into the cells and thus flows only through extracellular fluid. The tissue therefore shows mainly resistive characteristics.

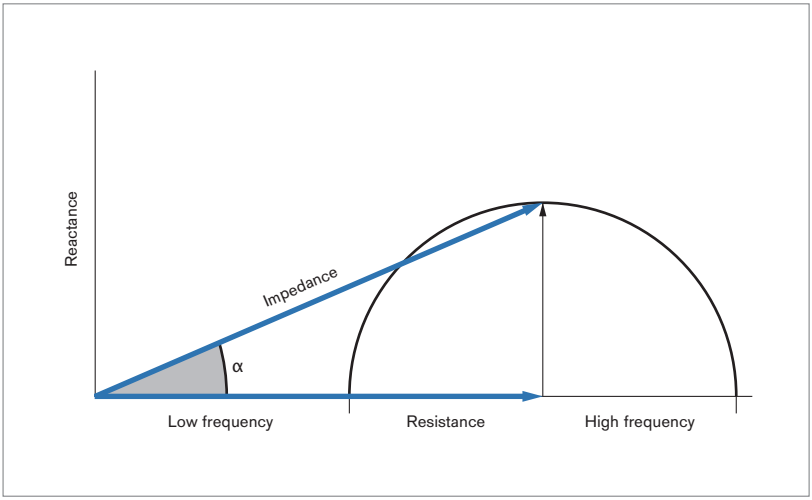

Fig. 63: Cole-Cole plot

The capacitive behaviour increases with increasing frequencies and reaches its maximum at about 50 kHz. Electrical currents are slightly deflected at the cell membranes.

At higher frequencies (> 100 kHz), the electrical current is directly passing the cell membranes, resulting in a decrease in the capacitive behaviour. As early as 1949, Kenneth S. Cole und Robert H. Cole described a model which explains this tissue specific impedance behaviour (Fig. 63).

BIOIMPEDANCE MEASUREMENTS WITH PULMOVISTA 500

PulmoVista 500 utilises alternating currents with a range of 80 – 130 kHz. It generally applies the current at a single frequency, which is automatically adjusted if a high level of electromagnetic background noise of a certain frequency would result in compromised data acquisition.

In contrast to bioelectrical impedance analysers (BIA), which utilise the frequency dependent responses of the tissue to determine body composition, PulmoVista 500 requires only a single frequency to determine ventilation or cardiac related impedance changes.

PulmoVista 500 is processing the absolute magnitude of impedance; however the information on the phase difference between voltage and current is not used for signal processing.

Within the frequency range of 80 – 130 kHz, the selection of the operating frequency does not have a substantial impact on the results of the measurements or the displayed information.

For many years, patient monitors have used bioimpedance measurements to monitor respiratory function. Like with PulmoVista 500, these patient monitors also make use of the fact that trans-thoracic impedance, which in this case is measured using ECG electrodes, increases in proportion to the intra-thoracic air content, which in turn is linked to the respiratory efforts of the patient.

CARDIAC RELATED IMPEDANCE CHANGES

The thoracic impedance changes related to cardiac activity are of the same interest as those brought about by ventilation. Typically, ventilation related impedance changes of the entire EIT sensitivity region are about 10 times higher than cardiac related impedance changes. However, it has to be taken into account that this ratio depends very strongly on the position of the electrodes relative to the heart, the lung water content, tidal volumes, stroke volumes and the end-expiratory lung volume, the latter suggesting that PEEP settings also will affect this ratio.

The underlying mechanisms of these cardiac related impedance changes are not completely understood.

The best explanation developed so far may be that, due to the contraction of the heart muscle during systole, low conductive lung tissue replaces high conductive heart volume. Simultaneously, lung tissue is displaced by the stroke volume distributed into the pulmonary circuit. Thus, the decrease in regional bioimpedance induced by perfusion would be a spatial dislocation effect of lung tissue caused by the expansion of major vessels and increased blood perfusion [98].

As typical tidal volumes in adults are about 500 to 600 ml and corresponding stroke volumes 70 ml, a rough correlation to the aforementioned 10:1 ratio of ventilation to cardiac related impedance changes is suggested, and actually can often be found in EIT data.

It requires further fundamental research and validation studies before information on cardiac activity or even lung perfusion derived from EIT data can be used for clinical decision making.

Appendix III: Glossary

TERM	ABBREVIATION	EXPLANATION
Acute Lung Injury	ALI	A severe, heterogeneous lung disease caused by a variety of direct and indirect issues. It is characterised by inflammation of the lung parenchyma leading to impaired gas exchange, non-cardiogenic pulmonary edema, low lung compliance with concomitant systemic release of inflammatory mediators causing inflammation, hypoxemia and frequently resulting in multiple organ failure. Acute Lung Injury is defined as [103]: – Bilateral pulmonary infiltrates on chest x-ray – Pulmonary Capillary Wedge Pressure < 18 mmHg (2.4 kPa) – PaO_2/FiO_2 <300
Acute Respiratory Distress Syndrome	ARDS	A more severe form of ALI. For many years, acute Respiratory Distress Syndrome was defined as [103]: – Bilateral pulmonary infiltrates on chest x-ray – Pulmonary Capillary Wedge Pressure < 18 mmHg (2.4 kPa) – PaO_2/FiO_2 <200 Recently this definition has been reviewed and redefined by a consensus panel [104]:

TERM	ABBREVIATION	EXPLANATION
Acute Respiratory Failure	ARF	Inadequate gas exchange by the respiratory system, with the result that arterial oxygen and/or carbon dioxide levels cannot be maintained within their normal ranges.
Aeration		Amount of gas contained within the lung at a certain moment of time.
Alternating Current	AC	A current, in which the movement of electric charge periodically reverses direction. The usual waveform of an AC is a sine wave.
Alveolar Recruitment		Alveolar recruitment describes the process of expanding collapsed parts of the lung over the entire ventilation cycle. It is one of the primary goals of respiratory care for acute lung injury. It is aimed at improving pulmonary gas exchange and, even more important, at protecting the lungs from VILI.
Atelectasis		A condition where alveoli are deflated and collapsed; it may be due to a blockage of airways, and/or excessive external pressure on the alveoli.

TERM	ABBREVIATION	EXPLANATION
Barotrauma		The damage to the lung caused by overdistension of alveoli due to excessive trans-pulmonary pressure during mechanical ventilation. Recent clinical data demonstrate that excessive tidal volumes, and not airway pressure, is the causal factor of VALI.
Change of End-Expiratory Lung Impedance	ΔEELI	Absolute impedance measurements cannot directly be related to the end-expiratory lung impedance. However, ΔEELI closely correlates with changes of end-expiratory lung volume of the EIT sensitivity region. The parameter ΔEELI as determined by PulmoVista 500 expresses deviations of the regional end-expiratory lung impedance in relation to the global tidal variation.
Chest X-Ray	CXR	A radiograph (frontal plane) of the chest used to diagnose conditions affecting the chest. Chest radiographs are among the most common films taken, being diagnostic of many conditions.

TERM	ABBREVIATION	EXPLANATION
Computed Tomography	CT, CAT	A medical imaging method employing tomography created by computer processing. CT is one of the most important methods of radiological diagnosis. It delivers non-superimposed, cross-sectional images of the body, which can show smaller contrast differences than conventional X-ray images. For lung imaging, CT images allow to differentiate between ventral and dorsal regions of the lung.
Cyclic Opening and Closing		Describes alveoli which are collapsed at the end of expiration and open during inspiration. This condition can cause VALI. Synonymously used with the term “tidal recruitment”.
Cytokines		Cytokines are substances released by cells of the immune system; they act as messengers between cells in the generation of an immune response. Lung cytokines can be released because of inadequate ventilator settings especially in patients with ALI and ARDS. An immune response triggered by cytokine activity may contribute to multiple system organ failure.

TERM	ABBREVIATION	EXPLANATION
Dependent Lung Regions		Area of the lungs, where the weight of the lung (and the heart) above this area acts as an additional weight, causing superimposed pressure. In supine position, the dependent lung regions are located in the dorsal part of the lung.
Derecruitment		Loss of end-expiratory lung volume leading to a lack of gas and respective ventilation within a lung area.
Differential Image		Is designed to display changes between two EIT images at different points in time. As these changes can generally be positive or negative, the zero value (representing no change) is always displayed in the mid-position of the colour scale, which uses – in contrast to the colour scale for Dynamic and Status Images – a turquoise colour for positive and an orange colour for negative changes.
Dorsal	D	Related to the position of the subject's spine, in EIT imaging the lower aspect of the image represents the part closest to the subject's spine. When the EIT image is subdivided into 4 layers, the dorsal part is represented by ROI 4.

TERM	ABBREVIATION	EXPLANATION
Dynamic Image		Continuously displays relative impedance changes induced by ventilation within the EIT sensitivity region as a series of tomograms. The relative impedance changes are referred to the end-expiratory impedance level.
EIT sensitivity region		The lens shaped intra-thoracic volume whose impedance changes contribute to the generation of EIT images. This plane is 4 cm thick at the periphery and increases towards the central region.
Electrode plane		The plane intersecting the centres of the body surface EIT electrodes. The most common is a transverse or oblique plane around the thorax.
Electron Beam Computed Tomography	EBCT	An experimental, specific form of CT in which the X-ray tube is not mechanically spun in order to rotate the source of X-ray photons. This different design was explicitly developed to better image heart structures which never stop moving, performing a complete cycle of movement with each heart beat.
End-Expiratory-Lung Impedance	EELI	End-expiratory lung impedance, which closely correlates with end-expiratory lung volume of the EIT sensitivity region. Thus ΔEELI represents the change in end-expiratory lung volume within the EIT sensitivity region.

TERM	ABBREVIATION	EXPLANATION
End-Expiratory-Lung Volume	EELV	Sometimes synonymously used with the term FRC. However, mechanically ventilated patients exhale against PEEP rather than ambient pressure, which is why physicians use the term EELV (End-Expiratory Lung Volume) instead of FRC. EELV (resp. FRC) describes the air volume which can contribute to gas exchange between two breaths. Adequate PEEP settings during mechanical ventilation help to keep alveoli and airways open thus maintaining a sufficient EELV.
Frame		A set of 208 voltage measurements taken after one complete rotation of the current injection, which is used to reconstruct one single EIT image.
Frame Rate		The frame rate is the frequency expressed as images per second at which Dynamic Images are generated.
Functional EIT	fEIT	PulmoVista 500 performs functional EIT, meaning that it mainly displays relative impedance changes as a result of lung function, i.e., ventilation and changing end-expiratory lung volume.

TERM	ABBREVIATION	EXPLANATION
Functional Residual Capacity	FRC	Physiological parameter, which describes the volume of air present in the lungs at the end of passive expiration (against ambient pressure).
Global Tidal Variation	TVglobal	The parameter TV global represents the difference between the minimum value and the maximum value in the Global impedance waveform for each breath. Regardless of the tidal volume, this figure is always 100%, it solely serves as a reference for the ROI tidal variations.
Hyperinflation		See Overdistension.
Impedance		Electrical impedance, or simply impedance, describes a measure of opposition to alternating current (AC). Lung tissue during end of inspiration causes more opposition to the current than during end of expiration, and thus the intra-thoracic impedance changes with ventilation.

TERM	ABBREVIATION	EXPLANATION
Magnetic Resonance Imaging	MRI	A medical imaging technique most commonly used in radiology to visualise detailed internal structure and function of the body. MRI provides much greater contrast between the different soft tissues of the body than CT, making it especially useful in neurological, musculoskeletal, cardiovascular, and oncological imaging.
Mid-dorsal	MD	An EIT imaging specific term, referring to the part of the image that is located above the dorsal aspect. When the EIT image is subdivided into 4 layers, the mid-dorsal part is represented by ROI 3.
Mid-ventral	MV	An EIT imaging specific term, referring to the part of the image that is located below the ventral aspect. When the EIT image is subdivided into 4 layers, the mid-ventral part is represented by ROI 2.
Minute Image		The Minute Image represents regional distribution of impedance changes over the last minute. The Minute Image displays Tidal Images averaged over the last minute.

TERM	ABBREVIATION	EXPLANATION
Multiple Inert Gas Elimination Technique	MIGET	An experimental technique used mainly in pneumology, that involves measuring mixed venous, arterial, and mixed expired concentrations of six infused inert gases. In many cases MIGET yields the crucial information about the physiology of gas exchange, i.e. shunt, dead space, and the general ventilation versus blood flow (Va/Q).
Non-dependent Lung Regions		Area of the lungs without superimposed pressure. In supine position, the non-dependent lung regions are located in the ventral part of the lung.
Overdistension		Excessive expansion of the lungs at the end of inspiration, commonly caused by either high tidal volumes or high end-expiratory lung volumes resulting from high PEEP levels. Recent findings suggest that overinflation is the predominant cause of VILI. Often synonymously used with Overinflation, Hyperdistension, and Hyperinflation. In EIT data, the effects of overdistension can only indirectly be seen, as overdistended lung regions have a low compliance and are thus less ventilated. Further studies are required to validate the capability of EIT to directly detect overdistension.

TERM	ABBREVIATION	EXPLANATION
Overinflation		See Overdistension.
Positive End Expiratory Pressure	PEEP	The pressure during mechanical ventilation used to oppose passive emptying of the lung and to keep the airway pressure above the atmospheric pressure. PEEP is used to maintain a sufficient end-expiratory lung volume.
Pulmonary Consolidation		The solidification of normally aerated lung tissue, that occurs as a result of accumulation of inflammatory cellular exudate in the alveoli and adjoining ducts. Consolidation may also occur due to the alveolar space filling with water or blood.
Pulmonary Shunt		Pulmonary shunt describes alveoli that are perfused but not ventilated, e.g. due to collapse or consolidation.

TERM	ABBREVIATION	EXPLANATION
Recruitment Manoeuvre	RM	A procedure, usually performed with a mechanical ventilator, aimed at expanding collapsed lung tissue. In order to recruit collapsed lung tissue, sufficiently high peak pressures and PEEP levels must be temporarily imposed to exceed the critical opening pressure of the affected lung region. After the recruitment manoeuvre the PEEP must be kept high enough that subsequent de-recruitment does not occur. Recruitment manoeuvres also have a time related component as the time required to open (heterogeneous) alveoli varies.
Region of Interest	ROI	A user-defined area within an EIT status image. The image can be divided horizontally or into quadrants. In PulmoVista 500, the area covered by each ROI is represented by a corresponding regional impedance waveform, a TV ROI and a regional ΔEELI.
ROI Tidal Variation	TV ROI	Regional Tidal Variations show the percentage of ventilation related impedance change which takes place in the corresponding ROI.

TERM	ABBREVIATION	EXPLANATION
Single Photon Emission Computed Tomography	SPECT	An experimental, nuclear tomographic imaging technique using gamma rays. Similar to CT, it delivers cross-sectional images of the body.
Status Image		A Tidal Image or Minute Image;
Tidal Image		The Tidal Image represents regional distribution of impedance changes of the last detected breath. The Tidal Image is a differential image of the end of inspiration compared to the beginning of inspiration.
Tidal Recruitment		See Cyclic Opening and Closing.
Tomogram		A cross-sectional image, created by a tomograph.
Tomograph		A device, used to create a tomogram.
Tomography		A method of producing a cross-sectional image, in slices, of a solid object.
Transverse Plane		PulmoVista 500 provides cross-sectional images as if looking through the subject's feet; the left side of the image represents the right side of the subject.

TERM	ABBREVIATION	EXPLANATION
Ventilation		Movement of gas into and out of the lung during breathing.
Ventilator Associated Lung Injury	VALI	Lung injury as a result of mechanical ventilation, caused by either excessive (regional) tidal volumes leading to overdistension and / or cyclic opening and closing of alveoli as a result of insufficient PEEP settings. In relation with mechanically ventilated patients, the term VALI has replaced the term VILI, as clinical data show that pre-existing lung injury seems to be mandatory for the observed adverse effects of mechanical ventilation.
Ventilator Induced Lung Injury	VILI	Sometimes used synonymously with VALI, but correctly the term VILI should only be used in the context of a purposely induced lung injury in laboratory settings.
Ventral	V	Related to the position of the subject's sternum (or belly), in EIT imaging the upper aspect of the image, regardless of whether the patient is lying in supine, lateral or prone position. When the EIT image is subdivided into 4 layers, the ventral part is represented by ROI 1.

TERM	ABBREVIATION	EXPLANATION
Volutrauma		The damage to the lung during mechanical ventilation, caused by excessive (regional) tidal volumes leading to overdistension of alveoli. It is not necessarily associated with barotrauma: the pressure in the alveoli may not be excessive but they may still be overdistended.

D-3415-2011

Eckhard Teschner, born in 1964 in Bremen, Germany, has a biomedical engineering background, but has also worked in emergency care and the intensive care environment. After his studies, he was employed as Senior Product Manager in the business fields of radiology, cardiology and heart surgery. He joined Dräger in 1999 and has been the responsible Product Manager for the EIT technology project since its launch in 2001 in cooperation with the EIT group Göttingen.

He has initialised and accompanied various scientific and clinical cooperations with international experts in lung mechanics and mechanical ventilation. He has been present during more than 100 EIT measurements on intensive care patients who were in some cases suffering from severe respiratory dysfunctions.

In the product development process of PulmoVista 500, he has specified its product requirements and designed its graphical user interface.

D-70-2011

Prof. Dr. med. Michael Imhoff is board certified in general surgery and intensive care medicine. Research areas include trauma surgery, intensive care medicine, patient monitoring, clinical data management, artificial intelligence in medicine and health economics, leading to over 300 publications and scientific presentations.

He teaches Medical Informatics and Statistics at the Ruhr-University Bochum, Germany, is a reviewer for the German Research Foundation, a member of the editorial boards of and reviewer for several international biomedical journals, and Chairman of the section for patient monitoring of the German Association of Biomedical Engineering (DGBMT).

D-676-2014

Prof. Dr. med. Dr.-Ing. Steffen Leonhardt was born in 1961 in Frankfurt, Germany. He obtained an M.S. in Electrical Engineering from SUNY at Buffalo, NY, USA, a Diploma and a Ph.D. in Electrical Engineering from Technical University of Darmstadt, Darmstadt, Germany, and an M.D. from Goethe University, Frankfurt, Germany. In 1999, he joined Dräger Medical GmbH in Luebeck, Germany, and he led the EIT-R&D team building the first prototypes of Pulmovista 500 from 2001 – 2003. In 2003, he was appointed Head of the newly established Philips Chair for Medical Information Technology at the Helmholtz-Institute for Biomedical Engineering, RWTH Aachen University, Germany.

Besides EIT, his research interests include medical measurement technologies, personal health care devices and closed loop systems in medicine.

CORPORATE HEADQUARTERS
Drägerwerk AG & Co. KGaA
Moislinger Allee 53–55
23558 Lübeck, Germany

www.draeger.com

Manufacturer:
Dräger Medical GmbH
Moislinger Allee 53–55
23558 Lübeck, Germany

As of August 2015:
Dräger Medical GmbH changes to Drägerwerk AG & Co. KGaA.

REGION EUROPE CENTRAL AND EUROPE NORTH
Dräger Medical GmbH
Moislinger Allee 53–55
23558 Lübeck, Germany
Tel +49 451 882 0
Fax +49 451 882 2080
info@draeger.com

REGION EUROPE SOUTH
Dräger Médical S.A.S.
Parc de Haute Technologie d'Antony 2
25, rue Georges Besse
92182 Antony Cedex, France
Tel +33 1 46 11 56 00
Fax +33 1 40 96 97 20
dlmfr-contact@draeger.com

REGION MIDDLE EAST, AFRICA
Dräger Medical GmbH
Branch Office
P.O. Box 505108
Dubai, United Arab Emirates
Tel +971 4 4294 600
Fax +971 4 4294 699
contactuae@draeger.com

REGION ASIA / PACIFIC
Draeger Medical South East Asia Pte Ltd.
25 International Business Park
#04-27/29 German Centre
Singapore 609916, Singapore
Tel +65 6572 4388
Fax +65 6572 4399
asia.pacific@draeger.com

REGION CENTRAL AND SOUTH AMERICA
Dräger Panama Comercial S. de R.L.
Complejo Business Park,
V tower, 10th floor
Panama City
Tel +507 377 9100
Fax +507 377 9130
contactcsa@draeger.com

90 66 788 | 1504-3 | Communications & Sales Marketing | PP | PR | LE | Printed in Germany | Chlorine-free – environmentally compatible | Subject to modifications | © 2015 Drägerwerk AG & Co. KGaA